A study of *cis-trans* isomerisation of the bis-chelated complexes of platinum(II) and palladium(II) with *N,N*-dialkyl-*N'*-aroyl(acyl)thiourea ligands

by

Dirk C. Hanekom

Thesis presented in fulfilment of the requirements for the degree of

Master of Science at the **University of Stellenbosch**

Supervisor: Prof. Klaus Koch

April 2006

I, the undersigned, hereby declare that the work contained in this thesis is my own original work and that I have not previously, in it's entirety or in part, submitted it at any university for a degree.

Signature:

Date: 28/02/2006

Abstract

The *N,N*-diakyl-*N'*-aroyl(acyl)thiourea ligands coordinate to platinum(II) and palladium(II) in solution to form stable chelated ***cis***-[M(L-***S,O***)$_2$] (M = Pt, Pd) complexes. Variation of solvent, mode of synthesis, starting material and the groups attached to the carbonyl moeity had no effect on the isomer distribution. The molecular structure of ***cis***-bis(*N,N*-dialkyl-*N'*-3,4,5-trimethoxybenzoylthioureato)-platinum(II), ***cis***-bis(*N,N*-dialkyl-*N'*-3,5-dimethoxybenzoylthioureato)platinum(II), ***cis***-bis(*N,N*-dialkyl-*N'*-3,4,5-trimethoxybenzoylthioureato)palladium(II) and ***cis***-bis(*N,N*-dialkyl-*N'*-3,5-dimethoxybenzoylthioureato)palladium(II) were determined and verified as *cis* geometries.

However, these ***cis***-[M(L-***S,O***)$_2$] [M = Pt, Pd] complexes have been shown to undergo a photo-induced ***cis***-[M(L-***S,O***)$_2$] to ***trans***-[M(L-***S,O***)$_2$] isomerisation with no such isomerisation observed in the absence of light. This process was followed and studied by Reversed Phase High Performance Liquid Chromatography. No thermal isomerisation reaction could be identified in the dark even when these solutions where heated to 80°C for 100 hours. Thereafter the addition of an excess of free ligand, to this heated solution, also had no effect on the *cis-trans* isomer distribution.

Irradiation and subsequent isomerisation of these complex solutions was studied in acetonitrile using yellow, blue, red and white light. No isomerisation took place with light of wavelenghts higher than 600nm. As with white light, when blue light (radiation cut-off ~ 300nm) and yellow light was used (radiation cut-off ~ 480nm) isomerisation did occur. In an experiment where yellow light was used for irradiation, it was shown that the intensity of the light passing through the solution (i.e. the flux of photons) has a direct effect on the steady-state *cis-trans* ratio of the molecules in solution.

When solutions of *cis* complexes were irradiated with white light to their respective steady-state *cis-trans* ratios, and then kept in the dark, the *trans* complex reverts to the *cis* complex again. This *trans-cis* isomerisation reaction was found to be thermally controlled; relative steady-state equilibruim constant (K_e = [*trans*]/[*cis*]) values for ***cis***-bis(*N,N*-dialkyl-*N'*-3,4,5-trimethoxybenzoylthioureato)palladium(II) in acetonitrile were determined at 0°C, 20°C and 40°C (no light) respectively.

The addition of electron donating methoxy groups to the benzoyl moeity did not lead to higher K_e-values, but the bulky camphanoyl moeity present in ***cis***-bis(*N,N*-diethyl-*N'*-camphanoylthioureato)platinum(II) led to a higher K_e-value than any of the bis(*N,N*-dialkyl-*N'*-3,4,5-trimethoxybenzoylthioureato)platinum(II), bis(*N,N*-dialkyl-*N'*-3,5-dimethoxybenzoylthioureato)platinum(II) and bis(*N,N*-dialkyl-*N'*-4-monomethoxy-benzoylthioureato)platinum(II) complexes. The *cis-trans* steady-state and K_e-values for ***cis***-bis(*N,N*-diethyl-*N'*-pivaloylthioureato)platinum(II) in acetonitrile were also determined.

A solvent study revealed that the *trans*-isomer, having a zero dipole moment by virtue of it's planar symmetrical structure, was not necessarily favoured by more non-polar solvents such as 1,4-dioxane and THF – as have previously been shown for similar monodentate complexes.

A ligand exhange reaction between two chelated complexes, ***cis***-bis(*N,N*-dialkyl-*N'*-3,4,5-trimethoxybenzoylthioureato)platinum(II) and ***cis***-bis(N,N-dialkyl-N'-naphthoyl-thioureato)platinum(II), was observed in acetonitrile in both the light and in the dark. In the presence of light both ligand exhange and isomerisation (also of the "mixed" complex) occurred, while in the dark only ligand exchange occurred with no evidence of isomerisation.

Prelimary ^{195}Pt NMR experiments have proved to be very promising and ^{195}Pt peaks for all the ***cis***- and ***trans***-[Pt(L-***S,O***)$_2$] isomers have been assigned after white light irradiation of the $CDCl_3$ solutions directly in the NMR tube.

Opsomming

N,N-diakyl-*N'*-aroyl(acyl)thiourea ligande koordineër met platinum(II) en palladium(II) in oplossing om stabiele, bidentate ***cis***-[M(L-***S,O***)$_2$] (M = Pt, Pd) komplekse te vorm. Variasie in oplosmiddel, metode van sintese, uitgangsstof en die funksionele groepe geheg aan die karboniel groep het geen effek gehad op die *cis-trans* isomeer verdeling nie. Die molekulêre struktuur van ***cis***-bis(*N,N*-dialkyl-*N'*-3,4,5-trimethoxybenzoylthioureato)platinum(II), ***cis***-bis(*N,N*-dialkyl-*N'*-3,5-dimethoxybenzoylthioureato)platinum(II), ***cis***-bis(*N,N*-dialkyl-*N'*-3,4,5-trimethoxybenzoylthioureato)palladium(II) en ***cis***-bis(*N,N*-dialkyl-*N'*-3,5-dimethoxybenzoylthioureato)palladium(II) is bepaal – dit het bevestig dat die geometrie van die molekules wel *cis* was.

Daar is egter gevind dat hierdie ***cis***-[M(L-***S,O***)$_2$] [M = Pt, Pd] komplekse 'n foto-geinduseerde ***cis***-[M(L-***S,O***)$_2$] na ***trans***-[M(L-***S,O***)$_2$] isomerisasie ondergaan. Geen bewys van 'n soortgelyke proses kon gevind word in die afwesigheid van lig nie. Hierdie proses is gevolg en bestudeer deur gebruik te maak van Reversed Phase High Performance Liquid Chromatography. Selfs toe oplossings tot en met 80°C verhit was vir 'n periode van 100 uur, kon geen termies-geinduseerde isomerisasie reaksie ge-indentifiseer word nie. Die byvoeging van ligand tot die verwarmde oplossing het ook geen effek gehad op die *cis-trans* isomeer verdeling nie.

Die effek wat bestraling met wit, geel, blou en rooi lig op oplossings van die komplekse het is bestudeer. Vir lig met golflengte hoër as 600nm is geen *cis-trans* isomerisasie waargeneem nie. Soos gevind is met wit lig het isomerisasie plaasgevind met blou lig (bestralings afsnypunt ~ 300nm) en met geel lig (bestralings afsnypunt ~ 480nm). In 'n eksperiment waar geel lig gebruik is vir bestraling, is dit bewys dat die intensiteit van die lig wat deur die oplossing beweeg 'n direkte invloed het op die *cis-trans* verdeling van molekules in oplossing.

In oplossings wat in die donker gelaat is, na bestraling met wit lig tot 'n *cis-trans* isomeer verdeling, het die *trans*-kompleks terug ge-isomeriseer na die

cis-kompleks. Dit is ook bevind dat hierdie *trans-cis* isomerisasie reaksie termies gekontrolleerd is. K_e = [*trans*]/[*cis*] waardes vir ***cis***-bis(*N,N*-dialkyl-*N'*-3,4,5-trimethoxybenzoylthioureato)palladium(II) in asetonitriel is bepaal by 0°C, 20°C en 40°C (geen lig).

Die byvoeging van elektron donerende metoksi groepe aan die benzoyl groep het nie gelei tot hoër K_e-waardes nie maar die bonkige camphanoyl groep in ***cis***-bis(*N,N*-diethyl-*N'*-camphanoylthioureato)platinum(II) lei tot 'n hoër K_e-waarde as vir enige van die bis(*N,N*-dialkyl-*N'*-3,4,5-trimethoxybenzoyl-thioureato)platinum(II), bis(*N,N*-dialkyl-*N'*-3,5-dimethoxybenzoylthioureato)-platinum(II) en bis(*N,N*-dialkyl-*N'*-4-monomethoxybenzoylthioureato)-platinum(II) komplekse. Die *cis-trans* bestendige-toestand K_e-waardes vir ***cis***-bis(*N,N*-diethyl-*N'*-pivaloylthioureato)platinum(II) is ook bepaal.

'n Oplosmiddel studie het gewys dat die *trans*-isomeer (wat 'n dipool moment gelyk aan nul het as gevolg van sy planêre, simmetriese struktuur) nie noodwendig – soos voorheen bewys is vir soortgelyke monodentate komplekse - bevoordeel word deur die meer nie-polêre oplosmiddels soos 1,4-dioksaan en THF nie.

'n Uitruilings meganisme wat plaasvind in die teenwoordigheid en afwesigheid van lig is waargeneem tussen die twee bidentaat gekoordineerde komplekse ***cis***-bis(*N,N*-dialkyl-*N'*-3,4,5-trimethoxybenzoylthioureato)platinum(II) and ***cis***-bis(N,N-dialkyl-N'-naphthoylthioureato)platinum(II). In die eksperiment waar lig wel teenwoordig was het uitruiling van ligande en isomerisasie (ook van die "gemengde kompleks") plaasgevind, terwyl slegs uitruiling in die donker eksperiment plaasgevind het.

Preliminêre ^{195}Pt KMR eksperimente wat gedoen is blyk belowend; ^{195}Pt pieke vir al die ***cis***- en ***trans***-[Pt(L-***S,O***)$_2$] isomere is aangewys na direkte wit lig bestraling van $CDCl_3$ oplossings in KMR buise.

Acknowledgements

I hereby would like to thank the following people and organisations that have each contributed in their own way to the success of this project:

- My parents and boet for their continued love, support and motivation.
- To my supervisor, Professor Klaus Koch, for the opportunity to spend 2 years in his research group – thereby adding to my education.
- To the members of the PGM-research group, specifically Gavin Blewett, Jocelyn Bruce, Andries Gie and Arjan Westra for their friendship, help and discussions.
- A special thank you to Dr. Catherine Esterhuysen for her help in solving the crystal structures.
- The University of Stellenbosch (US) and the National Research Foundation (NRF) for financial support.
- To Anja.
- Jesus Christ.

I thank you all.

Publications and awards

Sections of this work have been presented in the following manner:

- Dirk Hanekom, Jean M. McKenzie, Nocky M. Derix and Klaus R. Koch, *Chem. Commun.*, 2005, **6**, 767-769.

- Poster prize awarded at the 36th International Conference on Coordination Chemistry, Merida, Mexico, 18-23 July 2004 for a poster entitled: "A RP-HPLC study of the photochemically induced, thermally reversible, *cis-trans* isomerisation of M(L-***S,O***)$_2$ complexes [M = Pt, Pd]".

Photoinduced isomerisation of *cis*-[M(L-*S*,*O*)$_2$] (M = Pt^{II} and Pd^{II}) complexes of *N*,*N*-diethyl-*N*′-3,4,5-trimethoxybenzoylthiourea: key to preparation of the *trans* isomer

Dirk Hanekom, Jean M. McKenzie, Nocky M. Derix and Klaus R. Koch*

Received (in Cambridge, UK) 4th October 2004, Accepted 11th November 2004
First published as an Advance Article on the web 21st December 2004
DOI: 10.1039/b415306e

In acetonitrile solutions at room temperature, *cis*-[M(L-*S*,*O*)$_2$] Pt^{II} and Pd^{II} complexes of *N*,*N*-diethyl-*N*′-3,4,5-trimethoxybenzoylthiourea undergo reversible photoinduced isomerisation to the corresponding *trans* isomer upon irradiation with visible light in the 320–570 nm range, the rate and extent of isomerisation being significantly higher for the *cis*-[Pd(L-*S*,*O*)$_2$] complex compared to the Pt^{II} analogue; in the dark *trans*-[M(L-*S*,*O*)$_2$] cleanly reverts back to the *cis* complex at a rate dependent on the solution temperature, indicating a thermally controlled reverse process.

We have in the last decade extensively studied *N*,*N*-dialkyl-*N*′-aroylthioureas (RRNC(S)NHC(O)R′) for their potential analytical and process chemistry applications in the platinum group metals refining industry.[1] These ligands have long been known to readily form stable complexes with softer 1st row transition metal ions as shown from the studies of Hoyer and Beyer[2] and later König and Schuster.[3] Generally these molecules show an overwhelming tendency to coordinate particularly to d^8 metal ions resulting, upon loss of a proton, in a *cis*-*S*,*O* mode of coordination. We have exploited the favorable physiochemical properties of *N*,*N*-dialkyl-*N*′-acylthioureas (**HL**) for the convenient reversed-phase high performance liquid chromatographic (*rp*-HPLC) determination of Pt^{II}, Pd^{II} and Rh^{III} in acid chloride media.[4] Several years ago we serendipidously isolated a first example of a *trans*-bis(*N*,*N*-di(*n*-butyl)-*N*′-naphthoylthioureato)-platinum(II) complex in *ca.* 15% yield.[5] This is one of only two examples of *trans* complexes with these ligands of the more than 25 related crystal structures reported in the Cambridge Structural Database.[6] Despite considerable effort we have not been able to predictably prepare substantial quantities of *trans*-[Pt(L-*S*,*O*)$_2$] or *trans*-[Pd(L-*S*,*O*)$_2$] complexes with *N*,*N*-dialkyl-*N*′-aroylthioureas by any standard synthetic route.

We here report that the key to obtaining *trans*-[M(L-*S*,*O*)$_2$] complexes is a photoinduced isomerisation of the *cis*-[M(**L**^{1}-*S*,*O*)$_2$] complexes in acetonitrile solution[7] as monitored by *rp*-HPLC (M = Pt^{II}, Pd^{II} and *N*,*N*-diethyl-*N*′-3,4,5-trimethoxybenzoylthiourea (**HL**^{1}))†. Repeated injection of freshly prepared solutions (200 μg cm^{-3}) of authentic *cis*-[Pt(**L**^{1}-*S*,*O*)$_2$] in MeCN at room temperature, which are kept in the dark over a period of several weeks, show the elution of only a single peak (t_R ~ 10.5 min)‡. Identical solutions of *cis*-[Pt(**L**^{1}-*S*,*O*)$_2$] exposed to ambient daylight show the development of a second peak in the chromatogram within *ca.* 30–60 min of exposure, reaching a steady state within 25 h. As shown for *cis*-[Pt(**L**^{1}-*S*,*O*)$_2$] in Fig. 1, the area of the second peak at t_R ~ 8.6 min grows with length of exposure to light, while the major peak area correspondingly decreases, eventually reaching a steady state. The absorbance profiles of the two eluted species as obtained by a diode array photometric detector are virtually identical (λ_{max} = 307 nm), suggesting that the two peaks are due to *cis*–*trans* isomers. Moreover *rp*-HPLC coupled to electrospray mass spectrometry (ESMS) shows that the two peaks in the chromatogram of *cis*-[Pt(**L**^{1}-*S*,*O*)$_2$] solutions exposed to light have the same values (*m*/*z* 846.83 and 846.57, *calc.* for [$C_{30}H_{42}N_4O_8PtS_2$·H]$^+$ ≈ 846.22), confirming that the smaller peak corresponds to the *trans*-[Pt(**L**^{1}-*S*,*O*)$_2$] complex. Fig. 1 shows the peak area ratio K_c = [*trans*]/[*cis*] as a function of the time exposed to ambient light at room temperature. Similar observation can be made for *cis*-[Pd(**L**^{1}-*S*,*O*)$_2$], although the appearance of the second peak occurs much sooner, and steady state is reached within *ca.* 1 h.

Experiments show that the rate of photoisomerisation observed for *cis*-[Pt(**L**″-*S*,*O*)$_2$] or *cis*-[Pd(**L**″-*S*,*O*)$_2$] at room temperature in dilute acetonitrile solutions is significantly influenced by the relative intensity as well as the wavelength range of the light used for irradiation. Irradiation of solutions of *cis*-[Pt(**L**^{1}-*S*,*O*)$_2$] or *cis*-[Pd(**L**^{1}-*S*,*O*)$_2$] in a water jacketed, 15 cm glass cell using intense white light§ with relatively constant light flux (~320 μmol s^{-1} m^{-2}), results in isomerisation of *cis*-[Pt(**L**^{1}-*S*,*O*)$_2$] to a steady state within *ca.* 70 min (K_c = 0.14 ± 0.005), while *cis*-[Pd(**L**^{1}-*S*,*O*)$_2$] reaches a steady state within *ca.* 21 min (K_c = 0.43 ± 0.02). The relatively higher rate of isomerisation for *cis*-[Pd(**L**^{1}-*S*,*O*)$_2$] complexes at constant photon flux is consistent with the fact that Pd^{II} complexes

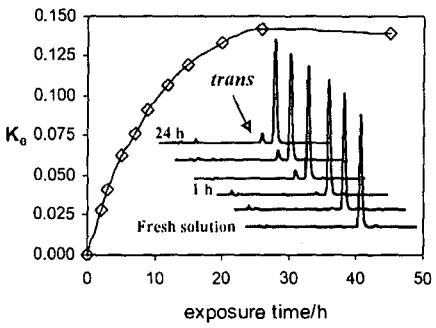

Fig. 1 K_c (ratio of *trans*/*cis* peak areas) for pure *cis*-[Pt(**L**^{1}-*S*,*O*)$_2$] in MeCN (*ca.* 100 μg cm^{-3}), as a function of the time exposed to ambient daylight at 20 °C, as monitored by *rp*-HPLC. The inset shows typical chromatograms obtained. Control dark experiments show only one peak.

*krk@sun.ac.za

are generally more kinetically labile compared to those of Pt^{II}. Experiments using optical filters to yield blue, yellow and red light respectively, show that light in the wavelength range of 320–570 nm is responsible for the observed photoisomerisation. Fig. 2 shows the influence of the wavelength range of visible light on the relative K_e values of *cis*-[Pd(L^1-*S*,*O*)$_2$] being 0.43 ± 0.02, 0.40 ± 0.05, 0.20 ± 0.01 and 0.01 for white, blue, yellow and red light respectively.

When the (yellow) light intensity is increased from ~ 320 to 2280 μmol s^{-1} m^{-2}, the K_e value increases from 0.20 to 0.40, at 20 °C for *cis*-[Pd(L^1-*S*,*O*)$_2$]. Similar trends are obtained for *cis*-[Pt(L^1-*S*,*O*)$_2$] in MeCN, showing relative K_e values of 0.14 ± 0.01, 0.10 ± 0.01, and 0 for white (and blue), yellow and red light respectively. These experiments confirm that *cis*-[M(L^1-*S*,*O*)$_2$] (M = Pt^{II}, Pd^{II}) in solution undergo wavelength dependent photoinduced *cis–trans* isomerisation in MeCN. In the absence of light the isomerisation is reversed resulting in pure *cis*-[M(L^1-*S*,*O*)$_2$] again, suggesting a thermally controlled reverse reaction.

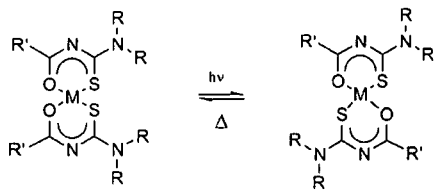

Fig. 3 clearly shows that K_e is temperature dependent, and that after an appropriate time in the dark, only the *cis* complex is again found in solution as monitored by *rp*-HPLC. Monitoring the isomerisation by *rp*-HPLC has the disadvantage of a time delay corresponding to the retention-time of the complexes on column. Thus monitoring the reverse *trans* to *cis* thermal reaction of *inter alia* *cis*-[Pd(L^1-*S*,*O*)$_2$] after irradiation with white light at various temperatures by means of ^{1}H NMR, confirms the results obtained with *rp*-HPLC. Fig. 4 shows a typical series of ^{1}H NMR spectra as a function of time after irradiation, confirming that the resonance at δ ~ 7.33 ppm (assigned to H2 and H6 of the trimethoxybenzoyl moiety) due to the *trans* complex decreases with time and the δ ~ 7.53 ppm resonance of the *cis* isomer grows to eventually dominate the spectrum again.

In conclusion, although photoinduced geometrical isomerizations of metal complexes particularly with monodentate ligands

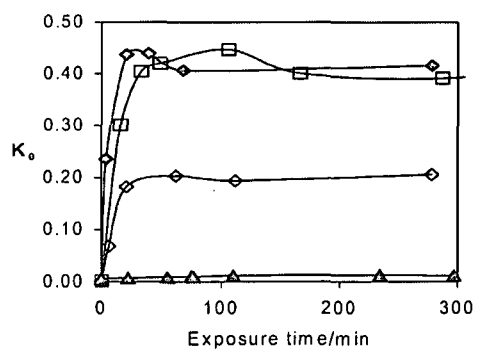

Fig. 2 K_e for pure *cis*-[Pd(L^1-*S*,*O*)$_2$] in MeCN (20 °C) as a function of wavelength of irradiation at relatively constant intensity. □ white; ◆ blue (cutoff 310 nm); ◇ yellow (465 nm); ▲ red (580 nm) light.

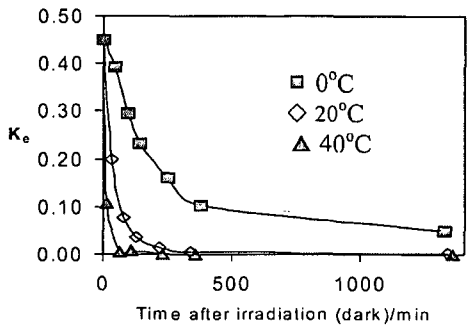

Fig. 3 K_e for *ca.* 200 μg cm^{-3} *cis*-[Pd(L^1-*S*,*O*)$_2$] in MeCN kept in the dark after irradiation at relatively constant intensity with white light as a function of temperature, as monitored by *rp*-HPLC.

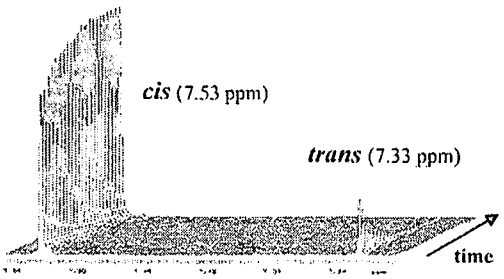

Fig. 4 Expanded ^{1}H NMR spectra of *cis*-[Pd(L^1-*S*,*O*)$_2$] in MeCN at 20 °C in the dark, showing a *trans* to *cis* isomerisation after irradiation with white light to steady state; ^{1}H(2,6) trimethoxyphenyl resonances.

are known,[8] such geometrical isomerisations are rare for chelating ligands, and there is to our knowledge only one well-studied case of a photoinduced *cis–trans* isomerisation observed for the [Pt(glycinato)$_2$] complex in the literature,[8] with no examples of comparable Pd^{II} complexes. The well studied facile *cis–trans* isomerism of bis(glycinato)copper(II) complexes,[9] is apparently *not* photoinduced, occurring spontaneously at ambient temperatures, presumably *via* an energetically favourable ring-twisting mechanism.[10] We are currently investigating in detail the possible mechanisms of the photoisomerisation of *cis*-[M(L-*S*,*O*)$_2$] reported here.

Financial support from the University of Stellenbosch, the NRF (GUN 2046827), THRIP (project 2921) and Angloplatinum is gratefully acknowledged.

Dirk Hanekom, Jean M. McKenzie, Nocky M. Derix and Klaus R. Koch*
Department of Chemistry, University of Stellenbosch, Private Bag X1, Matieland, 7602, Stellenbosch, South Africa. E-mail: krk@sun.ac.za; Fax: +27 21 808 3342; Tel: +27 21 808 3020

Notes and references

† Ligands **HL^1**, and the corresponding *cis*-[M(L^1-*S*,*O*)$_2$] complexes (M = Pt^{II} , Pd^{II}) were prepared as previously described,[1,4] fully characterised by elemental analysis, mp and ^{1}H and ^{13}C NMR in $CDCl_3$; *cis*-[Pt(L^1-*S*,*O*)$_2$] was confirmed by single crystal X-ray diffraction (unpublished results; K. R. Koch, J. Miller and L. Barbour, 2003).

‡ *rp*-HPLC conditions: 150 mm × 4.6 mm, Luna (end-capped) 5 μm C18 column, isocratic flow at 1 cm^3 min^{-1}, mobile phase: 90% CH_3CN, 10% 0.1 M sodium acetate buffer pH 6, 20 μL injections, photometric detection.

§ Light source 150 W quartz-halogen lamp from a conventional slide projector; intensity measured with an LI-250 quantum meter (Lincoln, LI-COR, USA). Photographic optical filters blue (80B), yellow (Y2) and red (25A) provided coloured light.

1 K. R. Koch, *Coord. Chem. Rev.*, 2001, **216**, 473; K. R. Koch, C. Sacht, T. Grimmbacher and S. Bourne, *S. Afr. J. Chem.*, 1995, **48**, 71.

2 L. Beyer, E. Hoyer, H. Hartman and J. Liebscher, *Z. Chem.*, 1981, **21**, 81; P. Mühl, K. Gloe, F. Dietze, E. Hoyer and L. Beyer, *Z. Chem.*, 1986, **26**, 81.

3 K.-H. König, M. Schuster, B. Steinbrech, G. Schneeweis and R. Schlodder, *Fresenius' Z. Anal. Chem.*, 1985, **321**, 457; K.-H. König, M. Schuster, G. Schneeweiss and B. Steinbrech, *Fresenius' Z. Anal. Chem.*, 1984, **319**, 66; M. Schuster, *Fresenius' Z. Anal. Chem.*, 1992, **342**, 791; M. Schuster and M. Schwarzer, *Anal. Chim. Acta*, 1996, **328**, 1; M. Schuster and M. Sandor, *Fresenius' Z. Anal. Chem.*, 1996, **356**, 326.

4 A. N. Mautjana, J. D. Miller, A. Gie, S. A. Bourne and K. R. Koch, *J. Chem. Soc., Dalton Trans.*, 2003, 1952.

5 K. R. Koch, J. du Toit, M. R. Caira and C. Sacht, *J. Chem. Soc., Dalton Trans.*, 1994, 785.

6 F. H. Allen, *Acta Crystallogr., Sect. B*, 2002, **58**, 380–388 CSC Version 5.25 updates (Jul 2004).

7 D. Hanekom and K. R. Koch, Presented in part as poster at the 36th International Conference on Coordination Chemistry, Merida, Mexico, 18–23 July, 2004. (Best poster in section award).

8 F. Scandola, O. Traverso, V. Balzani, G. L. Zucchini and V. Carassiti, *Inorg. Chim. Acta*, 1967, **1**, 76; C. R. Bock and A. E. Koerner von Gustorf, in *Advances in Photochemistry*, eds. J. N. Pitts, G. S. Hammond and K. Gollnick, Interscience Publication, John Wiley & Sons, New York, 1977, vol. 10, pp. 221–310.

9 P. O'Brien, *J. Chem. Educ.*, 1982, **59**, 1052–1053; S. M. Moussa, R. R. Fenton, B. A. Hunter and B. J. Kennedy, *Aust. J. Chem.*, 2002, **55**, 3319.

10 C. S. Trautermann, J. Sabolović, A. F. Voegele and K. R. Liedl, *J. Phys. Chem.*, 2004, **108**, 2098.

Abbreviations used

H_2L	:	*N*-alkyl-*N'*-aroyl(acyl)thiourea
HL	:	*N,N*-dialkyl-*N'*-aroyl(acyl)thiourea
X	:	a halide ion (Br^-, I^- or Cl^-) unless otherwise specified
(H_2L-***S***)	:	a H_2L ligand monodentately bound at the S atom
(L-***S,O***)	:	a HL ligand bidentately bound at the S and O atoms
$CDCl_3$	:	deuterated chloroform
HX	:	HBr or HI
L or L'	:	any neutral ligand unless otherwise specified
T	:	a ligand in a trans orientation to another ligand (X)
C	:	a ligand in a cis orientation to another ligand (X)
Y	:	a nucleophile unless otherwise specified
am	:	NH_3 or py
py	:	pyridine
DMSO	:	dimethyl sulfoxide
THF	:	tetrahydrofuran
MeCN	:	acetonitrile
NMR	:	nuclear magnetic resonance
MO	:	molecular orbital
MLCT	:	metal to ligand charge transfer
LMCT	:	ligand to metal charge transfer
CTTS	:	charge transfer to solvent
ITCT	:	interligand transmetallic charge transfer
IT	:	intervalence transfer
LC	:	liquid chromatography
HPLC	:	high performance liquid chromatography
RP-HPLC	:	reversed phase high performance liquid chromatography
GC	:	gas chromatography
FID	:	flame ionization detector
LC-ESMS	:	liquid chromatography electro spray mass spectrometry
t_r	:	retention time
R_s	:	resolution

Table of Contents

2. Experimental Approach

4. Concluding remarks

Chapter 1:

Introduction

1. Introduction

1.1 The platinum group metals (PGM) industry in South Africa: a brief overview

The six transition elements, platinum, palladium, ruthenium, rhodium, osmium and iridium, make up a collective group referred to as the PGM's (Platinum Group Metals). South Africa has been blessed with the world's largest proven PGM ore bearing deposits. These are contained in a large, irregularly shaped saucer-like geological intrusion known as the Bushveld Igneous Complex (BIC), being exposed over a surface area of 67 000km^2.[1] The main PGM containing reefs are the Merensky Reef and the Chromite Reefs, of which the Upper Group 2 (UG2) Reef, which is situated near the eastern and western limbs of the BIC (Figure 1), is the most important. A third PGM-rich layer is situated on the Potgietersrus limb and is referred to as Platreef.

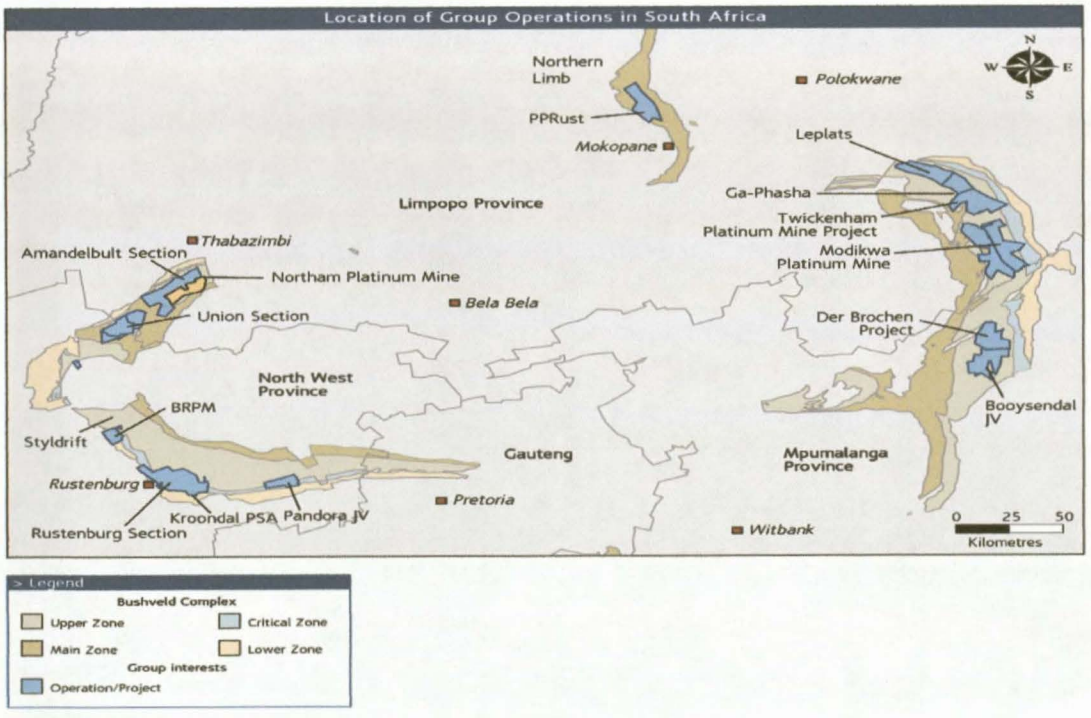

Figure 1. A map indicating the northern, eastern and western limbs of the BIC.[1]

South Africa, North America and Russia are the major role players in the global PGM market with South Africa, for example, producing more than 70% of the world's platinum in 2003 (Figure 2).

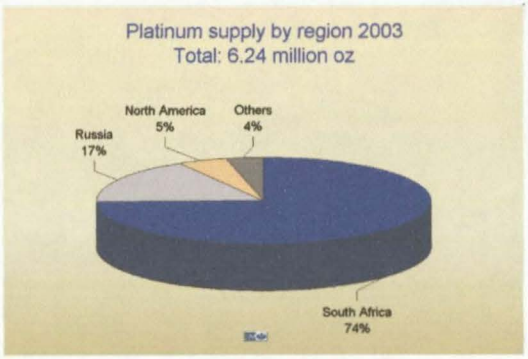

Figure 2. Platinum supply by region for the year 2003.[1]

Exhaust emission control legislation, referred to as Euro I, was introduced in 1992 resulting in automobile catalytic exhaust emission control devices being fitted to new cars in Europe, North America and Japan. These automobile catalytic exhaust emission control devices all contain Pt, Pd and Rh depending on their application. Euro IV has been introduced in 2004 and Euro V in 2008. The emissions (fine particles, hydrocarbons and NO_x) are measured in grams of pollutant per kilometre travelled and over 91% of new vehicles sold in the world today are sold with catalytic converters.[2] This has resulted in catalytic converters being the biggest application (see Figure 3 and 4) for platinum metal, surpassing its use for jewellery (which, unlike automobile catalytic exhaust emission control devices, is dependant on world economic growth).

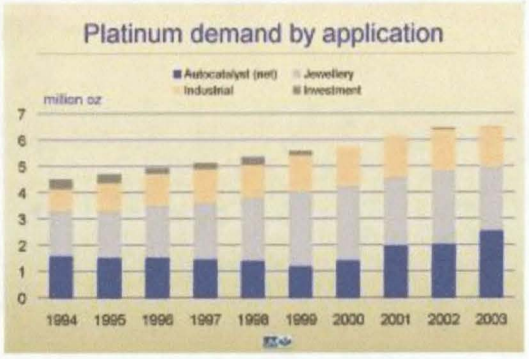

Figure 3. Platinum demand by application.[1]

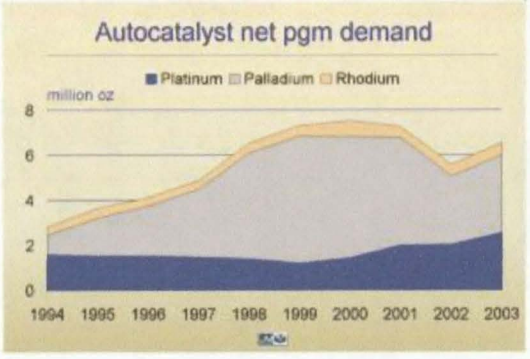

Figure 4. Autocatalyst net PGM demand.[1]

Industrial applications in the chemical-, electrical-, glass- and petroleum industries made up 23% of the market share in 2003.[3]

The PGM-industry is undeniably one of the largest contributors to the well-being of the South African economy. In Anglo Platinum's Annual Report of 2002 these were some of the "economic impact" highlights:

Employees:
Total Payroll and Benefits: R 4 134.4m
Public Sector:
Taxes Paid: R 3 667.0m
Donations: R 46.5m
Infrastructure development (non-business): R 11.5m
Service Suppliers:
Eskom: R 641.0m
Grinaker: R310.8m

Gross Sales Revenue Total: R 20 285.7m

Anglo Platinum has also been a leader in empowering historically disadvantaged South Africans. The Group has contributed by facilitating empowerment transactions on operations and projects with a total value of R 5 billion. Joint ventures include those with Mvelaphanda Platinum, African Rainbow Minerals and the Royal Bafokeng Nation.[3]

Anglo Platinum's expenditure on research and development (R&D) totalled R151.8 million in 2002. This includes research done at the Anglo Platinum Research Centre (ARC) and other programmes with universities and technical institutions, not only in South Africa, but also in Australia, Europe and Canada.

1.2 Literature survey

1.2.1 Coordination chemistry of *N*-alkyl and *N,N*-dialkyl-*N'*-aroyl(acyl)thiourea ligands and their complexes formed with platinum(II) and palladium(II)

For some time now our group (PGM Research Group, University of Stellenbosch) have been interested, with specific view to industrial application, in the coordination chemistry surrounding the *N*-alkyl (H_2L) and *N,N*-dialkyl-*N'*-aroyl(acyl)thiourea (HL) ligands (Figure 5).

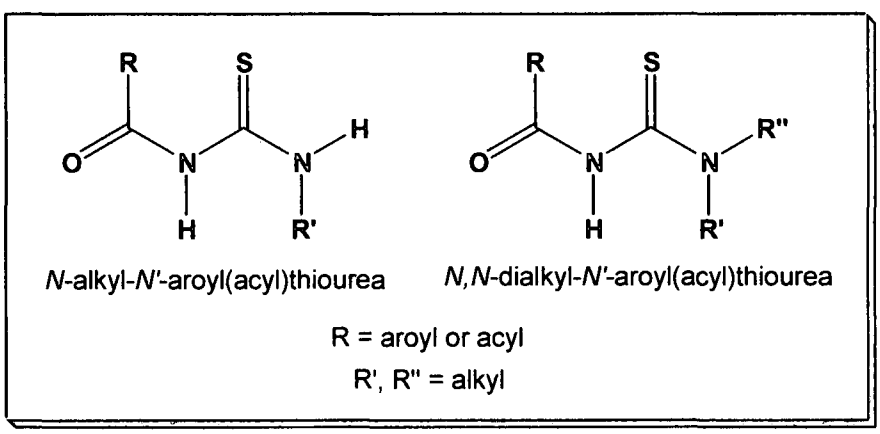

Figure 5. General structure of the *N*-alkyl and *N,N*-dialkyl-*N'*-aroyl(acyl)thiourea ligands.

These ligands have shown particular affinity towards the d^8 metal ions and the coordination to Pt(II), Pd(II), Rh(III) and Os(IV) have been thoroughly investigated and documented.[4-7]

The ligands, HL and H_2L, have been shown to coordinate to metal ions differently from one another.[7] This is due to an intramolecular hydrogen bond in H_2L (Figure 6). The crystal structure of H_2L shows this hydrogen bond to be between the thiourea –C(S)NHR moiety and the oxygen atom of the amidic group of H_2L resulting in a significant difference in conformation between these two ligands (H_2L and HL).[7] This hydrogen bond locks the C(O)NHC(S)NHR unit into a planar six-membered ring structure (Figure 6).

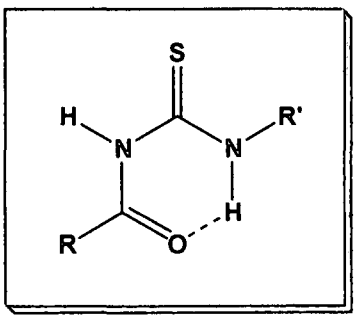

Figure 6. A schematic indicating hydrogen bonding in H_2L.

In the preparation of $[Pt(H_2L\text{-}\boldsymbol{S})_2X_2]^{\ddagger}$ (X = Cl^-, Br^-, and I^-) complexes[6] from the reaction of $[PtCl_4]^{2-}$ and H_2L it was found that when X was Cl^-, only the ***cis***-$[Pt(H_2L\text{-}\boldsymbol{S})_2X_2]$ complex was initially formed. However, when X = Br^- or I^-, mixtures of ***cis***- and ***trans***-$[Pt(H_2L\text{-}\boldsymbol{S})_2X_2]$ complexes are formed. When H_2L ligands are complexed with Pd(II), however, only mixtures of ***cis***- and ***trans***-$[Pd(H_2L\text{-}\boldsymbol{S})_2X_2]$ could be prepared, the *trans* isomer being dominant in all cases.[6]

The pure ***cis***-$[Pt(H_2L\text{-}\boldsymbol{S})_2Cl_2]$ complex undergoes spontaneous isomerisation in a variety of organic solvents. The equilibrium distribution of isomers at 25°C was also found to be directly dependant on the dipole moment of the solvent used for dissolution. K_e-values (K_e = [*trans*]/[*cis*]) ranged from 0.16 in nitromethane-d_3 to 0.88 in benzene-d_6.[7]

The intramolecular hydrogen bonding mentioned for H_2L is not evident in HL and therefore it assumes a twisted conformation with the sulphur and oxygen atoms pointing in approximately opposite directions. Ligands of the HL-type are relatively hydrophobic compounds with one dissociable proton on the amido – C(O)NHC(S) moiety (Figure 7).

‡ "(H_2L-***S***)" indicates a H_2L ligand bound to the metal atom only via the ***S*** atom.

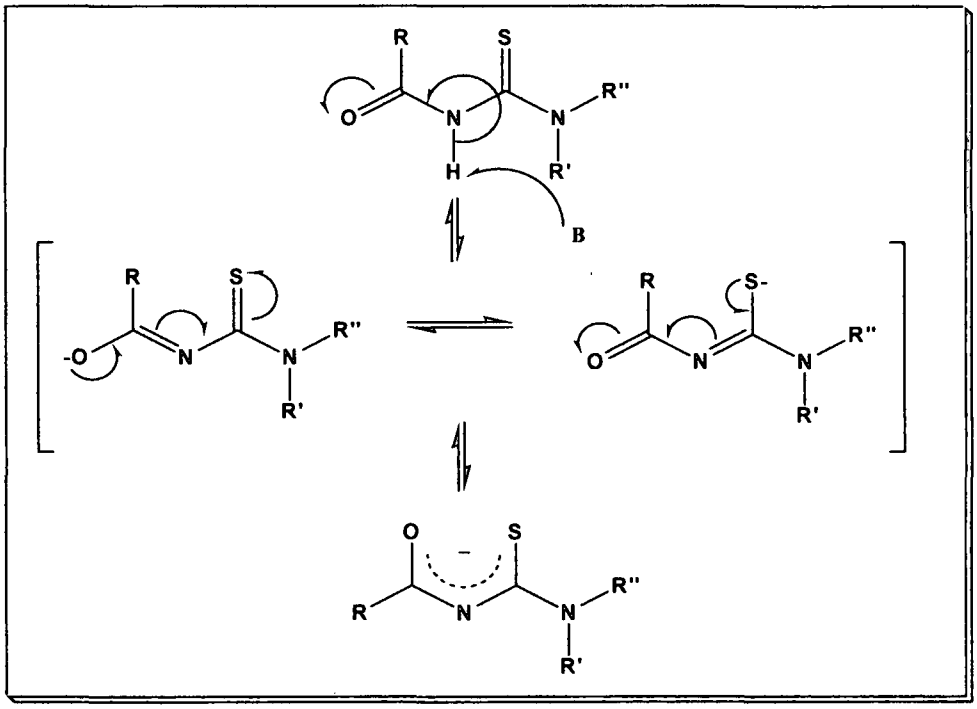

Figure 7. Schematic indicating the loss of the –NH proton, and appropriate resonance structures for *N,N*-dialkyl-*N'*-aroyl(acyl)thiourea.

Reactions between $[PtCl4]^{2-}$ or $[PdCl_4]^{2-}$ and HL, in the presence of a weak base, results in the formation of predominantly ***cis***-$[M(L\text{-}\boldsymbol{S,O})_2]$ complexes of Pt(II) (Figure 8) and Pd(II). Where "M" refers to the central metal atom and "***S,O***" refers to the coordinating atoms ***S*** and ***O***.

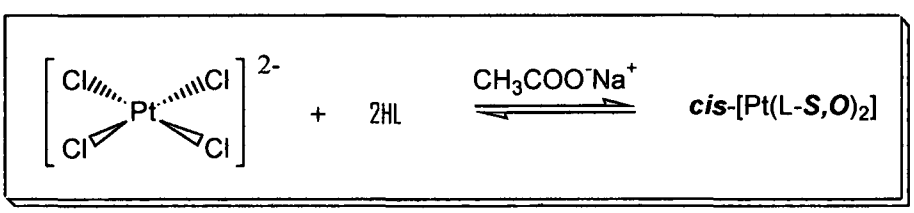

Figure 8. The reaction of $[PtCl_4]^{2-}$ and HL in the presence of base yielding ***cis***-$[Pt(L\text{-}\boldsymbol{S,O})_2]$.

Treatment of ***cis***-$[Pt(L\text{-}\boldsymbol{S,O})_2]$, in $CDCl_3$, with concentrated mineral acid HX (X = Br^- or I^-) led to the reversible protonation of the coordinated ligand.[8] These reactions with HX yielded mixtures of *cis*- and *trans*-$[Pt(HL\text{-}\boldsymbol{S})_2X_2]$ species as well as the partially ring-opened $[Pt(L\text{-}\boldsymbol{S,O})(HL\text{-}\boldsymbol{S})X]$ complex in solution.

When ***cis***-[Pt(L-***S,O***)$_2$] was treated with mixtures of HBr and HI it led to the formation of mixed halide species of ***cis***- and ***trans***-[Pt(HL-***S***)$_2$BrI] in addition to [Pt(HL-***S***)$_2$Br$_2$], [Pt(HL-***S***)$_2$I$_2$] as well as the partially ring-opened [Pt(L-***S,O***)(HL-***S***)X] complex.[8] Surprisingly, however, is the fact that on treatment of these solutions with aqueous base all the species present in solution reverted to the ***cis***-[Pt(L-***S,O***)$_2$] complex. This would imply that there must operate a rapid isomerisation mechanism on deprotonation and chelate ring-closure.

To date bis(*N,N*-dibutyl-*N'*-naphthoylthioureato)platinum(II) has been the only Pt(II) complex from ***S,O***-chelating ligands to form a mixture of ***cis***- and ***trans***-[Pt(L-***S,O***)$_2$] complexes.[5] The ***trans***-bis(*N,N*-dibutyl-*N'*-naphthoylthioureato)-platinum(II) complex is, at this stage, the only authenticated Pt(II) or Pd(II) example of such a *trans* complex, as by X-ray diffraction (Figure 9).

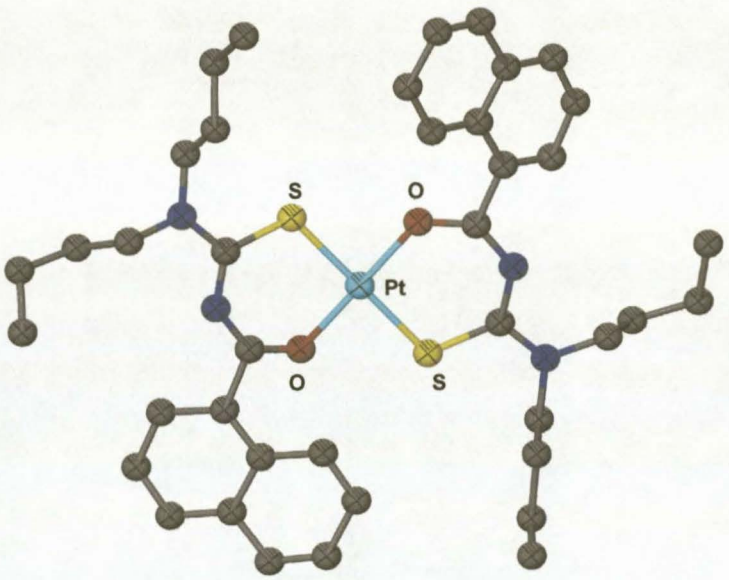

Figure 9. ***trans***-bis(*N,N*-dibutyl-*N'*-naphthoylthioureato)platinum(II).[5]

The ^{195}Pt shifts of these complexes were reported at –2708ppm (***cis***) and –3038ppm (***trans***) in $CDCl_3$ solution of the mixture of *cis* and *trans* complexes. In light of these results, it was speculated then that the *trans* complex might be obtained for bulky, electron-rich *N'*-aroylthiourea ligands because the electron-releasing aroyl groups might enhance the relative "softness" of the amidic oxygen donor atom, thereby stabilizing such a *trans* complex during synthesis.

1.2.2 Isomerisation of square-planar complexes of Pt(II) and Pd(II)

Square-planar geometry is common amongst complexes of d^8 2nd and 3rd row transition metals and geometric isomers are known for many derivatives. In these 4-coordinate complexes, geometric isomerisations have long been thought of as to take place *via* consecutive nucleophilic ligand substitution reactions.[9]

The majority of literature available on the *cis-trans* isomerisation of Pt(II) and Pd(II) specifically deals with square-planar complexes of metals with monodentate ligands and not with polydentate or bidentate ligands. Nevertheless, it is valuable to have a sound understanding of the basic principles involved, so that one can understand the possibly more complicated isomerisation involved in the $[M(L\text{-}\boldsymbol{S,O})_2]$ type complexes, with chelating bidentate ligands, as studied in this work.

Square-planar complexes of the d^8 metal ions Rh^{I}, Ir^{I}, Pd^{II}, Pt^{II}, and Au^{III} are all well known. Studies concerning geometric isomers or isomerisations have, however, been limited to platinum(II) and palladium(II). This is possibly due to the ease of preparation of the electronically neutral $[MX_2L_2]$, $[MXYL_2]$ and $[MX_2LL']$ (X and Y are ionic and L and L' are neutral ligands) of platinum(II) and palladium(II). For the platinum(II) and palladium(II) complexes $[MX_2L_2]$, it is generally thought that the *cis*-isomers are enthalpy favoured whereas the trans isomers appear to be entropy favoured (Figure 10).[11a]

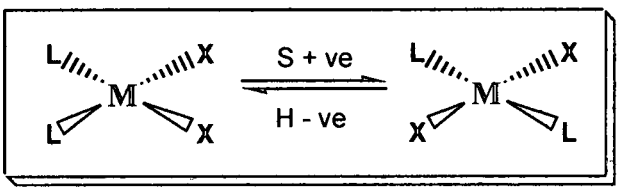

Figure 10. Enthaply and entropy considerations in the isomerisation of ***cis-*** and ***trans-*** $[MX_2L_2]$.[11a]

The position of the *cis-trans* equilibrium can be substantially affected by changes of the central metal atom, solvent of dissolution or temperature. It is

also apparent from literature that the *trans*-geometry is more favoured in palladium complexes as compared to the corresponding platinum complexes.[12] A marked solvent dependence was observed in a study of $[PdCl_2(PMePh_2)_2]$ and $[PdCl_2(PMe_2Ph)_2]$ in eleven solvents.[13] This was also reported for the complex *cis*-$[Pt(H_2L\text{-}S)_2Cl_2]$.[6] *Cis*-isomers of these complexes are strongly favoured by more polar solvents.

Although the distinction is often difficult to make, isomerisation reactions can be classified and treated as either catalysed or spontaneous. For example, both *cis*- and *trans*-$[PtCl_2(PEt_3)_2]$ are reported to remain unchanged in benzene at ambient temperature unless a trace amount of free phosphine is added. This then catalyses a rapid isomerisation to the equilibrium mixture. However, the palladium complex *cis*-$[PdCl_2(Sb^nPr_3)_2]$ rapidly and spontaneously isomerises to yield a mixture upon dissolution.[11]

As has been reported by Koch *et al.*[7], the complexes ***cis***-$[Pt(L\text{-}\boldsymbol{S,O})_2]$ and ***cis***-$[Pd(L\text{-}\boldsymbol{S,O})_2]$ are also relatively easy to prepare in a two-step, one-pot synthesis. It was found that the rates of isomerisation from ***cis***-$[M(L\text{-}\boldsymbol{S,O})_2]$ to ***trans***-$[M(L\text{-}\boldsymbol{S,O})_2]$ are such that it can conveniently be followed by means of RP-HPLC.[10]

1.2.2.1 Catalysed isomerisation reactions of square-planar complexes

A. The consecutive displacement mechanism

The mechanism of *cis-trans* isomerism which is best understood and supported by experimental data is shown in Figure 12. This is an associative mechanism involving only stereospecific ligand substitution steps. The *trans*-ligand, T, and *cis*-ligand, C, retain their relationship towards X. The reaction proceeds through a trigonal-bypiramidal intermediate (**B**) with T, X and the incoming ligand Y in the trigonal plane.[9] This is achieved through the trans-effect of T, which either weakens the bond M-X (a *trans*-influence) or stabilises the trigonal-bypiramidal intermediate by π-acceptor properties or both.

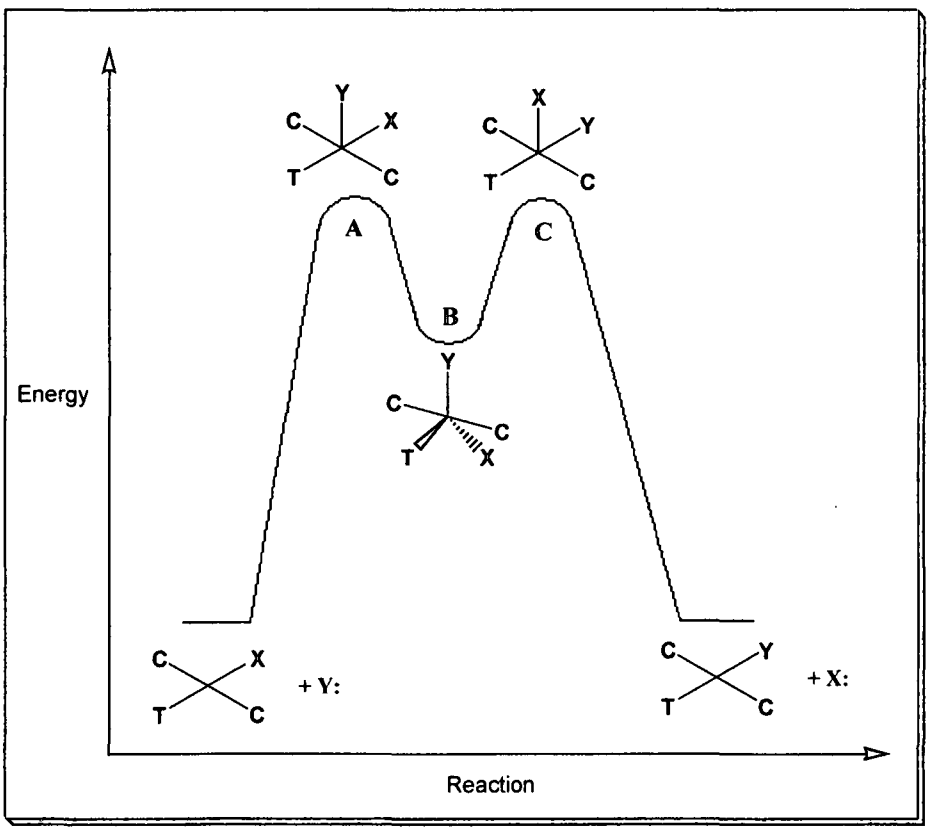

Figure 12. A reaction profile for the displacement of X by nucleophile Y.[11a]

The experimental kinetic rate law follows a two-term rate law, where k_2 relates to the direct associative attack of nucleophile Y, and k_1 applies to a solvent

association route, where X is displaced by solvent, which is then replaced by Y.[11a]

$$rate = (k_1 + k_2[Y])[MXTL_2]$$

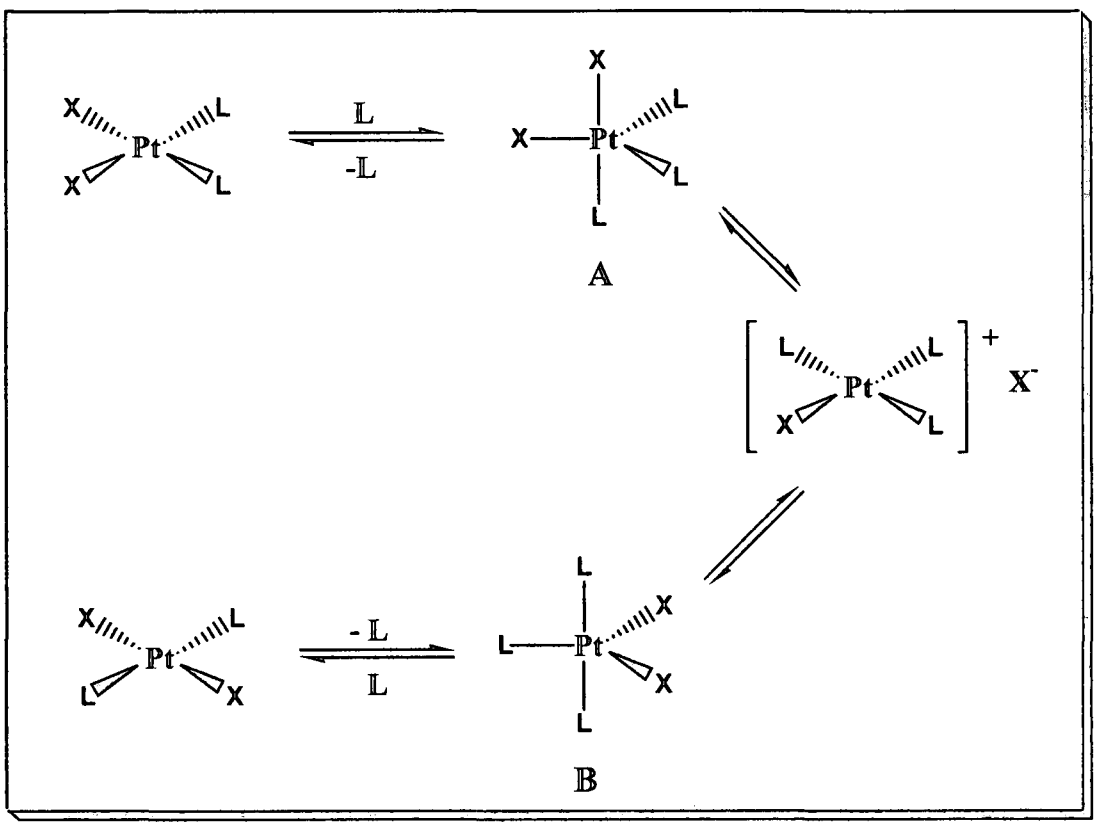

Figure 13. A schematic of the consecutive displacement mechanism.[11a]

The consecutive displacement mechanism shown in Figure 13 postulates that two-steps are needed to obtain isomerisation, as the substitutions at platinum are stereospecific. In the first step L (any neutral ligand) replaces a halide to form $[PtXL_3]^+X^-$. The second step involves attack of X^- on $[PtXL_3]^+$ again and, if it results in intermediate **A**, the original *cis*-isomer will be reformed but, if it proceeds through intermediate **B**, the *trans*-isomer is formed.[11a] It is also known[9, 15] that for $[PdX_2(am)_2]$, where X^- (N_3^-, Br^-, I^- or NCS^-) and (am) (NH_3 or py), the rate of the reaction increases when the dielectric constant of the solvent is increased, thus assisting in the formation of the postulated ionic intermediate.

B. The pseudorotation mechanism

The 5-coordinate intermediates **A** and **B** in Figure 13 may be interconverted via the ionic species $[PtXL_3]^+X^-$. **A** could, however, have been converted directly to **B** through a pseudorotation mechanism, should such a process be faster than either or both the steps linking **A** and **B** with the ionic intermediate.

Pseudorotation is a low-energy process possible in 5-coordinate main group element compounds.[11b] The problem in applying it to square planar complexes, however, is that geometry change of the intermediate would argue against the stereospecific nature of substitution reactions of square-planar complexes.[9] When added amounts of polar solvent slow the isomerisation reaction, it is often interpreted as evidence against the formation of an ionic intermediate.[16]

Louw[17] has probably presented the strongest support for a mechanism involving the 5-coordinate. He studied the isomerism of $[PtX_2L_2]$ (X^- is a halide, L is PEt_3 or PMe_2Ph) which is catalysed by either X^- or L, which suggests the following scheme (Figure 14) for isomerisation.

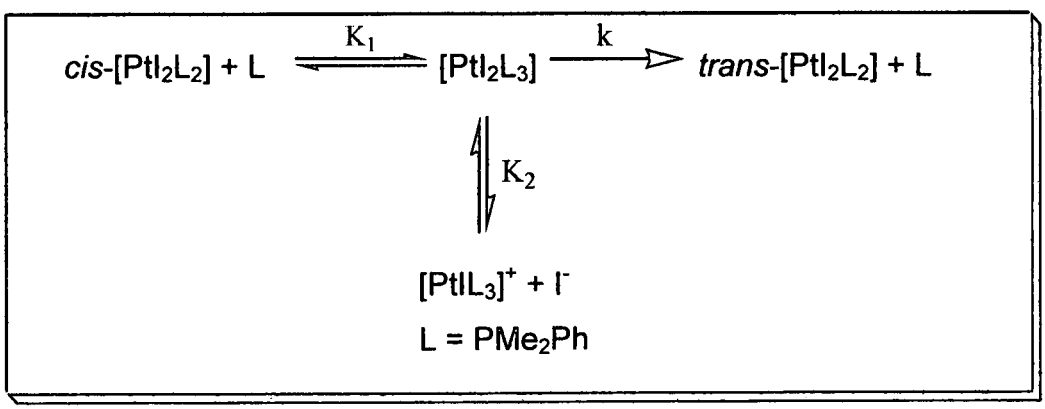

Figure 14. Proposed mechanism for the isomerisation of $[PtX_2L_2]$.[17]

In this study it was concluded that no isomerisation results from 4-coordinate ionic species; $[PdCl_2(PMePh)_3]$ was isolated and structurally characterised. Louw also points out that most studies of substitution reactions of square-

planar phosphine complexes where done in polar solvents, in which such 5-coordinate species would have a very sort lifetime. Pseudorotation might occur if such species had an appreciable lifetime, and such compounds are indeed attainable. Several phosphine halide complexes of platinum(II) and palladium(II), of the type $[MX_2L_3]$, have subsequently been described.[18] The geometries of those elucidated were close to either square-pyramidal or trigonal-bipyramidal.

These two mechanisms (consecutive displacement and pseudorotation) may best be viewed as two extreme situations of a single process. Polar solvents favour ionic intermediates and non-polar solvents lead to the formation of 5-coordinate intermediates. The energy difference between these two situations might be small; therefore it is not always possible to tell which, if indeed only one mechanism, might actually operate. Figure 15 effectively summarises the situation graphically.[11a]

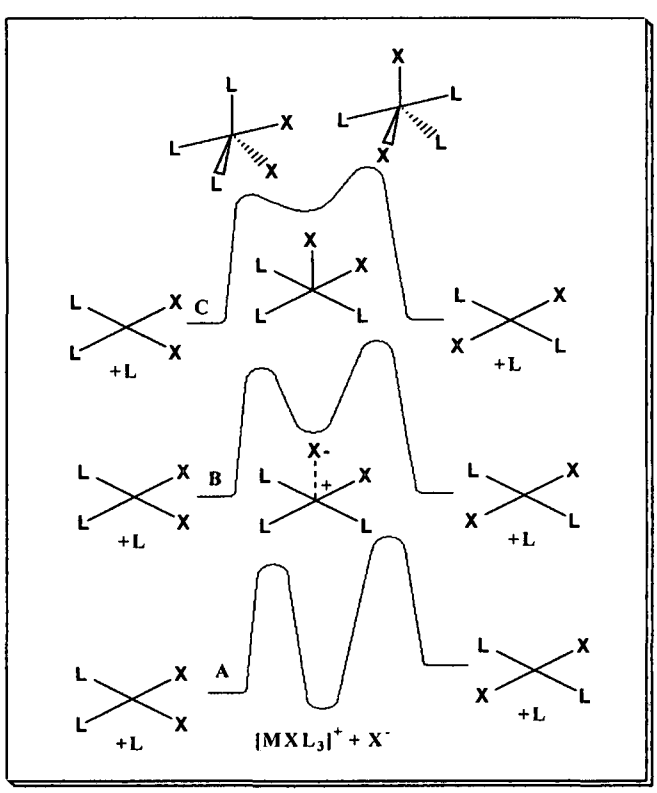

Figure 15. Reaction profiles for the L-catalysed isomerisation of $[MX_2L_2]$. A (consecutive displacement): polar solvent favouring an ionic intermediate, B: solvent of intermediate polarity, allowing ion-pair formation, C (pseudorotation): non-polar solvent, formation of 5-coordinate intermediate.

1.2.2.2 Spontaneous (uncatalysed) isomerisation reactions of square-planar complexes

These types of isomerisation reactions can be divided into three groups[10]:

1. Those that are actually catalysed, but for which the catalyst has not as yet been identified.
2. Isomerisation by means of a straightforward change in geometry.
3. Reactions where loss of a ligand forms a 3-coordinate system, with subsequent rearrangement.

A. Solvent catalysed and auto-catalysed reactions

Although not proven, it is possible according to literature that all the spontaneous isomerisations of palladium compounds, $[PdX_2L_2]$, could proceed *via* a 5-coordinate solvento species, $[PdX_2SL_2]$. As stated previously, a study done on $[PdCl_2L_2]$ (L = PMe_2Ph or $PMePh_2$) by NMR spectroscopy found a clear solvent dependence on the isomerisation process.[13] The solvents ranged from benzene and various chlorocarbons to acetone and nitrobenzene, and it seems quite possible that all these solvents can act in the same way as pyridine or DMSO by isomerisation through association. Such reactions are termed solvent-association catalysed isomerisations. When association of a solvent molecule results in the elimination of a ligand such as a tertiary phosphine, and that phosphine ligand catalyses an isomerisation process, this is termed autocatalysis.

B. Direct geometry change

Photochemical excitation of square-planar complexes could lead to *cis-trans* isomerisation via a pseudo-tetrahedral geometry of the excited state.[19] One process which appears to be a truly intramolecular process is the *cis-trans* isomerisation of the *N,O*-chelated bis(glycinato)platinum(II) complex.[19]

C. The dissociation mechanism

Because reactions of square-planar complexes have always been thought of as associative, this concept seems quite radical. However, like with consecutive displacement vs. pseudorotation, similar kinetic data have been used to argue for and against a dissociative pathway.

1.2.2.3 Conclusion

It is clear from literature that the field of *cis-trans* isomerisation of square-planar metal complexes is a vast and complicated one, and that there is much that still needs to be understood. Proposed mechanisms are as diverse as associative and dissociative.

Isomerisation reactions can generally be described as either catalysed isomerisations or spontaneous (uncatalysed) isomerisations. With the catalysed consecutive displacement mechanism the reaction proceeds *via* a 5-coordinate trigonal-bypiramidal intermediate or an ionic intermediate species. Pseudorotation isomerisation reactions takes place *via* a 5-coordinate intermediate species where such a 5-coordinate species has an appreciable lifetime, often in non-polar solvents.

Spontaneous isomerisation reactions can be solvent catalysed or auto-catalysed. Auto-catalysed reactions occur when a solvent molecule eliminates a ligand which then acts as a catalyst for the isomerisation process. Photochemical isomerisation reactions could occur when a square-planar molecule is excited to a pseudo-tetrahedral geometry, as in the work of Scandola *et al.*[19] As with solvent effects, the effect of visible light is often overlooked.

1.2.3 The theory of excited states and general photochemistry associated with platinum(II)

The photochemistry of platinum(II) has been a very active field of research in the middle to late 60's and throughout the 70's, with the main reactions observed and studied being substitution and *cis-trans* geometric isomerisation.[20] Haake and Hylton[21], for instance, studied the irradiation of the isomers of $[Pt(PEt_3)_2Cl_2]$ at wavelengths longer than 304nm, which presumably gave rise to ligand field transitions resulting in *cis-trans* isomerisation. When unfiltered light was used, decomposition occurred.

Further studies on the isomers of $[Pt(PEt_3)_2Cl_2]$ were done by Mastin[20] using chloroform as solvent at wavelengths longer than 300nm. Two possible isomerisation pathways were hypothesised. The first involved a triplet state with tetrahedral geometry.[9, 21] The other was analogous to the mechanism proposed for thermal catalysed isomerisation, but was thought to involve a trigonal bipyramid containing a solvent molecule.

A "primary process" was defined by Porter *et al.*[21] as: "Any continuous sequence of one or more primary steps which starts with a light absorption step". Here "primary step" refers to "any one of the elementary transformations of an excited state molecule of the species that absorbs light"; the absorption step being the first primary step. Primary processes can be seen to include absorption, dissociative reactions, intramolecular "twisting" isomerisations, intermolecular energy transfer, intermolecular electron transfer and luminescence.

Photoexcitation, obviously, is an important step in all primary photochemical processes. From a well-assigned electronic absorption spectrum one can get some knowledge concerning the types of states that can be produced by photoexcitation. These assignments can be extremely complex, but electronic absorption spectra of basic metal carbonyls have been successfully

interpreted with MO-theory[22], leading to the formation of the following frontier orbitals (Figure 16).

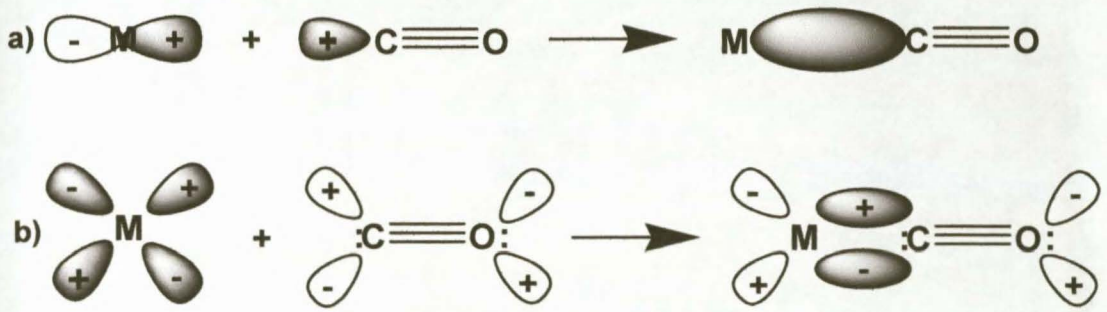

Figure 16. The MO-orbitals of the bonding interactions of MCO. a) Formation of the M-CO σ-bond. b) Formation of the M-CO π-bond.[22]

Three important categories of electronic transitions can be identified:

1. Electronic transitions referred to as *d,d*-transitions, which are between the MO's of predominantly *d*-orbital character (**blue**).
2. Transitions between MO's which are mainly ligand orbitals. These are referred to as internal ligand or ligand localised transitions (**black**).
3. Cross transitions are those that occur from a "metal-type" MO to a "ligand-type" MO (**red**) or *vise versa* (**green**). These are referred to as metal-to-ligand charge transfer (MLCT) or ligand-to-metal charge transfer (LMCT), respectively.

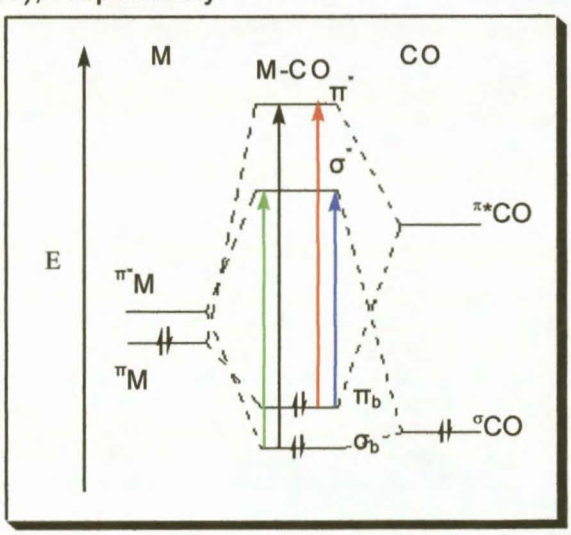

Figure 17. A MO diagram of MCO indicating the three important categories of electronic transitions.[22]

Other electronic transitions that could occur are: charge transfer to solvent (CTTS), interligand transmetallic charge transfer (ITCT), transitions between metal-metal bonds and intervalence transfer (IT).

An organo-transition metal compound can have a variety of orbitally different excited states compressed into a narrow energy range. These bands, however, have distinguishing characteristics that are affected by changes in either the molecule itself or its environment, thereby assisting in making the assignments. Some of the more important characteristics of the different types of electronic transitions are discussed below[22]:

Ligand Field Absorptions (*d*,*d*-transitions):

These absorptions are usually weak because they are overlap forbidden and in centrosymmetric complexes also Laporte forbidden. Intensities could be greater if there is mixing of ligand and metal orbitals or of *d*- and *p*-metal orbitals. If there is mixing of weakly allowed ligand field excited states with energetically close lying electronically allowed states, this could lead to intensity enhancement in ligand field transitions. If the ligand is a π-acceptor, such an electronic transition will lead to weakening, and subsequent lengthening, of the M-L bond. This occurs because an electron is promoted from a π-bonding to a σ-antibonding orbital.

Intra-ligand Absoprtions:

Intra-ligand transitions (between MO's having major contributions from ligand orbitals) of free ligands are slightly perturbed when complexed to a transition metal. Comparing the spectrum of the free ligand with that of the complex can therefore easily identify bands originating from intra-ligand transitions. However, it could be difficult to distinguish between intra-ligand bands and charge-transfer bands because both

are strongly allowed and therefore have maximum extinction coefficients of the same order of magnitude. By comparison with charge-transfer bands, inter-ligand bands are relatively insensitive to the oxidation state of the central metal atom, thereby allowing for assignment.

Charge Transfer Absorptions:

Because features of these spectral absorptions are so diverse, few general statements can be made concerning absorption bands of this type. One aspect by which charge-transfer bands can be identified is their dependence on solvent polarity (more so than for intra-ligand or ligand field bands). With increasing solvent polarity these bands can shift to higher or lower energies, but sometimes not at all. This effect is brought about by the different degrees to which solvent molecules stabilise the ground and excited states involved in such transition respectively.

The variety of orbitally different excited states possessed by these systems lead to different types of decay processes. Certain reactivity tendencies are associated with each type of excited state; for example, from ligand field excited states we expect ligand substitution because the M-L bond is weakened. Intramolecular redox processes are thought to arise from charge-transfer excited states and ligand rearrangements from inter-ligand transitions. There have been attempts to formulate models to predict the reactions leading from specific excited states. The models proposed by Zink[23] and Wrighton *et al.*[23] still have some deficiencies and need further development to be truly predictive.

Some photo-processes have quantum yields that are dependant on the wavelength of the exciting light. Such processes are referred to as "wavelength-dependant phenomena" or "wavelength effects".[22] From studies on the photochemical properties of organic compounds, it is evident that in

these systems chemical reactions (and luminescence), having high efficiency (high quantum yield), originate from the lowest excited electronic levels.

This behaviour can be explained as follows: Electronic transitions in a typical aromatic hydrocarbon are usually within the singlet manifold ($S_0 \rightarrow S_1$, n = 1, 2, 3...). The small oscillator strength of the singlet to triplet transitions prevents production of triplet excited states. S_1 will eventually be the only excited singlet state because of internal conversion as well as vibrational relaxation. Internal conversion between S_1 and S_0 is relatively slow, therefore other deactivating processes occur. Because of this, the only states that show any behaviour (other than internal conversion) are S_1 and T_1; therefore wavelength effects are not often come across in the photochemistry of organic molecules. Complexes with transition metals are different though in that they do show wavelength dependence, the reason being the possible existence of more than one reactive state.

Two of the best-described photochemical primary processes are ligand photo-substitution in solutions and geometrical photo-isomerisations. The latter shall be discussed.

Photochemically Induced Geometrical Isomerisation:

Photochemically induced isomerisations can be categorised into either intra- or intermolecular mechanisms.[22] Intramolecular reactions are subdivided into those operating via a "twisting" mechanism or those operating via bond breaking. In the latter case one ligand is partially dissociated for a while; in the former no bond breaking is involved.

Intermolecular photo-induced isomerisations, like photo-induced substitutions may involve association or dissociation of a ligand (Figure 18).

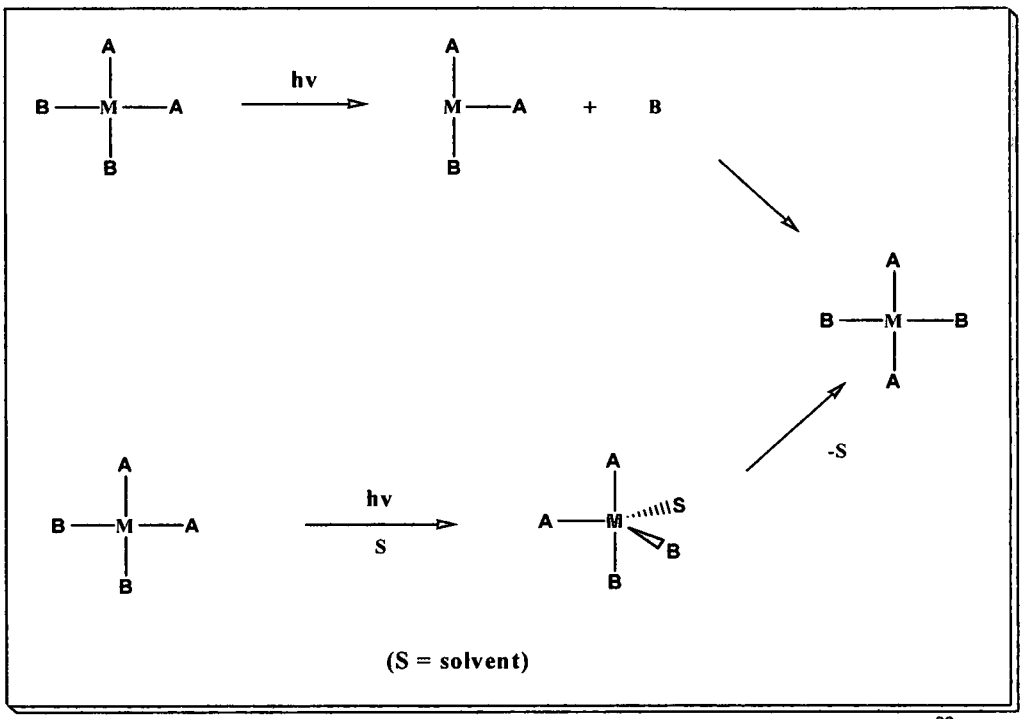

Figure 18. Schematic indicating two pathways for photo-induced isomerisations.[22]

Intramolecular "twisting" or pseudorotation mechanisms possibly involve the decay of a ligand field excited state complex. These excited state complexes are expected to show geometrical distortions and are therefore suspected as precursors in these reactions. In the study by Scandola *et al.*[19] it was shown that the isomerisation of *cis*-bis(glycinato)platinum(II) to *trans*-bis(glycinato)platinum(II) occurred with such a "twisting" mechanism facilitated by the pseudo-tetrahedral geometry of the thermally relaxed excited state.

For the six-coordinate, monodentate complex of ruthenium(II) a photo-induced *cis-trans* isomerisation with a thermal *trans-cis* isomerisation has been observed (Figure 19).[24]

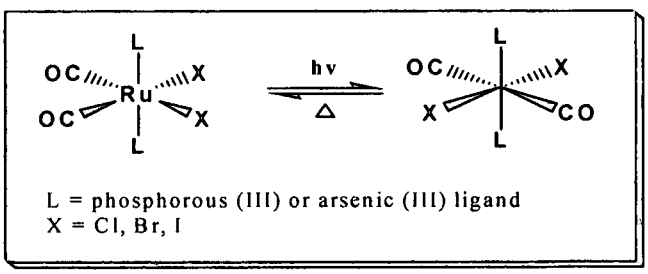

Figure 19. The isomerisation of $[Ru(CO)_2L_2X_2]$.[24]

1.3 High Performance Liquid Chromatography: A tool for the separation of *cis*-[M(L-*S*,*O*)$_2$] and *trans*-[M(L-*S*,*O*)$_2$]

Different chromatographic techniques can all be said to have one thing in common. Two immiscible phases are brought together, the one being stationary the other mobile. A sample is introduced into the system via the mobile phase and interacts with the stationary phase in the column. Figure 20 indicates how chromatography is divided into different sub-sections.

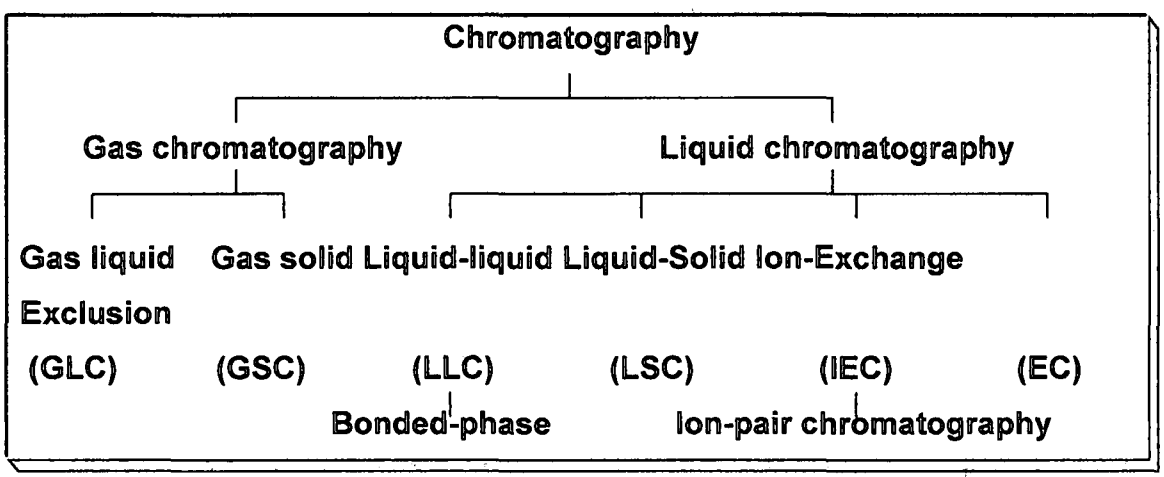

Figure 20. The different divisions of chromatography.[25]

Gas chromatography can only analyse about 20% of all known compounds. This is because the remaining 80% of compounds are not sufficiently volatile or because they are thermally unstable and decompose during separation. By using the theories associated with liquid chromatography (LC) and the instrumentation developed for gas chromatography (GC), a new technique was developed in the late 1960's. High performance liquid chromatography (HPLC) is not limited in this sense and can analyse anything from macromolecules and ionic species to high-molecular-weight polyfunctional groups.

In high-performance liquid chromatography, separation is achieved after the sample has undergone repeated interactions between the mobile phase and the stationary phase (in contrast with GC). At the end of the separation

process bands emerge in the order of increasing affinity towards the stationary phase relative to the mobile phase. One can say that the separation reflects the relative attraction and repulsion that molecules of the two phases show for the solute molecules.

An HPLC system consists of the following major components: a solvent reservoir for the mobile phase, a pulse-free pump system, a sampling valve, the column, a detector and a data handling device to view the output (Figure 21). Each of the devices will be discussed briefly.

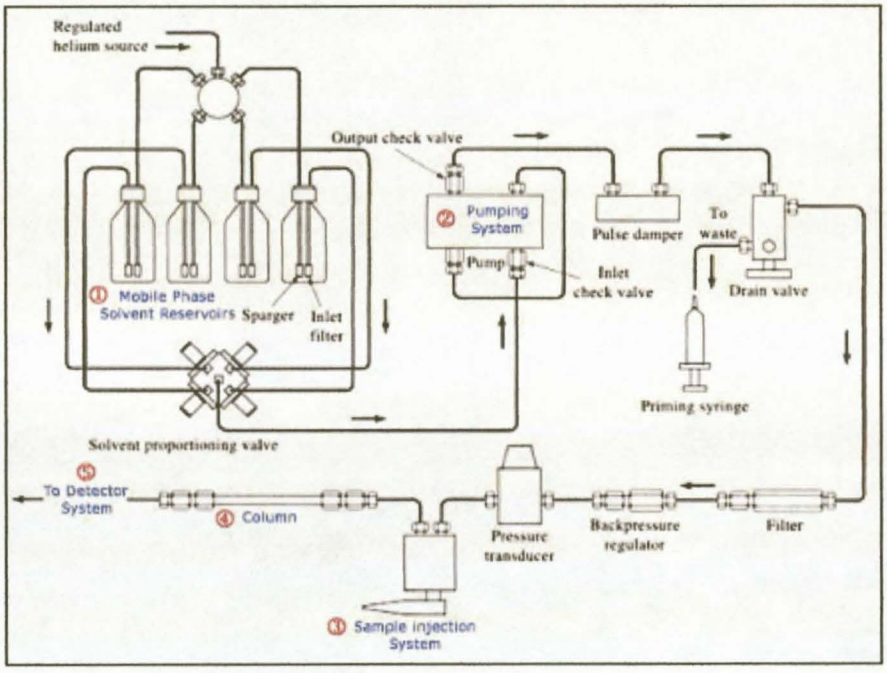

Figure 21. A detailed schematic of a HPLC system.[26]

Mobile phase delivery system:

The pump should be able to deliver the mobile phase to the column at a wide variety of flow rates and pressures. It should also be able to switch between mobile phases with relative ease for gradient elution. The system should obviously also be pulse-free, this is either attained by constant-pressure pumps or pulse dampeners. Because a wide variety of solvents can be used, the pumps, seals and connections

should all have a high level of chemical resistance. Solvents must be pure and degassed.

Sample injection system:

The injection system itself should have no void volume and should be as close as possible to the column. Sample loops, as illustrated in Figure 22, are the most widely used. These inject the sample into the mobile phase stream by simple rotation of the valve. The loop volume is usually between 10 μL and 20μL.

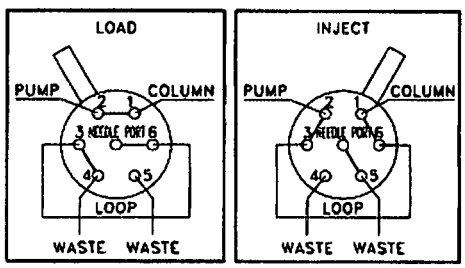

Figure 22. A typical sample injection system.

Column:

Straight stainless-steel columns, in the vertical position, are mainly used. The columns are usually constructed of heavy-wall, glass-lined metal tubing or stainless steel tubing designed to withstand the necessary high-pressures. Column fittings and connections are designed with no void volume. Columns range from 10 to 30cm, fast columns from 3 to 8cm and columns for size-exclusion chromatography from 50 to 100cm.

Detector:

A sensitive universal detector (like FID for GC) has still to be devised for HPLC. Therefore, at this stage, a detector has to be selected with a specific problem in mind. Optical detectors based on ultraviolet-visible absorption are currently the workhorse in HPLC detection. These are a 1000 times more sensitive than a refractive index detector, if not as versatile. UV-VIS detectors are also not sensitive to changes in mobile phase or temperature. Fixed-, variable- and scanning wavelength

detectors are available, the choice being dependant on the problem at hand and the capital available. Fluorescence and electrochemical detectors can also be employed.

1.4 Objectives of the study: A problem statement

The *N,N*-diakyl-*N'*aroyl(acyl)thiourea ligands (HL), in basic solution, react with the $[PtCl_4]^{2-}$ anion to form, quantitatively, the relevant ***cis***-[Pt(L-***S,O***)$_2$] complexes. An extensive series of HL ligands have been prepared within our group with variation of both the R-group on the carbonyl moiety and the R'-groups on the C(S)N- moiety (Figure 5). Except for one, all the complexes previously synthesised have been of the ***cis***-[Pt(L-***S,O***)$_2$] type. Koch *et al.* produced the first, and only, crystal structure of a ***trans***-[Pt(L-***S,O***)$_2$] complex, in the form of ***trans***-bis(*N,N*-dibutyl-*N'*-naphthoylthioureato)platinum(II).[5]

Given the fact that only one authentic ***trans***-[Pt(L-***S,O***)$_2$] complex exists amongst the many *cis* complexes in the Cambridge Structural Database (CSD)$^{\Psi}$, the question arises why these *trans* complexes are so rare.

In striving to elucidate the above question the objectives of this study are:

- to examine whether the method of complex synthesis could be altered in such a way as to yield a *trans* complex.
- to examine whether functional groups on the ligand have an effect on the *cis-trans* isomer distribution.
- to examine, within the selected group of ligands, if the metal centre has an effect on the *cis-trans* isomer distribution.
- to examine whether the solvents used during synthesis have an effect on the *cis-trans* isomer distribution.
- to examine other possible factors which might have an influence on the formation of a *trans* complex.

Ψ The Cambridge Structural Database: a quarter of a million structures and rising, *Acta Crystallogr.*, 2002, **B58**, 380-388.

Chapter 2:

Experimental Approach: Synthesis and Characterisation of Ligands and Complexes

2. Experimental Approach

2.1 Synthesis and characterisation of the *N,N*-dialkyl-*N'*-aroylthiourea ligands

The factors that we thought played a major role in the possible formation of both ***cis***-bis(*N,N*-dialkyl-*N'*-aroyl(acyl)thioureato)platinum(II) and ***trans***-bis(*N,N*-dialkyl-*N'*-aroyl(acyl)thioureato)platinum(II), in the crude product mixture, determined the choice of ligands synthesised. The ligands were synthesised according to the method described by Douglas and Dains.[27]

Each of these ligands would specifically address one of the factors that we thought could possibly lead to the presence of a ***trans***-[Pt(L-***S,O***)$_2$] complex as part of the product mixture after complexation with the specific platinum- or palladium-salt.

Table 1. A table of the ligands synthesised with their abbreviation and structure, HL^x (x = 1-7).

Name and Abbreviation	Structure	Name and Abbreviation	Structure
N,N-diethyl-*N'*-naphtoylthiourea HL^1	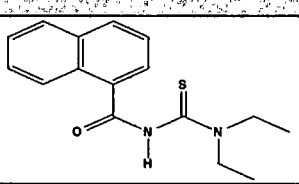	*N,N*-diethyl-*N'*-4-monomethoxy-benzoylthiourea HL^5	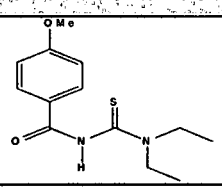
N,N-dibutyl-*N'*-naphtoylthiourea HL^2	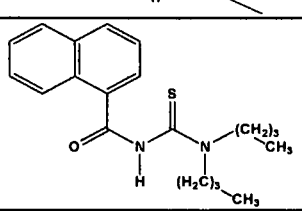	*N,N*-diethyl-*N'*-camphanoyl-thiourea HL^6	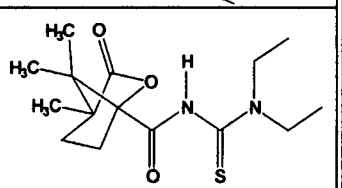
N,N-diethyl-*N'*-3,4,5-trimethoxy-benzoylthiourea HL^3	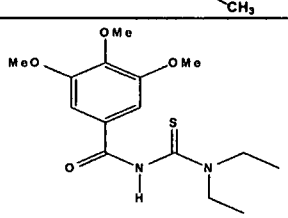	*N,N*-diethyl-*N'*-benzoylthiourea HL^7	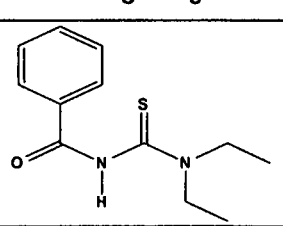
N,N-diethyl-*N'*-3,5-dimethoxy-benzoylthiourea HL^4	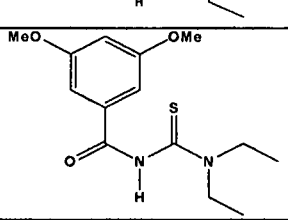		

N,N-diethyl-*N'*-benzoylthiourea (HL^7) was used as the first ligand to complex with platinum(II), as its coordination chemistry with Pt(II) is well-known and reported.[7] *N,N*-dibutyl-*N'*-naphthoylthiourea (HL^2) has been shown to complex with $PtCl_4^{2-}$ to afford a mixture of ***cis***- and ***trans***-[$Pt(L^2$-***S,O***$)_2$] and was therefore a obvious choice as an important ligand to be investigated.[5] It's *N,N*-diethyl derivative (HL^1) was synthesised to determine any possible changes to the product mixture in going from dibutyl to diethyl upon complexation with $PtCl_4^{2-}$. Along with *N,N*-diethyl-*N'*-camphanoylthiourea (HL^6), these two ligands (HL^1 and HL^2) were used to look at the effect that bulky substituents on the -C(O) moiety would have on the *cis-trans* distribution of the crude product mixture after complexation.

N,N-diethyl-*N'*-3,4,5-trimethoxybenzoylthiourea (HL^3), *N,N*-diethyl-*N'*-3,5-dimethoxybenzoylthiourea (HL^4) and *N,N*-diethyl-*N'*-4-monomethoxybenzoyl-thiourea (HL^5) were all synthesised with the aim of possibly giving us further insight into the effect (on the resultant products) of the addition of electron donating groups to the benzoyl moiety.

2.1.1 Results and discussion

The ligands synthesised produced no complications concerning either their purity or their stability. Percentage yields were all in the order of 75% and more. The ligands were all soluble in deuterated chloroform for the purposes of ^1H and ^{13}C NMR.

2.2 Synthesis and characterisation of the *cis*-bis(*N,N*-dialkyl-*N'*-aroylthioureato)platinum(II) complexes

The two-step, one-pot synthesis of the basic *cis*-coordinated, bis-chelated *N,N*-dialkyl-*N'*-aroyl(acyl)thiourea platinum(II) complexes are both well-known and well documented.[7] The potentially fluorescent *N,N*-dibutyl-*N'*-naphtoylthiourea has been shown to form a mixture of *cis* (85%) and *trans*

(15%) complexes of which the *trans* complex were isolated and characterised by means of X-ray crystallography.[5] At the time it was speculated that a possible steric effect, operating in the transition state during synthesis of these molecules, was playing a significant role in formation of the final product mixture. To test this idea, a number of synthetic methods and different ligands were tested to establish if it is possible to prepare at least some *trans*-Pt(II) complexes.

The formation of ***trans***-bis(*N,N*-dibutyl-*N'*-naphthoylthioureato)platinum(II) was attributed to the relatively large naphthoyl moieties on the ligand leading to steric hindrance in the transition state of the reaction reported by Koch *et al.*[5] Therefore, the change of the two butyl groups to two ethyl groups should not, according to that theory, significantly affect the *cis-trans* ratio of the product mixture. Aside from this slight change in the structure of the ligand, the only change to the synthetic route was that a mixture of acetonitrile and water was used where Koch *et al.* synthesised the complex using a mixture of dioxane and water. This change, as the change to the ligand, was not considered to affect the steric hindrance argument.

For differing reasons a photochemical and thermal isomerisation pathways were excluded as possible isomerisation mechanisms at the time.

2.2.1 *cis*-bis(*N,N*-diethyl-*N'*-naphthoylthioureato)platinum(II); *cis*-[Pt(L^1-*S,O*)$_2$]

cis-bis(*N,N*-diethyl-*N'*-naphthoylthioureato)platinum(II) was prepared according to the method followed by Koch *et al.*[5] This basic method of synthesis was followed for all the complexes, except where changes were made to investigate those specific factors on the crude product mixture. The complex was analysed by means of NMR (^{1}H, ^{13}C and ^{195}Pt), elemental analysis and a melting point determination (see section 2.5).

Interpretation of resultant ^{1}H and ^{13}C NMR spectra of the crude [Pt(L^{1}-***S,O***)$_2$] product revealed that a second, similar species was present in the mixture (Figure 23).

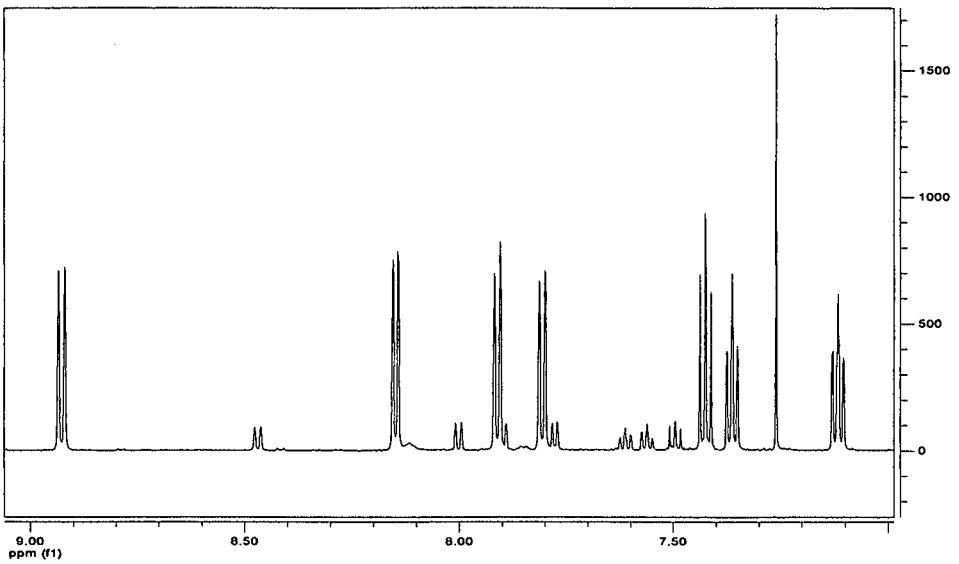

Figure 23. The aromatic region of the ^{1}H spectrum of [Pt(L^{1}-***S,O***)$_2$].

When one compares this to the two spectra[5] obtained for ***cis***- and ***trans***-crystals of bis(*N,N*-dibutyl-*N'*-naphthoylthioureato)platinum(II) it seems as though the second species present in both the ^{1}H and ^{13}C NMR spectra might well be ***trans***-[Pt(L^{1}-***S,O***)$_2$]. However, a thin layer chromatogram of product mixture confirmed that some unreacted ligand was present. The chemical shifts of the second species in the complex spectra also correlated well with those of pure *N,N*-diethyl-*N'*-naphthoylthiourea (Figure 24).

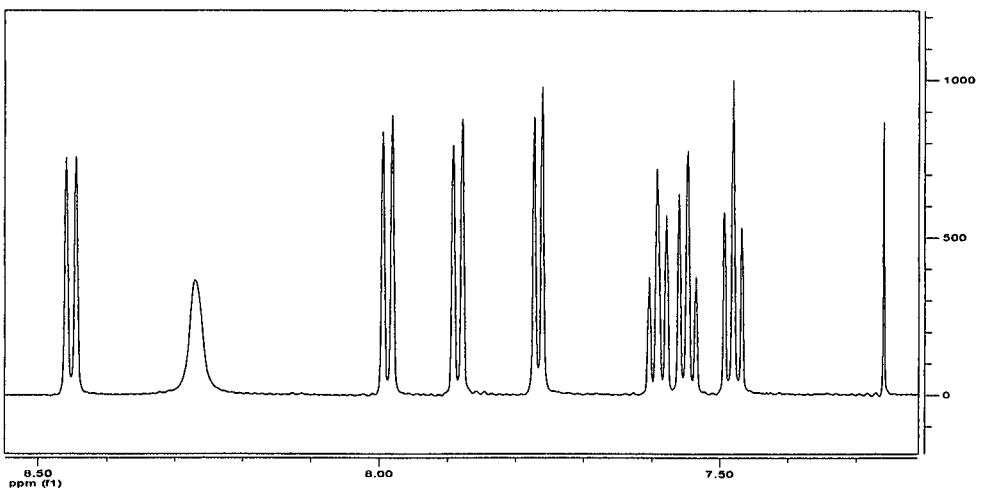

Figure 24. The aromatic region of the ^{1}H spectrum of *N,N*-diethyl-*N'*-naphthoylthiourea.

Also, thorough scrutiny of the ^{195}Pt spectra (window -1900 ppm to -3500 ppm) of the product revealed only one peak, corresponding to ***cis***-bis(*N*,*N*-diethyl-*N'*-naphthoylthioureato)platinum(II) at -2696.5 ppm (Figure 25).

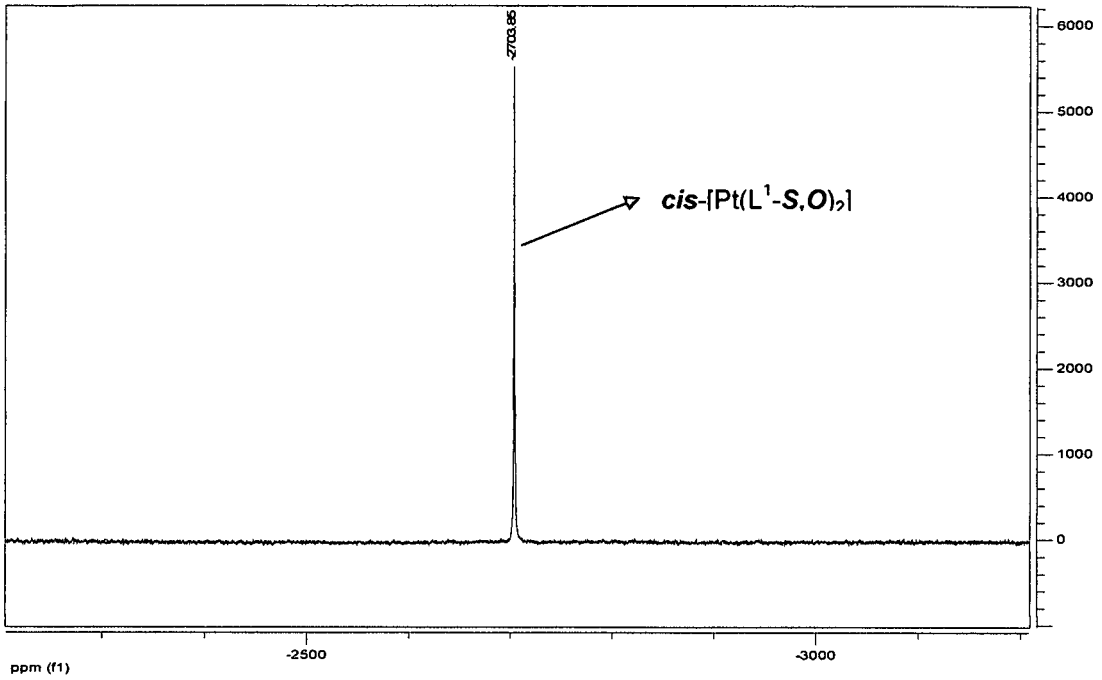

Figure 25. The downfield window of the ^{195}Pt spectra of ***cis***-[Pt(L^1-***S,O***)$_2$].

Based on the above spectroscopic evidence, and a single melting point at 142 – 145°C, it has to be concluded that the synthesis of [Pt(L^1-***S,O***)$_2$] from K_2PtCl_4 and HL^1 in acetonitrile and H_2O afforded only ***cis***-[Pt(L^1-***S,O***)$_2$].

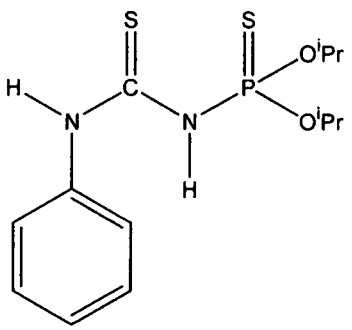

Figure 26. *N*-diisopropoxythiophosphoryl-*N'*-phenylthiourea.

Work done by Mtongana[28] on the ligand shown in Figure 26, and the resulting complexes, indicated that the mode of complex preparation (addition of the

metal solution to the ligand solution or the addition of the ligand solution to the metal solution) significantly affected the product or product mixture obtained. *N*-diisopropoxythiophosphoryl-*N'*-phenylthiourea complexed with platinum(II), either exclusively to yield the *trans* isomer or as a mixture of *cis* and *trans* isomers.

This prompted us to also synthesise of $[Pt(L^1\text{-}\boldsymbol{S,O})_2]$ with the dropwise addition of the deprotonated ligand solution to the $[PtCl_4]^{2-}$ solution, keeping all other factors (temperature, solvent, starting material) constant. The ligand (HL^1) and sodium acetate were dissolved in 30 mL of a mixture of acetonitrile-water (2:1, v/v) at 50°C before being transferred to a dropping funnel. The conventional route of synthesis was followed for the remaining steps of the synthetic procedure. ^1H, ^{13}C and ^{195}Pt NMR, as well as a melting point determination (see section 2.5) indicated that, as with the addition of ligand solution to metal solution, only ***cis***-$[Pt(L^1\text{-}\boldsymbol{S,O})_2]$ was present in the crude product mixture.

As the exact mechanism and dynamics for the complexation of deprotonated ligand and $PtCl_4^{2-}$ is as yet not clear, the mechanism could be affected by the net charge of the starting material. $[PtCl_2(NC\text{-}^iPr)_2]$ was received as a donation from V.Y. Kukushkin (Department of Chemistry, St. Petersburg State University, Russia), and used in the same synthetic procedure as outlined in section 2.5. The synthesis of *bis*(*N,N*-diethyl-*N'*-naphthoylthioureato)-platinum(II) from HL^1 and dichloroisopropionitrileplatinate in acetonitrile and water also led to the *cis*-isomer as the solitary product.

2.2.2 *cis*-bis(*N,N*-dibutyl-*N'*-naphthoylthioureato)platinum(II); *cis*-$[Pt(L^2\text{-}\boldsymbol{S,O})_2]$

The basic synthetic procedure for the synthesis of ***cis***-bis(*N,N*-dibutyl-*N'*-naphthoylthioureato)platinum(II) was the same as that followed for $[Pt(L^1\text{-}\boldsymbol{S,O})_2]$. $[Pt(L^2\text{-}\boldsymbol{S,O})_2]$ was synthesised to investigate the possible changes in the product mixture in going from the diethyl-group to the longer more non-

polar dibutyl-group as the synthesis of the very similar [Pt(L^2-***S,O***)$_2$] molecule has been reported to lead to a mixture of *cis*- and *trans*-isomers. As seen in section 2.2.1 this was not the case for [Pt(L^1-***S,O***)$_2$], despite our efforts.

From the ^{1}H NMR spectra obtained for the crude synthesis product of [Pt(L^2-***S,O***)$_2$] it can been seen that a second species is present (Figure 27). Once again however, as for [Pt(L^1-***S,O***)$_2$] the shifts of the second species are nearly identical to the shifts of the same peaks in the ^{1}H NMR spectra of HL^2. Also, analysis of the ^{195}Pt NMR spectra of [Pt(L^2-***S,O***)$_2$] only reveals one peak at -2703.25 ppm.

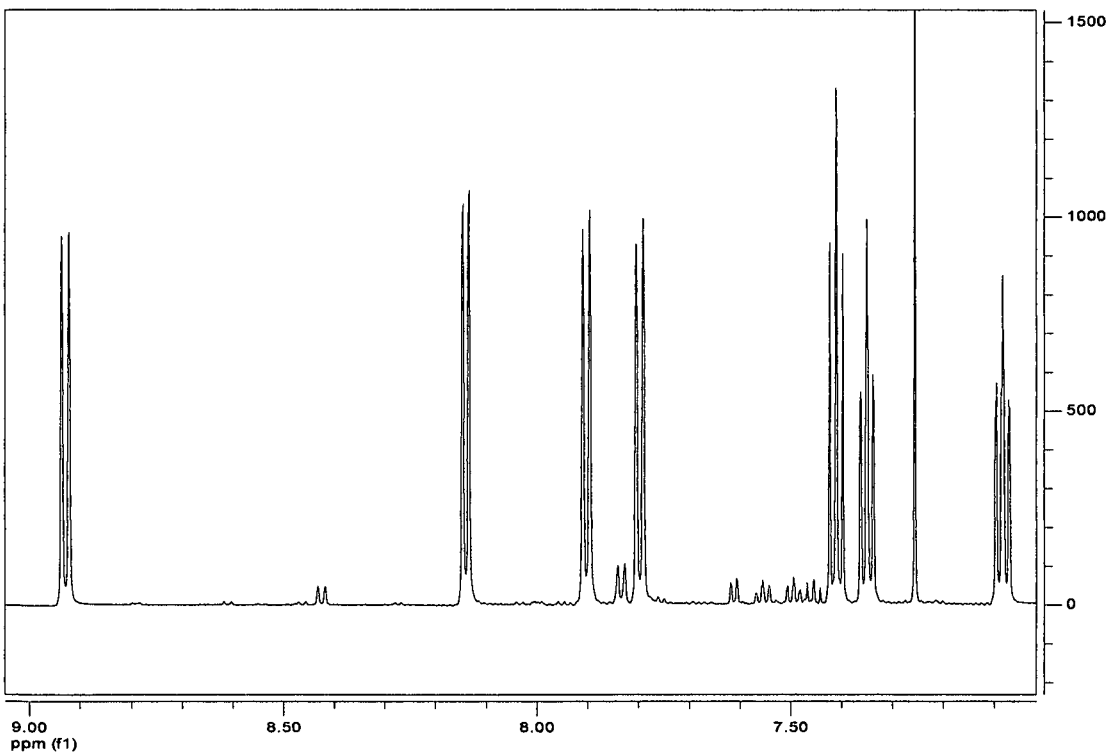

Figure 27. The aromatic region of the ^{1}H spectrum of [Pt(L^2-***S,O***)$_2$].

The second synthesis of this complex was done by adding the ligand solution dropwise to the metal solution. Because it was previously seen that the second species in the crude product mixture of [Pt(L^x-***S,O***)$_2$] (x = 1, 2) was possibly free ligand (from NMR results), it was argued that most of this free ligand in solution should react, and therefore disappear from the spectra if the reacting mixture was allowed to stir at 70°C for a considerably longer period of time. Therefore, the second synthesis of [Pt(L^2-***S,O***)$_2$] was done stirring for 48

hours instead of 60 minutes. The ^{1}H NMR spectra obtained clearly indicated that when the reaction mixture is given enough time to react the "second species" virtually disappears (Figure 28).

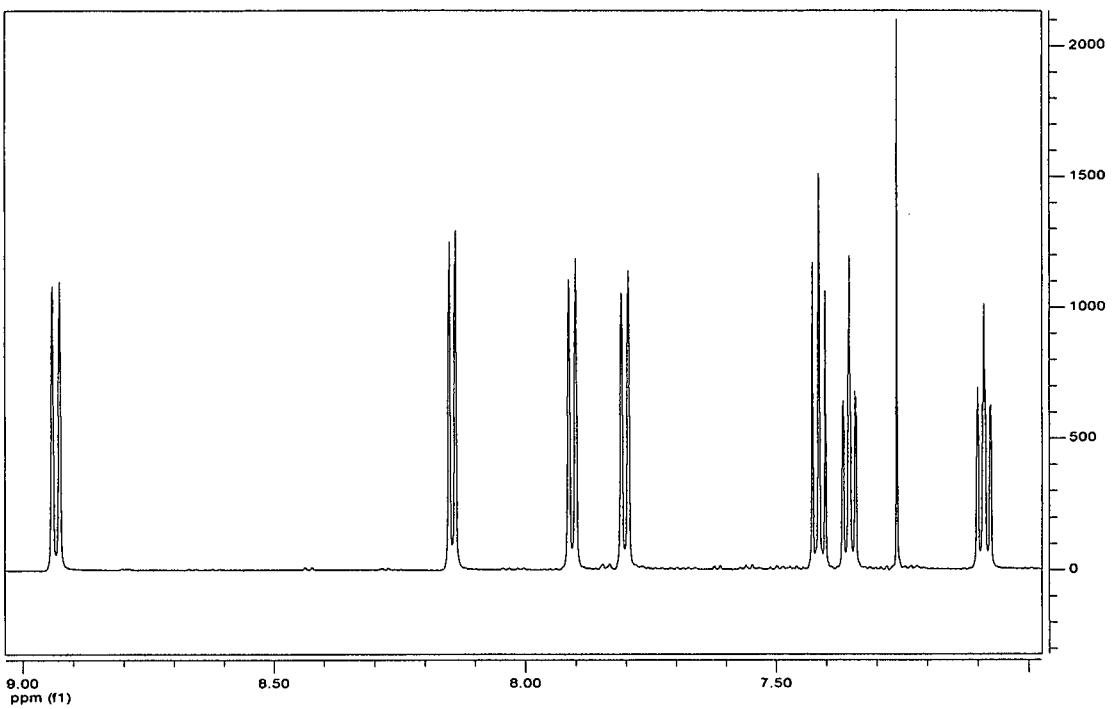

Figure 28. The aromatic region of the ^{1}H NMR spectra of ***cis***-Pt(L^2-***S,O***)$_2$ after 48 hours of continuous stirring (addition of ligand to metal).

In a further attempt to synthesise ***trans***-[Pt(L^2-***S,O***)$_2$] we followed the exact method previously used to synthesise this molecule.[5] The acetonitrile component of the solvent mixture was therefore replaced by dioxane. This change of acetonitrile to dioxane renders the solvent mixture more non-polar and could hence favour the more non-polar *trans*-isomer. HL^2 and sodium acetate were dissolved in 30mL of a mixture of dioxane-water (2:1, v/v) and K_2PtCl_4 was dissolved in 30mL of a second mixture of dioxane-water (1:1, v/v).

In a final synthesis of [Pt(L^2-***S,O***)$_2$] the aqueous component of the solvent mixture was completely removed. *N,N*-dibutyl-*N'*-dibutylnaphthoylthiourea and sodium acetate were dissolved in 30mL of pure MeCN. K_2PtCl_4 was also dissolved in 30mL of pure MeCN and the added dropwise to the deprotonated

ligand solution. The reaction mixture was stirred for *ca.* 24 hours. The solvent was removed using a rotary evaporator, after which the product was dried in a vacuum dessicator.

^{1}H, ^{13}C and ^{195}Pt NMR, as well as a melting point determination (see section 2.5) on the products of both the above mentioned reactions confirmed the presence of only the ***cis***-Pt[L^{2}-***S,O***$)_2$] complex.

2.2.3 *cis*-bis(*N,N*-diethyl-*N'*-3,4,5-trimethoxybenzoylthioureato)Pt(II); *cis*-[Pt(L^{3}-*S,O*)$_2$]

In their article on the ***trans***-bis(*N,N*-dibutyl-*N'*-naphthoylthioureato)platinum(II) complex, Koch *et al.* suggested that, due to the steric bulkiness of the naphthoyl moieties, these groups might be orientated out of the plane or perpendicular to the six-membered chelate rings around the metal centre in the transition state of the complex synthesis, thereby leading to the *trans* conformation.

The *cis* geometry can also be thought of as being more stable, since the two sulphur atoms (having a more significant *trans* influence) are not orientated *trans* to one another but rather *trans* to the oxygen donor atoms (smaller *trans* influence). Therefore it can also be argued that the electron-rich naphthoyl moieties, because they are electron donating, have a softening effect on the oxygen donor atoms. The stabilising effect of having a sulphur atom *trans* to an oxygen atom would therefore be diminished, leading to the greater likelihood of a *trans* conformation being present as part of the crude product of complexation. In work by Mtongana[28] on similar molecules, it was seen that if both of the two chelating atoms are sulphur atoms, *trans*-isomers of these types of molecules would form readily.

As methoxy groups are known to be resonance donating, the above-argued hypothesis was investigated by the synthesis of a series of methoxy-enriched molecules.

The synthesis of [Pt(L^3-***S,O***)$_2$] proceeded according to the method previously described for ***cis***-[Pt(L^1-***S,O***)$_2$]. The purity of [Pt(L^3-***S,O***)$_2$] was determined by means of ^{1}H, ^{13}C, ^{195}Pt NMR spectra, elemental analysis (C, H, N and S) and melting point determination (see section 2.5). It is evident from Figure 29 (two resonances arising from the three methoxy groups) that only one isomer can be identified.

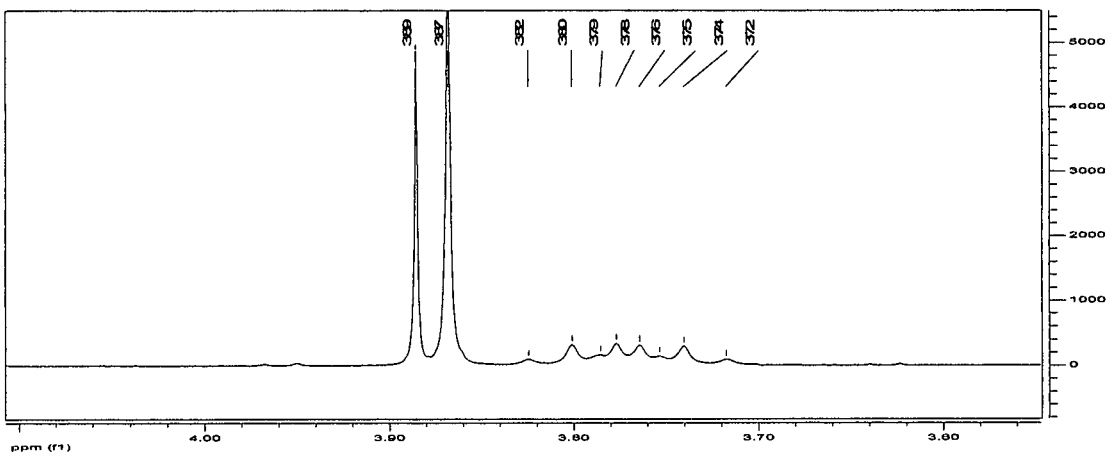

Figure 29. The 3.6 ppm – 4.1ppm region of the ^{1}H NMR spectrum of ***cis***-[Pt(L^3-***S,O***)$_2$]. Only one isomer can be identified as inferred from the presence of only two resonances corresponding to methoxy groups.

2.2.3.1 Crystal structure determination of *cis*-[Pt(L^3-*S,O*)$_2$]

The crude product, ***cis***-[Pt(L^3-***S,O***)$_2$], was recrystallised from an acetonitrile-chloroform solvent mixture (*ca.* 80:20, %(v/v)). Crystals were grown in a vial sealed with parafilm.

The complex is air and moisture stable and was dried by suction. Intensity data were collected using a SMART APEX CCD diffractometer (Bruker-Nonius), followed by cell refinement and data reduction using SAINT (Bruker-Nonius). Initial structure solution was performed using SHELXS 97[29] and the structure was expanded using difference electron density maps. The refinement method was full matrix least squares on F^2 using SHELXL 97.[30] Molecular graphics were generated using X-Seed[31] and POV-Ray.

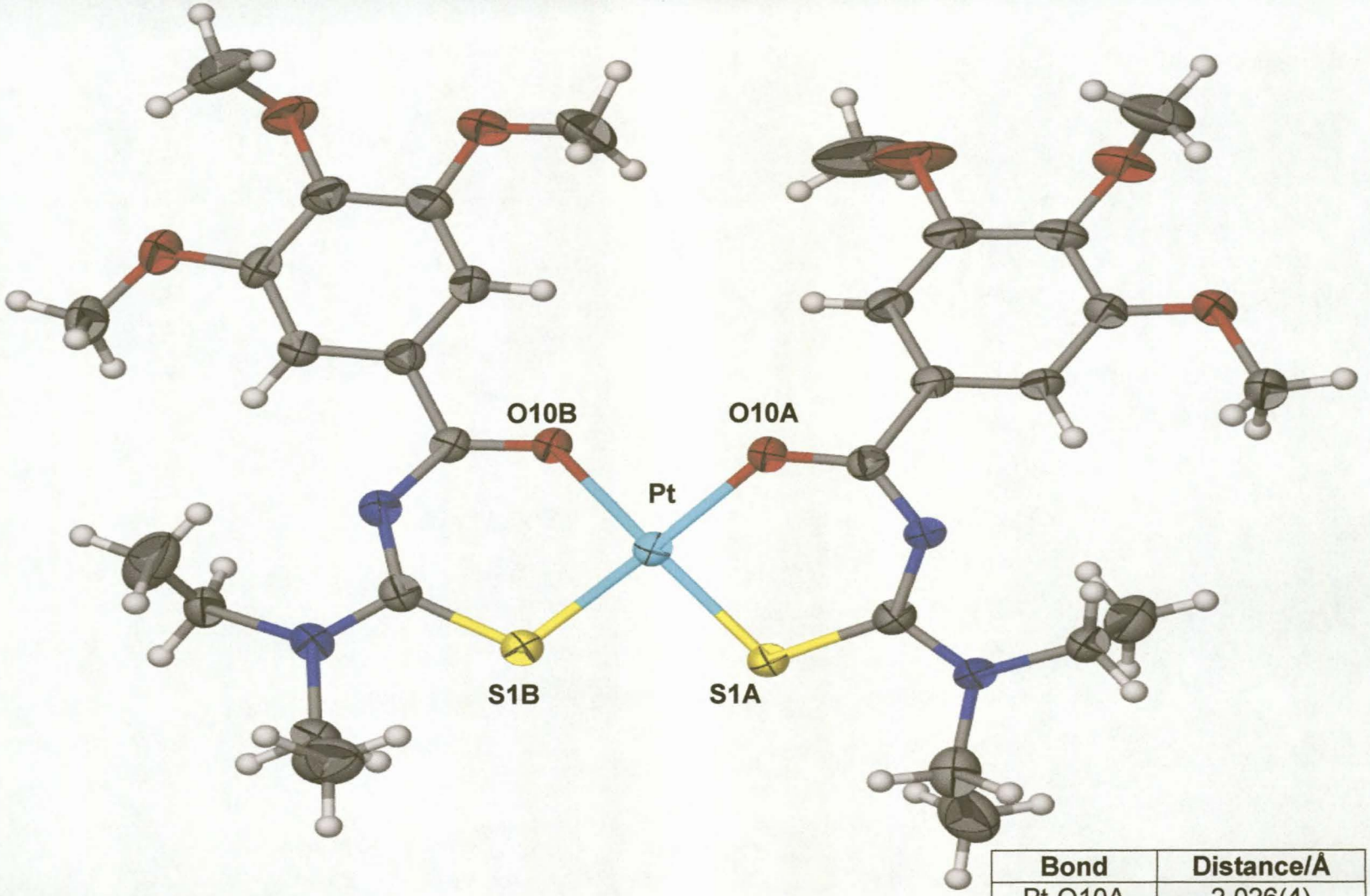

Figure 30. The molecular structure of ***cis***-bis(*N,N*-diethyl-*N'*-3,4,5-trimethoxybenzoylthioureato)-platinum(II), R1 = 5.7%. Structural data can be obtained from Dr. C Esterhuysen, Department of Chemistry, University of Stellenbosch.

Bond	Distance/Å
Pt-O10A	2.026(4)
Pt-O10B	2.041(4)
Pt-S1A	2.2320(17)
Pt-S1B	2.2377(19)

2.2.4 *cis*-bis(*N,N*-diethyl-*N'*-3, 5-dimethoxybenzoylthioureato)Pt(II); *cis*-[Pt(L^4-*S,O*)$_2$]

[Pt(L^4-*S,O*)$_2$] was synthesised to form part of the series of methoxy compounds. The synthesis of bis(*N,N*-diethyl-*N'*-3,5-dimethoxybenzoyl-thioureato)-platinum(II) proceeded according to the method previously described for *cis*-[Pt(L^1-*S,O*)$_2$]. The purity of [Pt(L^4-*S,O*)$_2$] was determined by means of ^{1}H, ^{13}C, ^{195}Pt NMR spectra, elemental analysis (C, H, N and S) and melting point determination (see section 2.5).

As for the previously discussed complexes, the only isomer identified was *cis*-[Pt(L^4-*S,O*)$_2$].

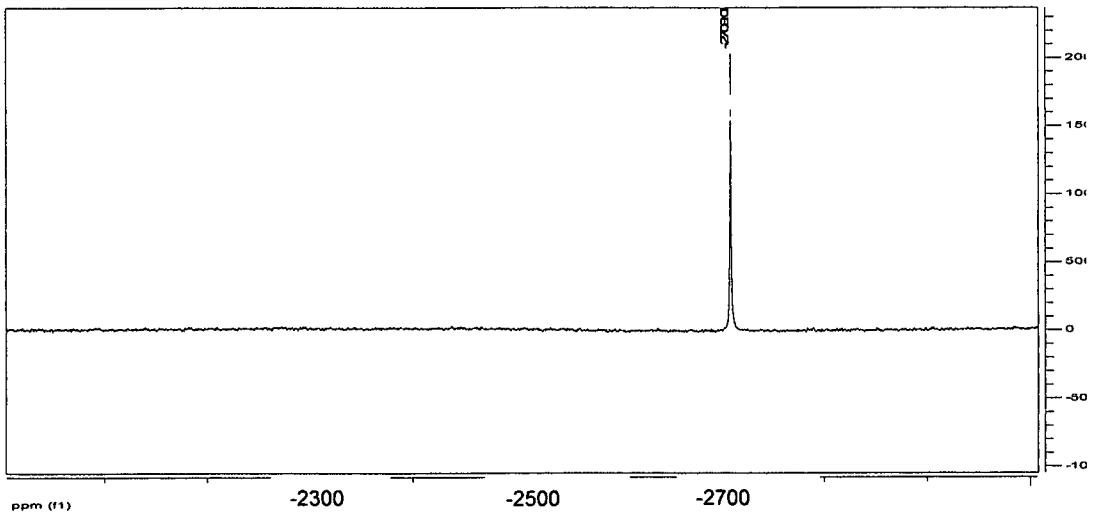

Figure 31. The ^{195}Pt NMR of *cis*-[Pt(L^4-*S,O*)$_2$].

2.2.4.1 Crystal structure determination of *cis*-[Pt(L^4-*S,O*)$_2$]

The crude product, *cis*-[Pt(L^3-*S,O*)$_2$], was recrystallised from an acetonitrile-chloroform solvent mixture (*ca.* 80:20, %(v/v)). Crystals were grown glass vial sealed with parafilm.

The complex is air and moisture stable and was dried by suction. Details as per section 2.2.3.1.

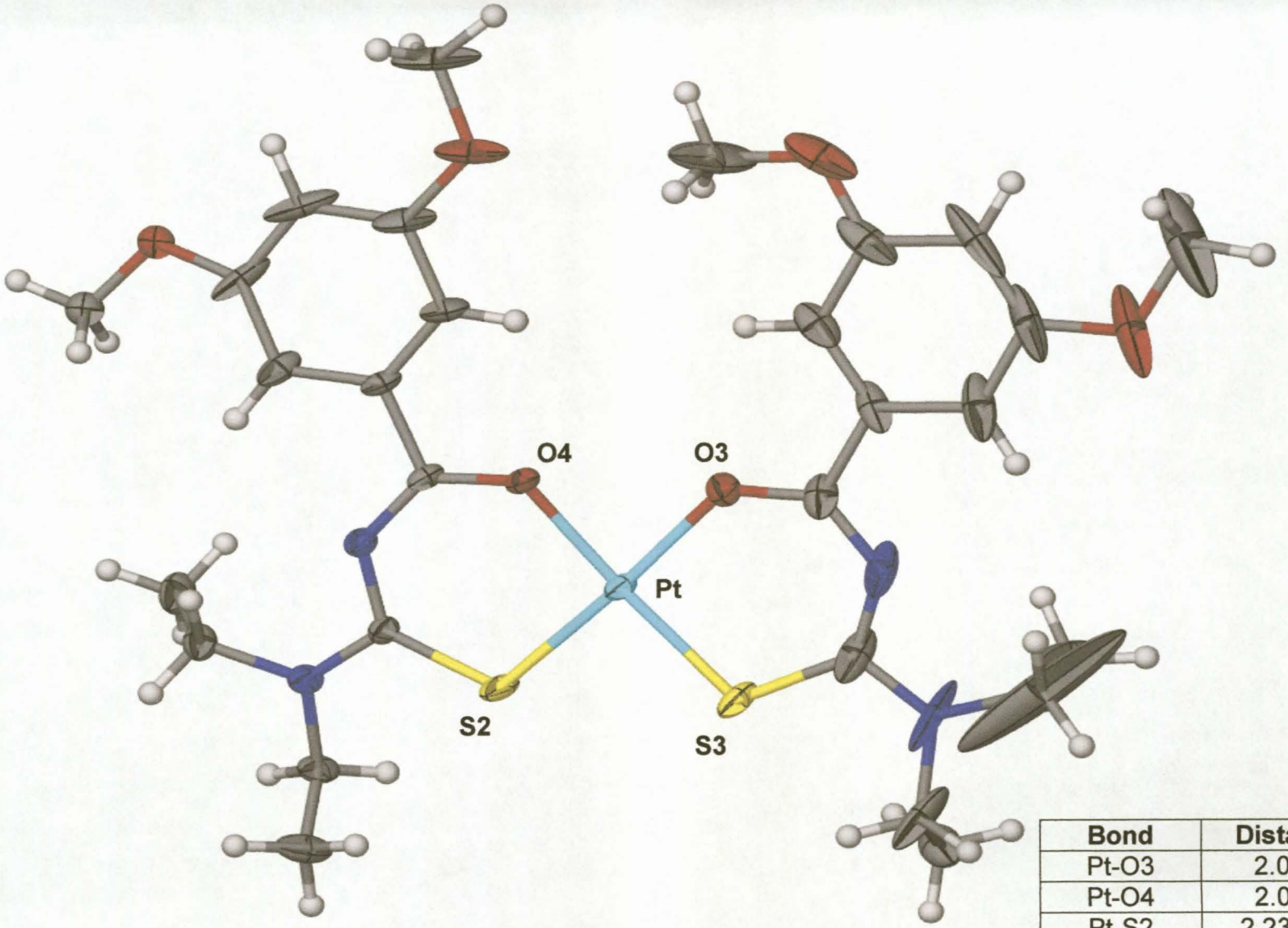

Bond	Distance/Å
Pt-O3	2.010(3)
Pt-O4	2.014(3)
Pt-S2	2.2310(12)
Pt-S3	2.2360(11)

Figure 32. The molecular structure of ***cis***-bis(*N,N*-diethyl-*N'*-3,5-dimethoxybenzoylthioureato)-platinum(II), R1 = 3.3%. Structural data can be obtained from Dr. C Esterhuysen, Department of Chemistry, University of Stellenbosch

2.2.5 *cis*-bis(*N,N*-diethyl-*N'*-4-monomethoxybenzoylthioureato)Pt(II); *cis*-[Pt(L^5-*S,O*)$_2$]

[Pt(L^5-***S,O***)$_2$] was synthesised to form part of the series of methoxy compounds. The synthesis of bis(*N,N*-diethyl-*N'*-4-monomethoxybenzoyl-thioureato)platinum(II) proceeded according to the method previously described for ***cis***-[Pt(L^1-***S,O***)$_2$]. The purity of [Pt(L^5-***S,O***)$_2$] was determined by means of ^{1}H, ^{13}C, ^{195}Pt NMR spectra, elemental analysis (C, H, N and S) and melting point determination (see section 2.5).

As for the previously discussed complexes, the only isomer identified was ***cis***-[Pt(L^5-**S,O**)$_2$].

2.2.6 Discussion of crystal structures: *cis*-[Pt(L^3-*S,O*)$_2$] and *cis*-[Pt(L^4-*S,O*)$_2$]

As discussed in section 2.2.3, the *cis* geometry is thought to be more stable, since the two sulphur atoms are not *trans* to each other but rather *trans* to the oxygen donor atoms (smaller *trans* influence compared to sulphur atoms).

When electron-rich, resonance-donating groups such as the 3,4,5-trimethoxy- and 3,5-dimethoxybenzoyl are adjacent to the carbonyl moiety (as opposed to a benzoyl group) the softening effect of the electron donating methoxy groups should increase the lengths of the Pt-O bonds when compared to ***cis***-bis(*N,N*-diethyl-*N'*-benzoylthioureato)platinum(II). The stabilising effect of having a sulphur atom *trans* to an oxygen atom would therefore be diminished, thus leading to the greater likelihood of a *trans* conformation being present as part of the crude product of complexation.

The difference between the Pt-O bonds and the Pt-S bonds should be smaller in ***cis***-bis(*N,N*-diethyl-*N'*-3,4,5-trimethoxybenzoylthioureato)Pt(II) than in ***cis***-bis(*N,N*-diethyl-*N'*-3,5-dimethoxybenzoylthioureato)Pt(II).

Mtongana, working on similar molecules where both chelating atoms are sulphur atoms, was able to readily prepare *trans*-isomers. [28]

Table 2. A comparison of the difference between the average Pt-S and Pt-O bond lengths for three relevant complexes.

Comparison of Pt-S and Pt-O bond length differences					
cis-[Pt(L^3-***S,O***)$_2$]		***cis***-[Pt(L^4-***S,O***)$_2$]		***trans***-[Pt(L-***S,S***)$_2$]	
Bond	**Length (Å)**	**Bond**	**Length (Å)**	**Bond**	**Length (Å)**
Pt1 O10A	2.026(4)	Pt1 O3	2.010(3)	Pt1 S1	2.3034(7)
Pt1 O10B	2.041(4)	Pt1 O4	2.014(3)	Pt1 S1a	2.3034(7)
Avg_{Pt-O}	2.0335	**Avg_{Pt-O}**	2.0120	**Avg_{Pt-S1}**	2.3034
Pt1 S1A	2.2320(17)	Pt1 S3	2.2310(12)	Pt1 S2	2.3367(7)
Pt1 S1B	2.2377(19)	Pt1 S2	2.2360(11)	Pt1 S2a	2.3367(7)
Avg_{Pt-S}	2.2349	**Avg_{Pt-S}**	2.2335	**Avg_{Pt-S2}**	2.3367
$(Pt-S)_{AVG}$ - $(Pt-O)_{AVG}$	0.20135	**$(Pt-S)_{AVG}$ - $(Pt-O)_{AVG}$**	0.2215	**$(Pt-S2)_{AVG}$ - $(Pt-S1)_{AVG}$**	0.0333

In table 2 the differences between the average Pt-S and Pt-O bond distances for the various molecules are given (Pt-S1 and Pt-S2 in the case of ***trans***-[Pt(L-***S,S***)$_2$]). This data would suggest that electron donation by the methoxy groups renders the oxygen more sulphur-like (difference for ***cis***-[Pt(L^3-***S,O***)$_2$] smaller than for ***cis***-[Pt(L^4-***S,O***)$_2$]). The stabilising effect (*trans* influence) of having an oxygen atom *trans* to a sulphur atom would therefore be diminished. However, this small decrease in stabilisation is not sufficient for the formation of the *trans* isomer.

2.2.7 Additional platinum(II) complexes synthesised *cis*-[Pt(L^6-*S,O*)$_2$], *cis*-[Pt(L^7-*S,O*)$_2$]

cis-bis(*N,N*-diethyl-*N'*-camphanoylthioureato)platinum(II), (***cis***-[Pt(L^6-***S,O***)$_2$]), was synthesised to investigate, according to the argument followed in section 2.2.3, the effect of an even larger group than a naphthoyl group attached to the carbonyl moiety of the ligand. ***cis***-bis(*N,N*-diethyl-*N'*-benzoylthioureato)-platinum(II), (***cis***-[Pt(L^7-***S,O***)$_2$]), was synthesised and used with two ideas in mind. Firstly, this molecule has been studied extensively and is therefore well understood, and secondly from a "baseline" point of view, this molecule also forms part of the methoxy complex series which was synthesised with the aim of investigating the effect of adding electron-donating groups to the benzoyl moiety of the thiourea ligand.

cis-[Pt(L^7-***S,O***)$_2$] was analysed by means of ^{1}H-, ^{13}C-, ^{195}Pt NMR, elemental analysis (C, H, N and S) and a melting point determination. ***cis***-[Pt(L^6-***S,O***)$_2$] was analysed by means of elemental analysis (C, H, N and S), melting point determination§ and ^{195}Pt NMR. In both cases only the *cis* isomer could be identified.

§ Compares favourably with literature value. [34b]

2.3 Synthesis and characterisation of the *cis*-bis(*N,N*-dialkyl-*N'*-aroylthioureato)palladium(II) complexes

The synthesis and coordination chemistry of the palladium complexes of the *N,N*-dialkyl-*N'*-aroyl(acyl)thiourea ligands have also been reported by Koch *et al.*[7] As for the platinum analogues (with the notable exception of the *N,N*-dibutyl-*N'*-naphthoyl platinum complex), the complexes of palladium reported to date have all been of the *cis* conformation.

Anderson and Cross, in their review of the isomerisation of square-planar metal complexes[11], state that studies concerning the isomer distribution, isomerisation and subsequent detection of these isomers have largely been confined to platinum(II) and palladium(II). The reason being: ease of preparation and reaction rates (allowing for the spectroscopic detection of the isomer distribution up to the point of equilibrium). Both of these factors, and our knowledge of the reactions of *N,N*-dialkyl-*N'*-aroyl(acyl)thiourea with palladium(II), prompted us to synthesise some molecules similar to those discussed in section 2.2.

Only the effect of electron donation (on the crude product of synthesis), rendering the oxygen atom softer and more sulphur-like, was investigated for palladium. In keeping with the methoxy-series synthesised in section 2.2, bis-(*N,N*-diethyl-*N'*-3,4,5-trimethoxybenzoylthioureato)palladium(II), bis(*N,N*-di-ethyl-*N'*-3,5-dimethoxybenzoylthioureao)palladium(II) and bis(*N,N*-diethyl-*N'*-4-monomethoxybenzoylthioureato)palladium(II) were synthesised.

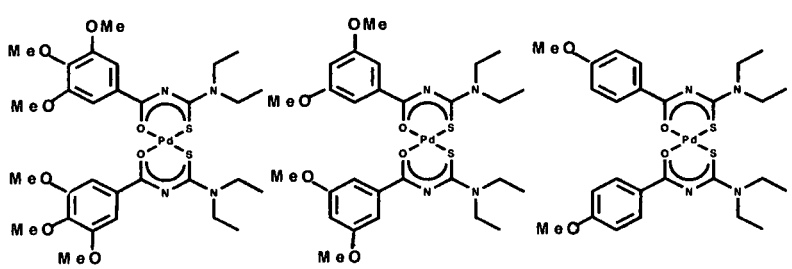

$Pd(L^3\text{-}S,O)_2$: *N,N*-diethyl-*N'*-3,4,5-trimethoxybenzoylthioreato)palladium(II)
$Pd(L^4\text{-}S,O)_2$: *N,N*-diethyl-*N'*-3,5-dimethoxybenzoylthioreato)palladium(II)
$Pd(L^5\text{-}S,O)_2$: *N,N*-diethyl-*N'*-4-monomethoxybenzoylthioreato)palladium(II)

Figure 33. Structures of the methoxy-series of palladium complexes.

Other factors that could aid the formation of a *trans* complex and which were investigated for the platinum(II) metal centre, were not considered with regard to palladium. These include the question of possible steric hindrance operating in a transition state during complex formation, the kinetic effect of alternating between the addition of metal to ligand or ligand to metal and the polarity of the solvent of synthesis.

The synthetic route, except for the use of $K_2[PdCl_4]$ as starting material, was exactly that followed for ***cis***-bis(*N,N*-diethyl-*N'*-naphthoylthioureato)-platinum(II) outlined in section 2.5.

The three palladium complexes that were synthesised all complexed in the *cis* conformation with no spectroscopic evidence supporting the formation of the *trans* isomer (see Figure 34).

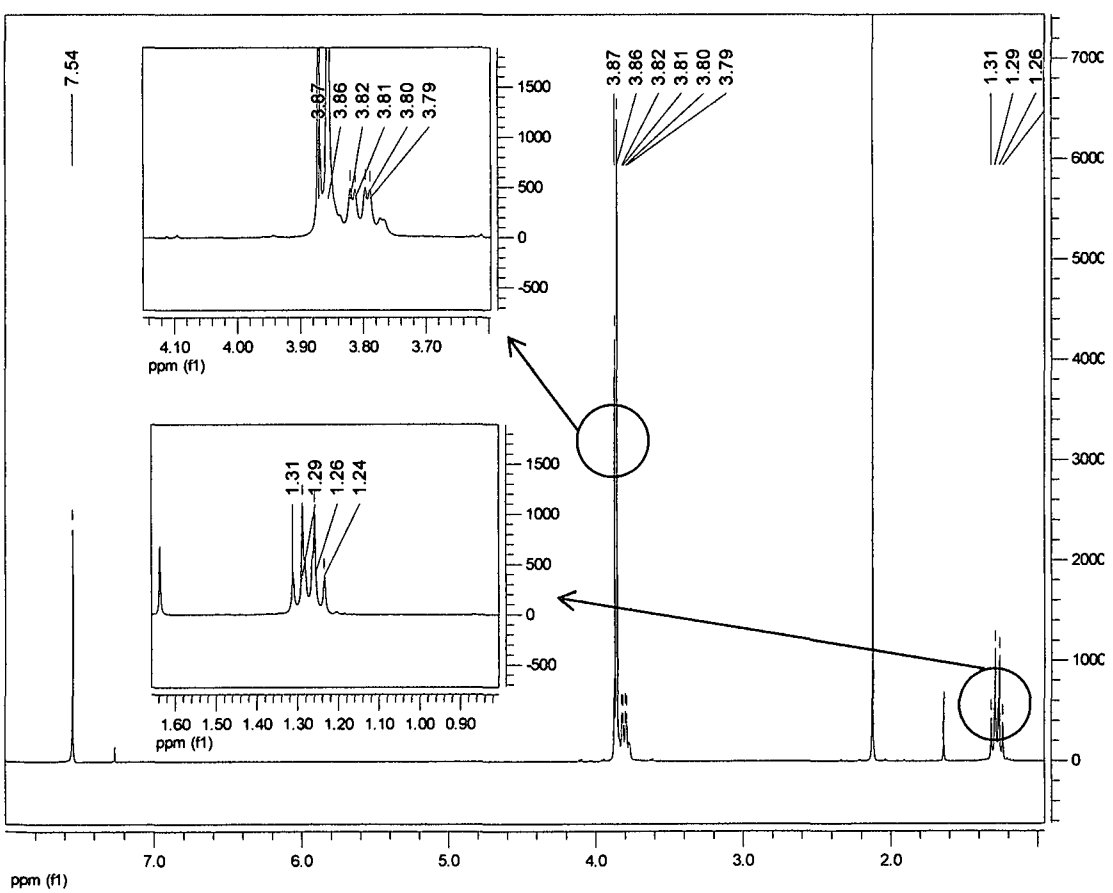

Figure 34. From the ^{1}H spectrum of ***cis***-[Pd(L^3-***S,O***)$_2$] it is clear from the methyl (1.29ppm), methylene (3.81ppm) and ortho-H (7.54ppm) regions of the spectrum, that only the *cis*-isomer can be identified in the crude product mixture.

2.3.1 Crystal structure determination of *cis*-[Pd(L^3-*S,O*)$_2$]

The crude product, ***cis***-[Pd(L^3-***S,O***)$_2$], was recrystallised from an acetonitrile-chloroform solvent mixture (*ca.* 80:20, %(v/v)). Crystals were grown in a glass vial sealed with parafilm.

The complex is air and moisture stable and was dried by suction. Intensity data were collected using a SMART APEX CCD diffractometer (Bruker-Nonius), followed by cell refinement and data reduction using SAINT (Bruker-Nonius). Initial structure solution was performed using SHELXS 97[29] and the structure was expanded using difference electron density maps. The refinement method was full matrix least squares on F^2 using SHELXL 97. [30] Molecular graphics were generated using X-Seed[31] and POV-Ray.

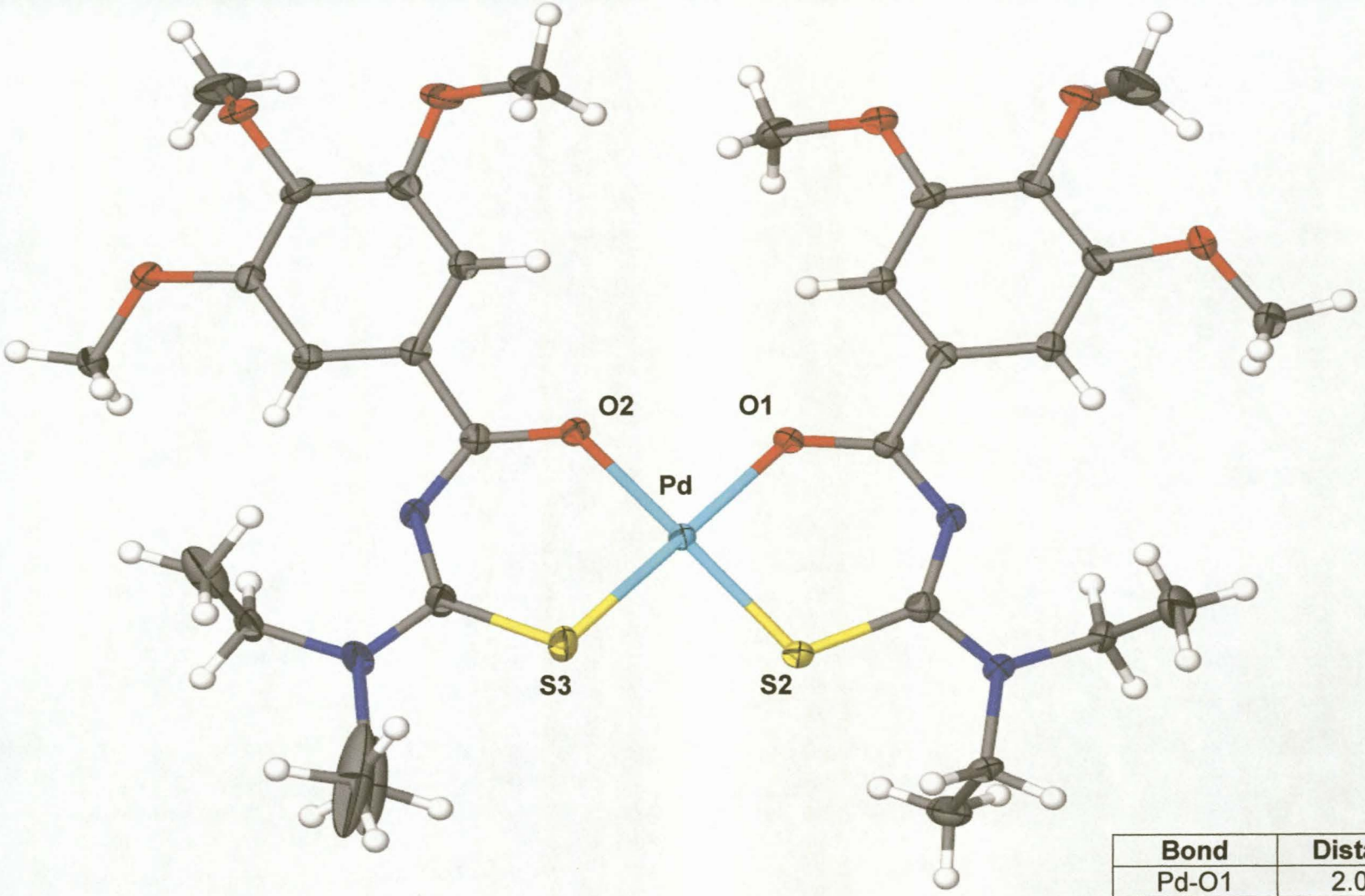

Bond	Distance/Å
Pd-O1	2.012(2)
Pd-O2	2.040(2)
Pd-S2	2.2344(9)
Pd-S3	2.2400(10)

Figure 35. The molecular structure of ***cis***-bis(*N,N*-diethyl-*N'*-3,4,5-trimethoxybenzoylthioureato)-palladium(II), R1 = 5.2%. Structural data can be obtained from Dr. C Esterhuysen, Department of Chemistry, University of Stellenbosch.

2.3.2 Crystal structure determination of *cis*-[Pd(L^4-*S,O*)$_2$]

The crude product, ***cis***-[Pd(L^4-***S,O***)$_2$], was recrystallised from an acetonitrile-chloroform solvent mixture (*ca.* 80:20, %(v/v)). Crystals were grown in a glass vial sealed with parafilm.

The complex is air and moisture stable and was dried by suction. Intensity data were collected using a SMART APEX CCD diffractometer (Bruker-Nonius), followed by cell refinement and data reduction using SAINT (Bruker-Nonius). Initial structure solution was performed using SHELXS 97[29] and the structure was expanded using difference electron density maps. The refinement method was full matrix least squares on F^2 using SHELXL 97. [30] Molecular graphics were generated using X-Seed[31] and POV-Ray.

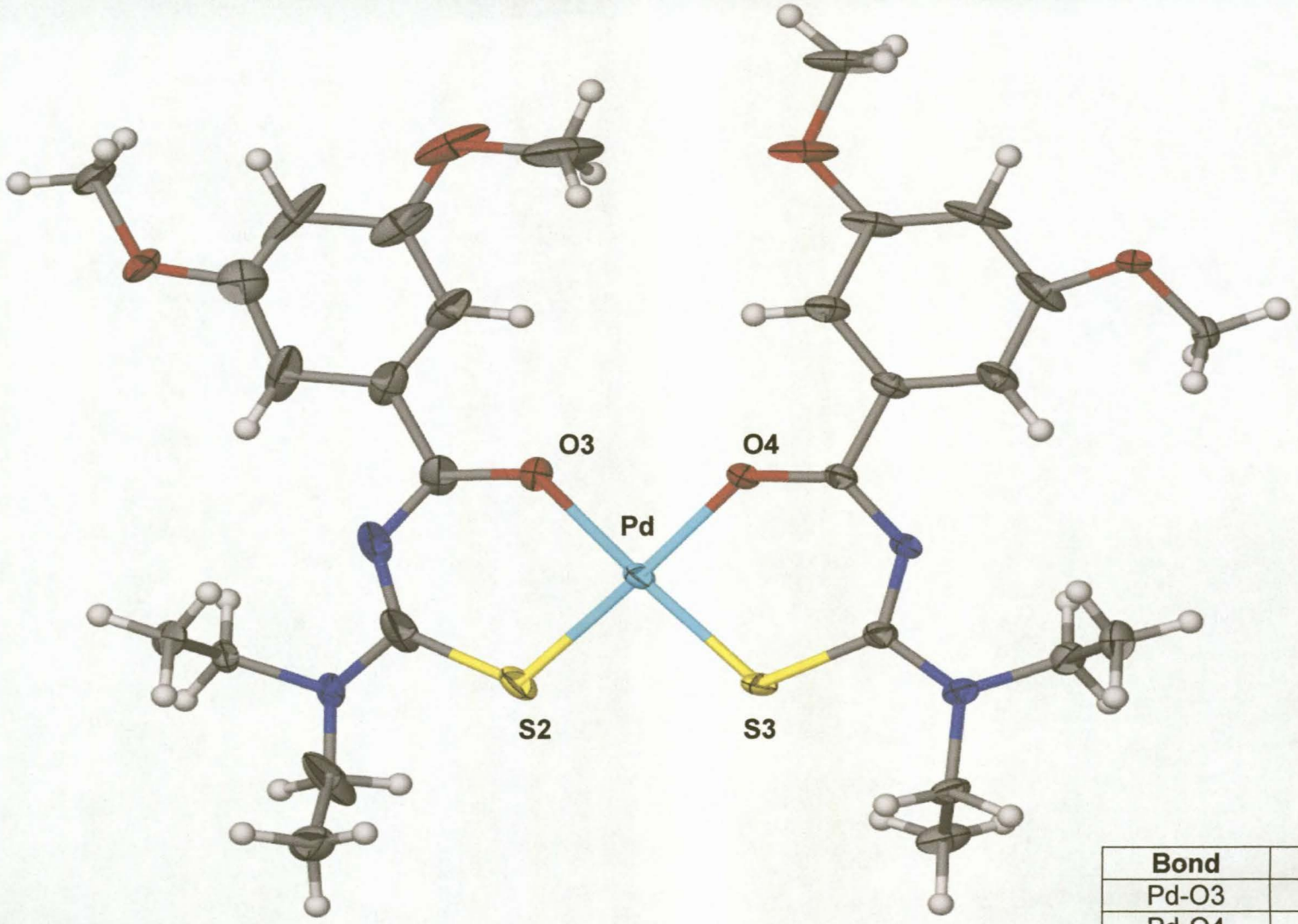

Bond	Distance/Å
Pd-O3	2.007(2)
Pd-O4	2.013(3)
Pd-S2	2.2376(10)
Pd-S3	2.2392(10)

Figure 36. The molecular structure of ***cis***-bis(*N,N*-diethyl-*N'*-3,5-dimethoxybenzoylthioureato)-palladium(II), R1 =3.9%. Structural data can be obtained from Dr. C Esterhuysen, Department of Chemistry, University of Stellenbosch.

2.3.3 Discussion of crystal structures: *cis*-[Pd(L^3-*S,O*)$_2$] and *cis*-[Pd(L^4-*S,O*)$_2$]

As argued in section 2.2.6, the effect of adding methoxy groups to the benzoyl moiety could soften the oxygen atom, leading to a smaller *trans* influence effect and therefore the increased possibility of forming a mixture of *cis* and *trans* complexes.

Table 3. A comparison of the difference between the average Pt-S and Pt-O bond lengths for *cis*-[Pd(L^3-*S,O*)$_2$] and *cis*-[Pd(L^4-*S,O*)$_2$].

Comparison of Pt-S and Pt-O bond length differences			
cis-[Pd(L^3-*S,O*)$_2$]		*cis*-[Pd(L^4-*S,O*)$_2$]	
Bond	Length (Å)	Bond	Length (Å)
Pd O1	2.012(2)	Pt O3	2.007(2)
Pd O2	2.040(2)	Pt O4	2.013(3)
Avg_{Pd-O}	2.0262	Avg_{Pd-O}	2.0103
Pd1 S2	2.2344(9)	Pt S2	2.2376(10)
Pd1 S3	2.2400(10)	Pt S3	2.2392(10)
Avg_{Pd-S}	2.2373	Avg_{Pd-S}	2.2384
$(Pd-S)_{AVG}$ - $(Pd-O)_{AVG}$	0.2111	$(Pd-S)_{AVG}$ - $(Pd-O)_{AVG}$	0.2281

Again, as for table 2, this data suggest that electron donation by the methoxy groups renders the oxygen more sulphur-like (difference for *cis*-[Pd(L^3-*S,O*)$_2$] smaller than for *cis*-[Pd(L^4-*S,O*)$_2$]). The stabilising effect (*trans* influence) of having an oxygen atom *trans* to a sulphur atom would therefore be diminished, but again, this small decrease in stabilisation is not sufficient for the formation of the *trans* isomer.

2.4 Experimental details: Ligands

The ligands, *N,N*-dibutyl-*N'*-naphthoylthiourea (HL^2), *N,N*-diethyl-*N'*-benzoylthiourea (HL^7) and *N,N*-diethyl-*N'*-3,4,5-trimethoxybenzoylthiourea (HL^3) were prepared and donated by Mr. Arjan Westra, Department of

Chemistry, University of Stellenbosch. The purity of these ligands were evaluated by means of ^{1}H and ^{13}C NMR spectroscopy, melting point determination and elemental analysis (C, H, N and S). All other ligands were synthesised via a similar synthetic procedure described in detail below for *N,N*-diethyl-*N'*-naphthoylthiourea (HL^1).

Vacuum-oven-dried potassium thiocyanate (1.4570g, 14.99mmol) was dissolved in a 500mL two-necked round bottom flask, under nitrogen, using anhydrous acetone (50mL). Naphthoyl chloride (2.8492g, 14.95mmol) in anhydrous acetone (50mL) was added dropwise at room temperature with continuous stirring under inert atmosphere. The reaction mixture was refluxed with stirring for approximately 45 minutes. The flask, now containing naphthoyl isothiocyanate, was allowed to cool to room temperature. Diethylamine (1.1g) in 50mL of anhydrous acetone was added dropwise with continuous stirring over a period of 30 minutes. The reaction mixture was then heated to reflux for a further 45 minutes with stirring. The flask was allowed to cool to room temperature before the contents were poured into a 600mL beaker containing 75mL of water. Approximately 130mL of acetone was allowed to evaporate before the crude product was collected by suction. The crude product was washed with an excess of water to remove any inorganic salts possibly still present. The crude product was recrystallised from a mixture of acetone and water and collected by means of filtration. The final product was dried in a vacuum dessicator. The reaction is thought of as proceeding via the pathway illustrated in Figure 37.

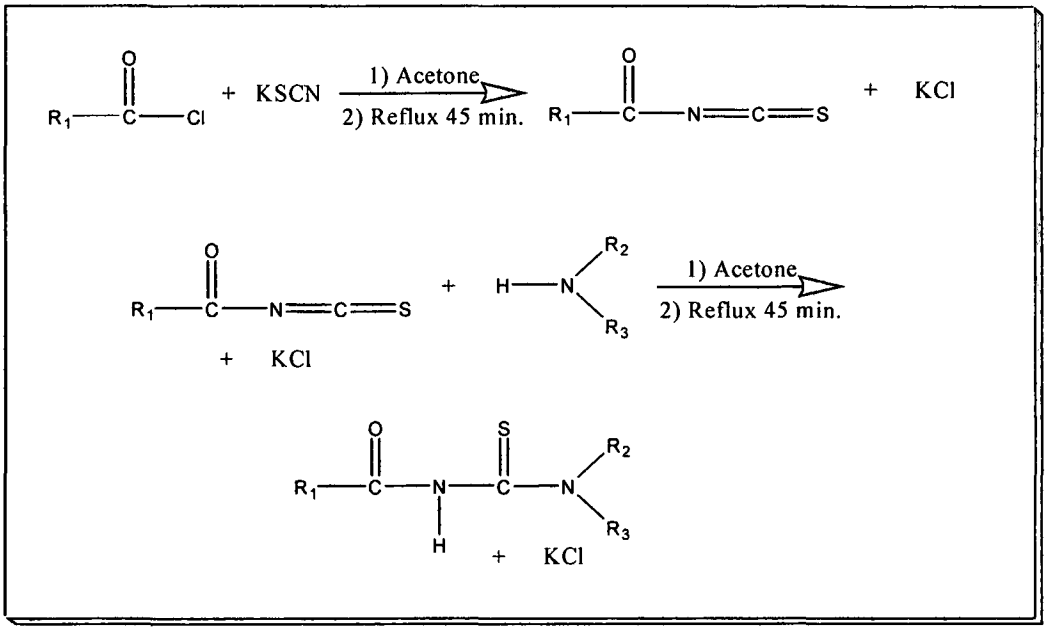

Figure 37. A proposed reaction pathway for the synthesis of *N,N*-dialkyl-*N'*-aroyl(acyl)thiourea (R_1 = alkyl- or benzyl derivative group, R_2 = R_3 = alkyl group).

The melting points of the ligands were determined using an Electrothermal 9300 melting point apparatus. The C, H, N and S elemental analysis was carried out using a Carlo Erba EA 1108 elemental analyser in the microanalytical laboratory of the University of Cape Town, South Africa. The ^{1}H and ^{13}C nuclear magnetic resonance spectra were all recorded in 5mm tubes in $CDCl_3$. The instrument used was either a Varian Unity 300 spectrometer or a Varian Unity 600 spectrometer operating at 300 and 600MHz for ^{1}H spectra and 75 and 150MHz for ^{13}C spectra. All the ^{1}H and ^{13}C spectra were acquired at 25°C and the chemical shifts are referenced relative to $CDCl_3$ at 7.25ppm and 77.0ppm respectively. All the reagents used are commercially available and were used without further purification (except for being dried in the appropriate fashion).

_N,N_-diethyl-_N'_-naphthoylthiourea; HL^1

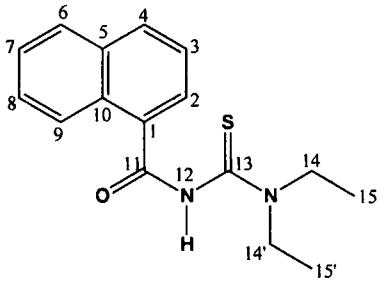

A recrystallised yield of (3.4g, 11.87mmol) 79% was recovered. For characterization m.p. 142-145°C, (Found: C, 67.22; H, 6.55; N, 9.93; S, 10.86; calculated for $C_{16}H_{18}N_2OS$ C, 67.1; H, 6.33; N, 9.78; S, 11.26); NMR δ_H (300MHz, $CDCl_3$): 1.37 (6H, unresolved, $H_{15/15'}$), 3.80 (4H, unresolved, $H_{14/14'}$), 7.49 (1H, triplet, H_8), 7.56 (1H, triplet, H_3), 7.60 (1H, triplet, H_7), 7.77 (1H, doublet, H_6), 7.89 (1H, doublet, H_4), 7.99 (1H, doublet, H_9), 8.27 (1H, singlet, H_{12}), 8.46 (1H, doublet, H_2) δ_C (75MHz, $CDCl_3$): 11.79, 13.58, 48.09, 48.20, 124.71, 125.40, 126.65, 126.99, 128.77, 130.49, 131.78, 132.69, 134.10, 165.62, 179.15.

_N,N_-dibutyl-_N'_-naphthoylthiourea; HL^2

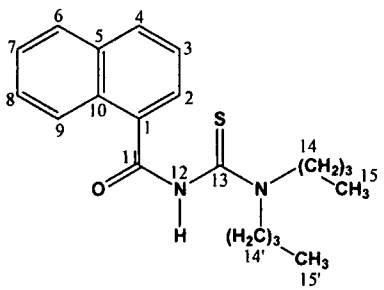

Donation. For characterisation m.p. 96-98°C, (Found: C, 70.33; H, 7.80; N, 8.00; S, 9.68; calculated for $C_{20}H_{26}N_2OS$ C, 70.14; H, 7.65; N, 8.18; S, 9.36); NMR δ_H (300MHz, $CDCl_3$): 0.97 (3H, triplet, $-CH_2CH_3$), 1.01 (3H, triplet, $-CH_2CH_3$), 1.38 (2H, sextet, CH_3CH_2-), 1.49 (2H, sextet, CH_3CH_2-), 1.75 (2H, heptet, NCH_2CH_2), 1.85 (2H, heptet, NCH_2CH_2), 3.69 (2H, triplet NCH_2), 4.01 (2H, triplet NCH_2), 7.50 (1H, triplet, H_7), 7.57 (1H, triplet, H_3), 7.60 (1H, triplet, H_7), 7.76 (1H, triplet, H_6), 7.91 (1H, doublet, H_4), 8.02 (1H, doublet, H_2), 8.19 (1H, singlet, NH), 8.46 (1H, d, H_9), δ_C (75MHz, $CDCl_3$): 13.82, 13.86, 20.20, 29.28, 30.08, 30.90, 51.33, 52.42, 124.46, 125.53, 126.65, 127.11, 127.96, 128.63, 131.16, 131.31, 133.95, 135.69, 167.15, 171.47.

_N,N_-diethyl-_N'_-3,4,5-trimethoxybenzoylthiourea; HL^3

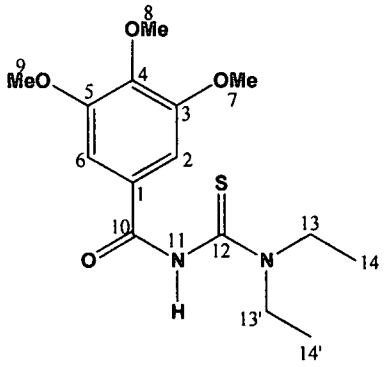

Donation. For characterisation m.p. 143 –145°C, (Found: C, 55.30; H, 7.16; N, 8.62; S, 9.37; calculated for $C_{15}H_{22}N_2O_4S$ C, 55.19; H, 6.79; N, 8.58; S, 9.82); NMR δ_H (300MHz, $CDCl_3$): 1.31 (6H, unresolved, $H_{14/14'}$), 3.55 (2H, unresolved, H_{13} or $H_{13'}$), 3.85 (3H, singlet, H_8), 3.87 (6H, singlet, $H_{7/9}$), 3.98 (2H, unresolved, H_{13} or $H_{13'}$), 7.05 (2H, singlet, $H_{2/6}$), 8.82 (1H, singlet, H_{11}), δ_C (75MHz, $CDCl_3$): 11.41, 13.30, 47.54, 47.71, 56.38, 60.91, 105.23, 127.36, 142.05, 153,12, 163.34, 179.62.

_N,N_-diethyl-_N'_-3,5-dimethoxybenzoylthiourea; HL^4

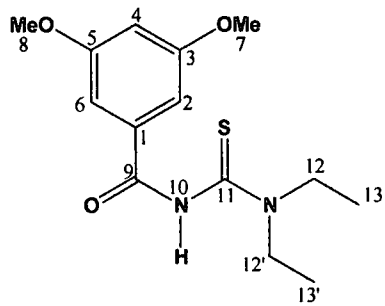

A recrystallised yield of (3.56g, 12.01mmol) 80% was recovered. For characterization m.p. 122-124°C, (Found: C, 57.06; H, 6.89; N, 9.51; S, 10.49; calculated for $C_{14}H_{20}N_2O_3S$ C, 56.73; H, 6.80; N, 9.45; S, 10.82); NMR δ_H (300MHz, $CDCl_3$): 1.27 (6H, unresolved, $H_{13/13'}$), 3.55 (2H, unresolved, H_{12} or $H_{12'}$), 3.79 (6H, singlet, $H_{7/8}$), 4.00 (2H, unresolved, H_{12} or $H_{12'}$), 6.61 (1H, triplet, H_4), 6.93 (2H, doublet, $H_{2/6}$), 8.38 (1H, singlet, H_{10}), δ_C (75MHz, $CDCl_3$): 11.19, 12.98, 47.53, 55.40, 105.32, 105.37, 134.79, 161.23, 163.83, 179.50.

N,N-diethyl-*N'*-4-monomethoxybenzoylthiourea; HL[5]

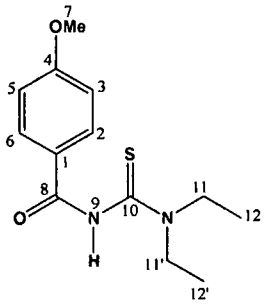

A recrystallised yield of (3.12g, 11.71mmol) 78% was recovered. For characterization m.p. 134 – 135°C, (Found: C, 59.12; H, 7.45; N, 10.74; S, 11.74; calculated for $C_{13}H_{18}N_2O_2S$ C, 56.73; H, 6.80; N, 9.45; S, 10.82); NMR δ_H (300MHz, $CDCl_3$): 1.27 (6H, unresolved, $H_{12/12'}$), 3.57 (2H, unresolved, H_{11} or $H_{11'}$), 3.84 (3H, singlet, H_7), 4.00 (2H, unresolved, H_{11} or $H_{11'}$), 6.93 (2H, doublet, $H_{2/6}$), 7.79 (2H, doublet, $H_{3/5}$), 8.21 (1H, singlet, H_9), δ_C (75MHz, $CDCl_3$): 11.28, 12.95, 47.66, 51.41, 114.17, 124.97, 130.00, 163.57, 179.93.

N,N-diethyl-*N'*-camphanoylthiourea; HL[6]

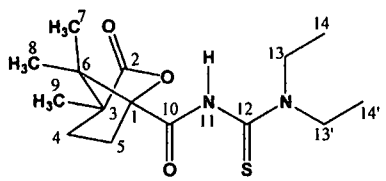

A recrystallised yield of (2.76g, 12.75mmmol) 85% was recovered. For characterization m.p. 148 – 150°C, (Found: C, 57.83; H, 8.18; N, 8.90; S, 10.00; calculated for $C_{15}H_{24}N_2O_3S$ C, 57.66; H, 7.74; N, 8.97; S, 10.26); NMR δ_H (300MHz, $CDCl_3$): 1.03 (6H, unresolved, $H_{14/14'}$), 1.12 (3H, singlet, $H_{7/8}$), 1.14 (3H, singlet, $H_{7/8}$), 1.31 (3H, unresolved, H_9), 1.97 (3H, multiplet, $H_{4/5}$), 2.48 (3H, multiplet, $C_{5/4}$), 3.52 (2H, unresolved, NCH_2), 3.95 (2H, unresolved, NCH_2), 8.36 (1H, singlet, NH), δ_C (75MHz, $CDCl_3$): 13.4, 13.4, 13.8, 18.1, 18.1, 23.8, 24.8, 35.4, 55.6, 101.8, 176.0, 180.3, 183.0.

_N,N_-diethyl-_N'_-benzoylthiourea; HL^7

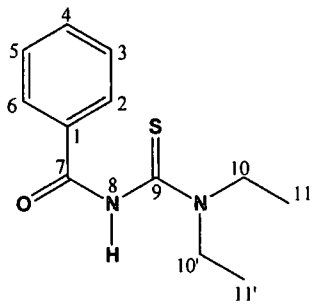

Donation. For characterisation m.p. 98 – 100°C, (Found: C, 61.15; H, 6.93; N, 12.00; S, 13.61; calculated for $C_{12}H_{16}N_2OS$ C, 60.98; H, 6.82; N, 11.85; S, 13.57); NMR δ_H (300MHz, $CDCl_3$): 1.25 (6H, unresolved, $H_{11/11'}$), 3.54 (2H, unresolved, H_{10} or $H_{10'}$), 4.01 (2H, unresolved, H_{10} or $H_{10'}$), 7.54 (2H, triplet, $H_{3/5}$), 7.68 (1H, triplet, H_4), 8.11 (2H, doublet, $H_{2/6}$), δ_C (75MHz, $CDCl_3$): 11.32, 13.14, 47.54, 50.85, 129.25, 131.68, 134.11, 137.89, 164.23, 179.97.

2.4.1 Table of structures and general information for ligands

Table 4: A list of the ligands synthesised with their respective abbreviations, percentage yields and melting points in degrees Celsius.

Abbreviation	Structure	m.p. (°C)	% Isolated Yield
HL^1	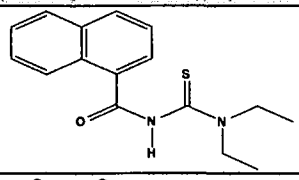	142 – 145	79
HL^2	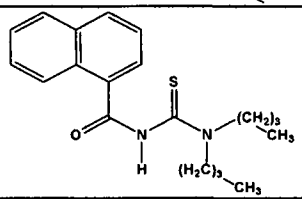	96 - 98	*
HL^3	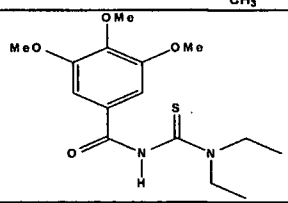	143 – 145	*
HL^4	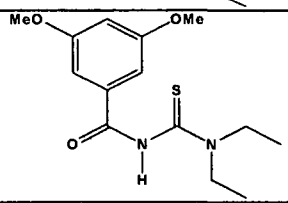	122 – 124	80
HL^5	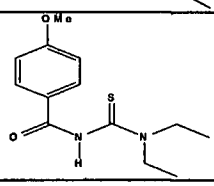	134 – 135	76
HL^6	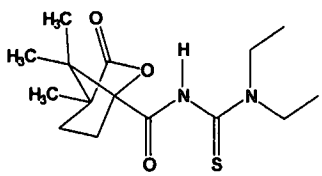	148 – 150	82
HL^7	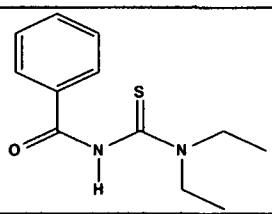	98 – 100	*

* The percentage yields for HL^2, HL^3 and HL^5 are not available as these were donations received from Mr. Arjan Westra, Department of Chemistry, University of Stellenbosch.

2.5 Experimental details: Platinum complexes

N,N-diethyl-*N'*-naphthoylthiourea (0.1401g, 0.4880mmol) and sodium acetate (0.1350g, 0.9920mmol) were dissolved in a 100mL round bottom flask (in an oil bath at 50°C) by the addition of 30mL of a mixture of acetonitrile-water (2:1, v/v) and continuous stirring under inert atmosphere (N_2 gas). Dipotassium tetrachloroplatinate (0.1014g, 0.2443mmol) was dissolved in a dropping funnel by the addition of 30mL of a mixture of acetonitrile-water (1:2, v/v). When no more solid ligand or base was visible in solution, the oil bath temperature was increased to 80°C and the metal solution was added dropwise over a period of 15 minutes with continuous stirring under nitrogen gas. The reacting mixture was stirred for a further hour at the same temperature. The bright yellow product was subsequently allowed to cool down to room temperature before an excess of water was added. The water-insoluble Pt-complex still dissolved in the acetonitrile layer was forced out of solution in this manner. The reaction flask (now consisting of a clear MeCN layer, a clear H_2O layer and the precipitate) was sealed with parafilm and placed in the freezer for a period of *ca.* 24 hours. The crude product mixture was centrifuged and thereafter washed with water.

The melting points of the complexes were obtained using an Electrothermal 9300 melting point apparatus. The C, H, N and S elemental analysis was carried out using a Carlo Erba EA 1108 elemental analyser in the microanalytical laboratory of the University of Cape Town, South Africa. The ^{1}H and ^{13}C nuclear magnetic resonance spectra were all recorded in 5mm tubes in $CDCl_3$. The instrument used was either a Varian Unity 300 spectrometer or a Varian Unity 600 spectrometer operating at 300 and 600MHz for ^{1}H spectra and 75 and 150MHz for ^{13}C spectra. All the ^{1}H and ^{13}C spectra were acquired at 25°C and the chemical shifts are referenced relative to $CDCl_3$ at 7.25ppm and 77.0ppm respectively. All the reagents used were either commercially available or were donations. All chemicals were used without further purification (except for being dried in the appropriate fashion).

***cis*-bis(*N,N*-diethyl-*N'*-naphthoylthioureato)platinum(II); *cis*-[Pt(L^1-*S,O*)$_2$]**

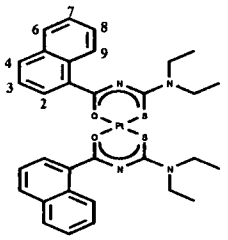

A recrystallised yield of (0.1542g, 0.2018mmol) 84% was recovered. For characterization m.p. 150-154°C, (Found: C, 50.57; H, 4.59; N, 7.39; S, 8.63; calculated for $C_{32}H_{38}N_4O_2PtS_2$ C, 49.92; H, 4.98; N, 7.28; S, 8.33); NMR $\delta_{H/ppm}$ (600MHz, $CDCl_3$): 1.25 (6H, triplet, CH_3), 1.38 (6H, triplet, CH_3), 3.80 (4H, quartet, NCH_2), 3.83 (4H, quartet, NCH_2), 7.12 (2H, triplet, H_8), 7.35 (2H, triplet, H_3), 7.43 (2H, triplet, H_7), 7.81 (2H, doublet, H_6), 7.92 (2H, doublet, H_4), 8.15 (2H, doublet, H_2), 8.93 (2H, doublet, H_9) $\delta_{C/ppm}$ (75MHz, $CDCl_3$): 12.66, 13.46, 45.93, 47.02, 124.82, 125.83, 126.83, 127.34, 128.25, 128.86, 131.44, 132.73, 134.19, 135.95, 167.10, 171.85 $\delta_{Pt/ppm}$ -2700.41 (*cis*), -1980.26 (*trans,* post irradiation).

***cis*-bis(*N,N*-dibutyl-*N'*-naphthoylthioureato)platinum(II); *cis*-[Pt(L^2-*S,O*)$_2$]**

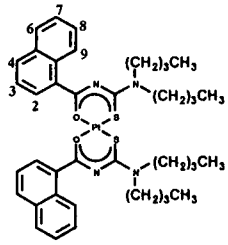

A recrystallised yield of (0.1548g, 0.1763mmol) 73% was recovered. For characterization m.p. 106-109°C, (Found: C, 54.15; H, 6.08; N, 6.02; S, 7.20; calculated for $C_{40}H_{54}N_4O_2PtS_2$ C, 54.46; H, 6.17; N, 6.35; S, 7.27); NMR $\delta_{H/ppm}$ (600MHz, $CDCl_3$): 0.89 (6H, triplet, CH_3), 1.01 (6H, triplet, CH_3), 1.32 (4H, sextet, CH_3CH_2), 1.42 (4H, sextet, CH_3CH_2), 1.67 (4H, heptet, NCH_2CH_2), 1.80 (4H, heptet, NCH_2CH_2), 3.72 (4H, triplet, NCH_2), 3.74 (4H, triplet, NCH_2), 7.09 (2H, triplet, H_8), 7.35 (2H, triplet, H_3), 7.42 (2H, triplet, H_7), 7.81 (2H, doublet, H_4), 7.90 (2H, doublet, H_4), 8.15 (2H, doublet, H_2), 8.94 (2H, doublet, H_9) $\delta_{C/ppm}$ (75MHz, $CDCl_3$): 13.82, 13.86, 20.20, 29.28, 30.08,

30.90, 51.33, 52.42, 124.46, 125.53, 126.65, 127.11, 127.96, 128.63, 131.16, 131.31, 133.95, 135.69, 167.15, 171.47.

***cis*-bis(*N,N*-diethyl-*N'*-3,4,5-trimethoxybenzoylthioureato)platinum(II); *cis*-[Pt(L^3-*S,O*)$_2$]**

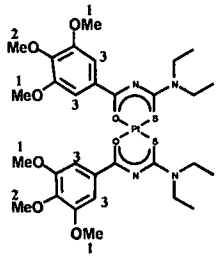

A recrystallised yield of (0.1617g, 0.1903mmol) 79% was recovered. For characterization m.p. 218-221°C (decomposition), (Found: C, 42.43; H, 4.88; N, 6.55; S, 7.00; calculated for $C_{30}H_{46}N_4O_8PtS_2$ C, 42.39; H, 5.46; N, 6.59; S, 7.55); NMR $\delta_{H/ppm}$ (600MHz, $CDCl_3$): 1.29 (6H, triplet, CH_3), 1.32 (6H, triplet, CH_3), 3.75 (4H, quartet, NCH_2), 3.80 (4H, quartet, NCH_2), 3.87 (12H, singlet, H_1), 3.88 (6H, singlet, H_2), 7.55 (4H, singlet, H_3) $\delta_{C/ppm}$ (75MHz, $CDCl_3$): 12.44, 13.09, 30.84, 46.01, 47.06, 56.34, 60.76, 107.45, 132.89, 141.61, 152.62, 166.88, 167.89 $\delta_{Pt/ppm}$ -2723.49 (*cis*), -1982.51 (*trans,* post irradiation).

***cis*-bis(*N,N*-diethyl-*N'*-3,5-dimethoxybenzoylthioureato)platinum(II); *cis*-[Pt(L^4-*S,O*)$_2$]**

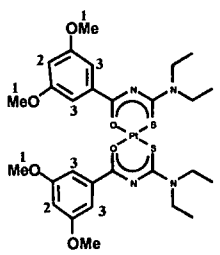

A recrystallised yield of (0.1758g, 0.2237mmol) 88% was recovered. For characterization m.p. 211-212°C, (Found: C, 42.96; H, 4.47; N, 7.06; S, 7.82; calculated for $C_{28}H_{42}N_4O_6PtS_2$ C, 42.58; H, 5.36; N, 7.09; S, 8.17); NMR $\delta_{H/ppm}$ (600MHz, $CDCl_3$): 1.29 (6H, triplet, CH_3), 1.33 (6H, triplet, CH_3), 3.75 (4H, quartet, NCH_2), 3.81 (4H, quartet, NCH_2), 3.84 (12H, singlet, H_1), 6.61 (2H, singlet, H_2), 7.47 (4H, singlet, H_3) $\delta_{C/ppm}$ (75MHz, $CDCl_3$): 12.37, 13.11,

46.09, 47.06, 55.38, 103.72, 107.19, 139.66, 160.39, 167.00, 167.73 $\delta_{Pt/ppm}$ -2706.55 (*cis*), -1974.51 (*trans,* post irradiation).

cis-bis(_N,N_-diethyl-_N'_-4-monomethoxybenzoylthioureato)platinum(II); _cis_-[Pt(L^5-_S,O_)$_2$]

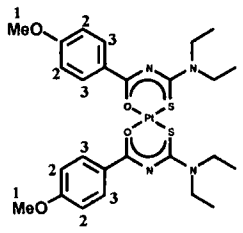

A recrystallised yield of (0.1444g, 0.1989mmol) 82% was recovered. For characterization m.p. 198-200°C, (Found: C, 43.57; H, 4.58; N, 8.91; S, 7.82; calculated for $C_{28}H_{34}N_4O_4PtS_2$ C, 42.79; H, 5.25; N, 7.68; S, 8.79); NMR $\delta_{H/ppm}$ (600MHz, $CDCl_3$): 1.27 (6H, triplet, CH_3), 1.33 (6H, triplet, CH_3), 3.77 (4H, quartet, NCH_2), 3.81 (4H, quartet, NCH_2), 3.87 (6H, singlet, H_1), 6.92 (4H, doublet, H_3), 8.22 (4H, doublet, H_2) $\delta_{Pt/ppm}$ -2733.79 (*cis*), -1990.95 (*trans,* post irradiation).

cis-bis(_N,N_-diethyl-_N'_-camphanoylthioureato)platinum(II); _cis_-[Pt(L^6-_S,O_)$_2$]

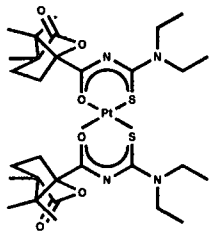

A recrystallised yield of (0.0932g, 0.1140mmol) 47% was recovered. For characterization m.p. 219-222°C§, (Found: C, 43.63; H, 5.51; N, 6.73; S, 7.20; calculated for $C_{30}H_{46}N_4O_6PtS_2$ C, 45.35; H, 6.26; N, 5.12; S, 7.81); $\delta_{Pt/ppm}$ -2691.08 (*cis*), -1972.04 (*trans,* post irradiation).

§ Compares favourably with literature value.[34b]

cis-bis(_N,N_-diethyl-_N'_-benzoylthioureato)platinum(II); _cis_-[Pt(L^7-_S,O_)$_2$]

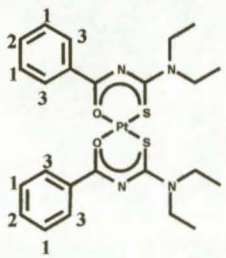

A recrystallised yield of (0.1025g, 0.1539mmol) 63% was recovered. For characterization m.p. 152-156°C, (Found: C, 43.57; H, 4.58; N, 8.91; S, 9.32; calculated for $C_{28}H_{30}N_4O_2PtS_2$ C, 43.30; H, 4.54; N, 8.42; S, 9.63); NMR $\delta_{H/ppm}$ (600MHz, $CDCl_3$): 1.28 (6H, triplet, CH_3), 1.34 (6H, triplet, CH_3), 3.77 (4H, quartet, CH_2), 3.83 (4H, quartet, CH_2), 7.42 (4H, triplet, H_1), 7.51 (2H, triplet, H_2), 8.26 (4H, doublet, H_3) $\delta_{C/ppm}$ (75MHz, $CDCl_3$): 12.34, 13.10, 45.90, 46.97, 128.05, 129.35, 131.34, 137.57, 167.00, 168.42 $\delta_{Pt/ppm}$ -2720.14 (*cis*), -1980.83 (*trans,* post irradiation).

2.5.1 Summary of the structures, synthetic routes and general information for the Pt(II)-complexes synthesised

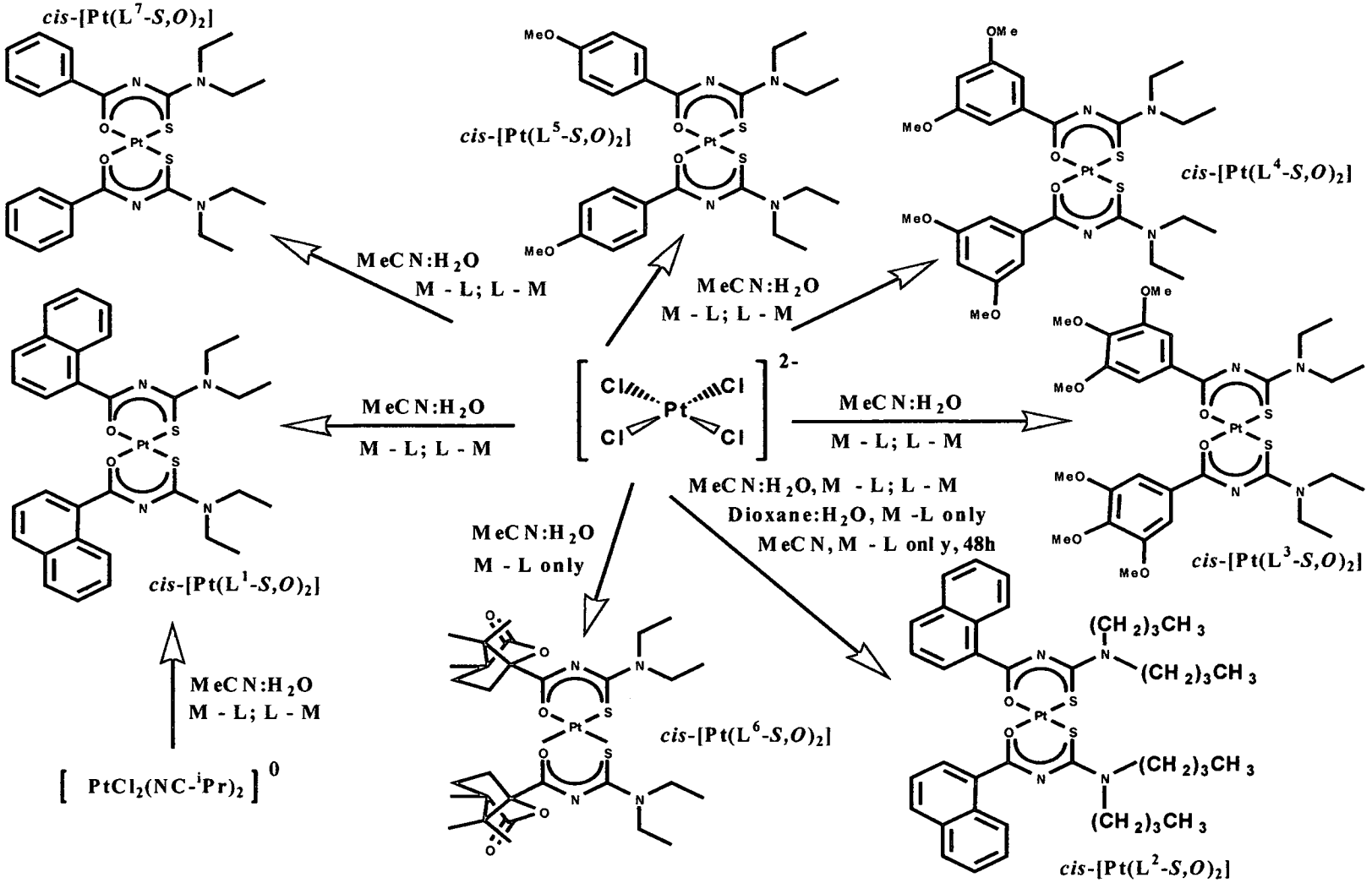

2.6 Experimental details: Palladium complexes

The melting points of the complexes were obtained using an Electrothermal 9300 melting point apparatus. The C, H, N and S elemental analysis was carried out using a Carlo Erba EA 1108 elemental analyser in the microanalytical laboratory of the University of Cape Town, South Africa. The ^{1}H and ^{13}C nuclear magnetic resonance spectra were all recorded in 5mm tubes in $CDCl_3$. The instrument used was either a Varian Unity 300 spectrometer or a Varian Unity 600 spectrometer operating at 300 and 600MHz for ^{1}H spectra and 75 and 150MHz for ^{13}C spectra. All the ^{1}H and ^{13}C spectra were acquired at 25°C and the chemical shifts are referenced relative to $CDCl_3$ at 7.25ppm and 77.0ppm respectively. All the reagents used were either commercially available or were donations. All chemicals were used without further purification (except for being dried in the appropriate fashion).

***cis*-bis(*N,N*-diethyl-*N'*-3,4,5-trimethoxybenzoylthioureato)palladium(II); *cis*-[Pd(L^3-*S,O*)$_2$]**

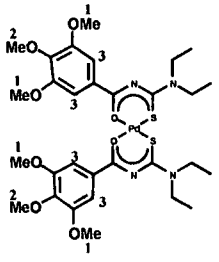

A recrystallised yield of (0.1518g, 0.2005mmol) 87% was recovered. For characterization m.p. 205-208°C, (Found: C, 47.62; H, 5.59; N, 6.55; S, 7.37; calculated for $C_{30}H_{42}N_4O_8PdS_2$ C, 47.33; H, 6.09; N, 7.36; S, 8.42); NMR $\delta_{H/ppm}$ (600MHz, $CDCl_3$): 1.26 (6H, triplet, CH_3), 1.29 (6H, triplet, CH_3), 3.80 (4H, quartet, NCH_2), 3.82 (4H, quartet, NCH_2), 3.86 (12H, singlet, H_1), 3.87 (6H, singlet, H_2), 7.54 (4H, singlet, H_3) $\delta_{C/ppm}$ (75MHz, $CDCl_3$): 12.46, 12.88, 30.70, 46.05, 47.18, 56.13, 60.80, 107.62, 132.60, 141.79, 152.74, 170.36, 171.22.

cis-bis(_N,N_-diethyl-_N'_-3,5-dimethoxybenzoylthioureato)palladium(II); _cis_-[Pd(L^4-_S,O_)$_2$]

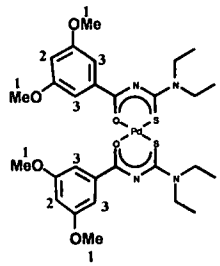

A recrystallised yield of (0.1489g, 0.2136mmol) 92.9% was recovered. For characterization m.p. 198-202°C, (Found: C, 48.22; H, 5.69; N, 7.98; S, 9.15; calculated for $C_{28}H_{42}N_4O_6PtS_2$ C, 47.96; H, 6.04; N, 7.99; S, 9.15); NMR $\delta_{H/ppm}$ (600MHz, $CDCl_3$): 1.28 (6H, triplet, CH_3), 1.32 (6H, triplet, CH_3), 3.82 (4H, quartet, NCH_2), 3.84 (4H, quartet, NCH_2), 3.83 (12H, singlet, H_1), 6.58 (2H, triplet, H_2), 7.44 (4H, doublet, H_3) $\delta_{C/ppm}$ (75MHz, $CDCl_3$): 12.26, 13.10, 46.21, 47.27, 55.35, 103.88, 107.45, 139.17, 160.25, 169.97, 171.18.

cis-bis(_N,N_-diethyl-_N'_-4-monomethoxybenzoylthioureato)palladium(II); _cis_-[Pd(L^5-_S,O_)$_2$]

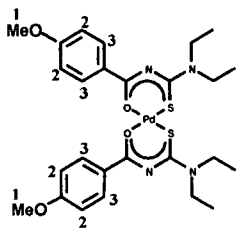

A recrystallised yield of (0.1705g, 0.2675mmol) 86.8% was recovered. For characterization m.p. 186-190°C, (Found: C, 49.60; H, 5.56; N, 8.91; S, 10.10; calculated for $C_{28}H_{34}N_4O_4PtS_2$ C, 48.71; H, 5.97; N, 8.74; S, 10.00); NMR $\delta_{H/ppm}$ (600MHz, $CDCl_3$): 1.27 (6H, triplet, CH_3), 1.32 (6H, triplet, CH_3), 3.83 (4H, quartet, NCH_2), 3.84 (4H, quartet, NCH_2), 3.87 (6H, singlet, H_1), 6.92 (4H, doublet, H_3), 8.19 (4H, doublet, H_2).

2.6.1 Summary of the structures, synthetic routes and general information for the Pd(II)-complexes synthesised.

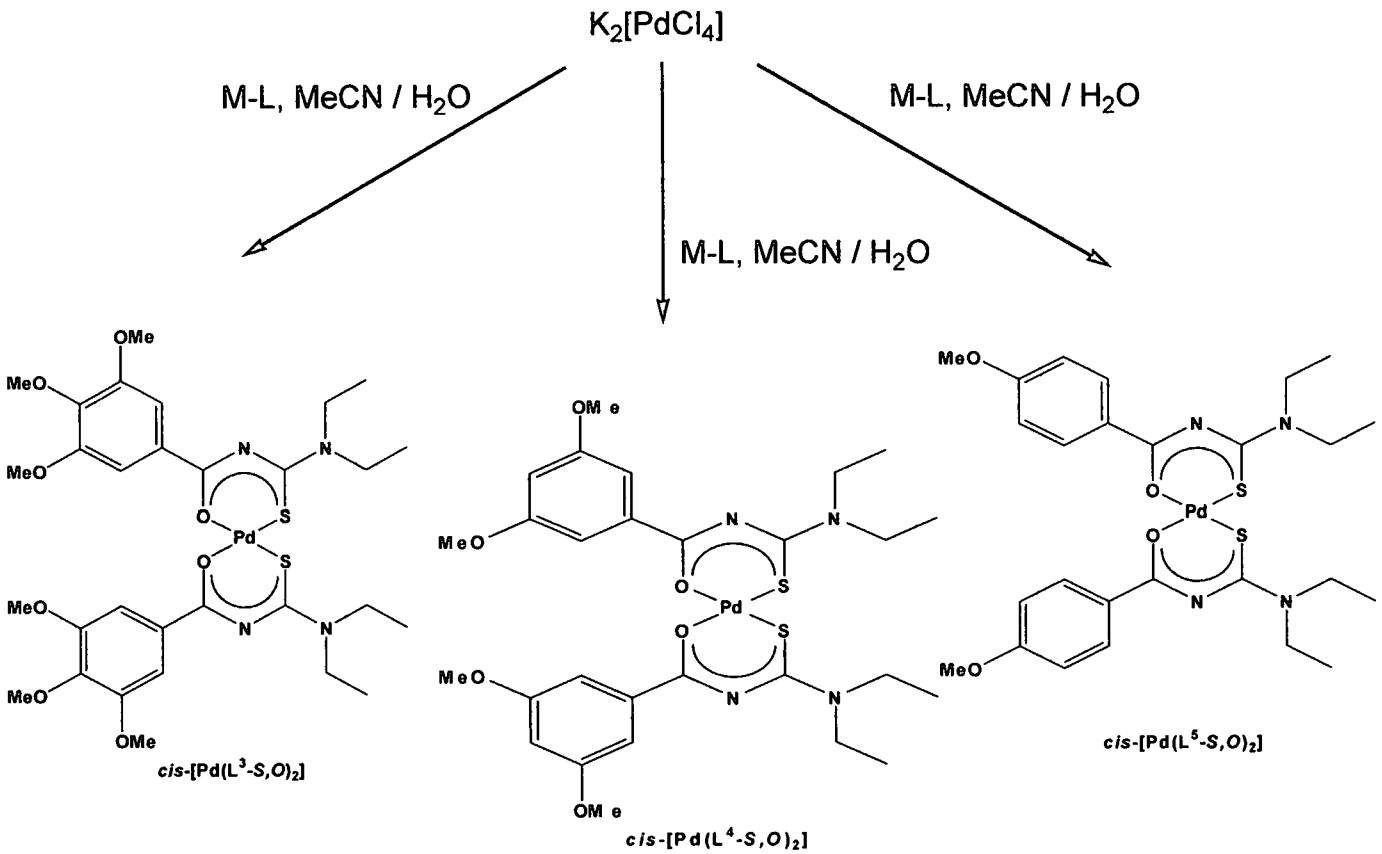

2.7 Conclusion

It is clear from our systematic synthetic study, outlined in this chapter, that the *cis-trans* isomer distribution of these Pd(II)- and Pt(II)-complexes is not determined by the mode or method of synthesis.

Chapter 3:

A RP-HPLC study of the *cis-trans* isomerisation of Pt(II) and Pd(II) complexes: photochemically induced *cis-trans* isomerisation

3. A RP-HPLC study of the *cis-trans* isomerisation of Pt(II) and Pd(II) complexes: photochemically induced *cis-trans* isomerisation

3.1 Separation of *cis*-[M(L-*S,O*)$_2$] and *trans*-[M(L-*S,O*)$_2$] complexes by Reversed Phase High Performance Liquid Chromatography

The platinum(II), palladium(II) and rhodium(III) complexes of some *N,N*-dialkyl-*N'*-acylthioureas, especially the metal complexes of *N*-pyrrolidyl-*N'*-(2,2-dimethylpropanoyl)thiourea, have been shown to be suitable for separation and determination by means of RP-HPLC.[32] Moreover, the favourable physiochemical properties and ease of preparation makes these ligands suitable for the determination of traces of metal ions in process effluents.[10]

As part of the RP-HPLC studies it was noticed that small additional peaks started to appear in the chromatograms after leaving these solutions on the bench top for some period of time. Serendipitously it was then discovered that, when these metal complex solutions (in vials) were left inside the sampling chamber of the HPLC instrument, no significant secondary peaks appeared (see Figures 38 and 39).

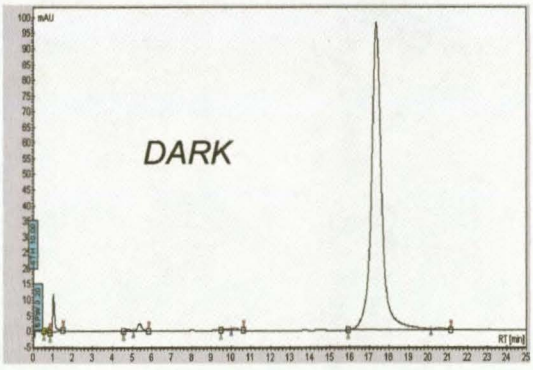

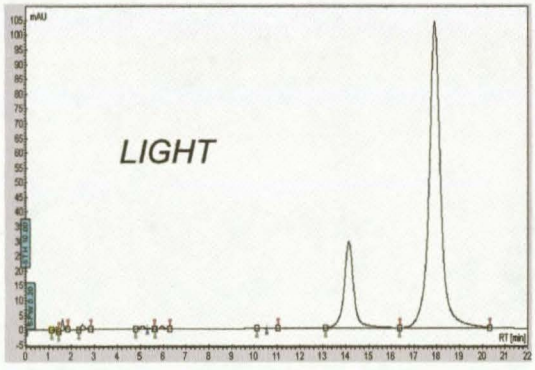

Figures 38 and 39. Chromatograms of a M(L-***S,O***)$_2$ solution in acetonitrile left standing obscured from and exposed to light, respectively.

The absorbance profiles of the two species in Figure 39, obtained by using a diode array photometric detector, (see section 3.9) are nearly identical, suggesting that the two peaks are *cis-trans* isomers of the same compound.

Furthermore, liquid chromatography coupled to electrospray mass spectrometry (LC-ESMS) showed that the two peaks in the Figure 39 (pg. 65) have values of m/z 846.83 and 846.57, respectively (Figure 40). This confirms that the second peak in the chromatogram is most likely the *trans*-isomer of the starting *cis*-complex.

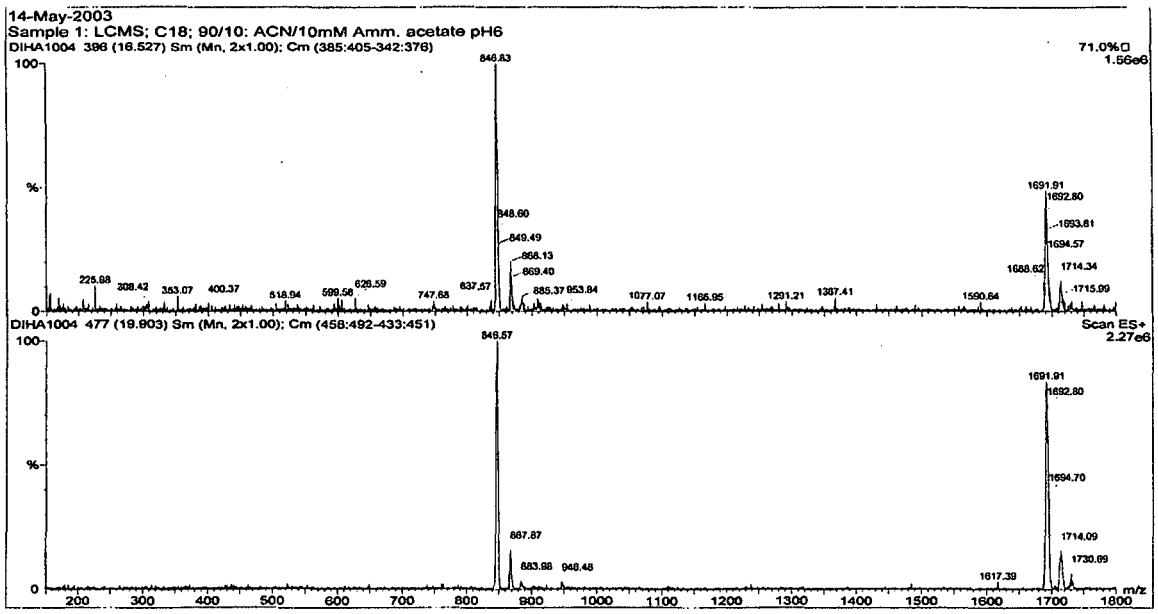

Figure 40. LC-ESMS data confirming that the two peaks in the chromatograms obtained were indeed *cis* and *trans* isomers of one compound.

3.2 The isomerisation of *cis*-[Pt(L^3-*S,O*)$_2$] to *trans*-[Pt(L^3-*S,O*)$_2$]

After the observations of section 3.1 were made (photo-induced isomerisation of the platinum complexes) it was apparent that a more controlled experiment had to be set up where all factors possibly contributing to the isomerisation process could be controlled and systematically varied. These factors included: flux of photons used to irradiate the solutions, the wavelength of the light used, the solvent, concentration and temperature (Figure 41).

The following items were used in the experiments that followed: a conventional slide projector (150 W quartz-halogen lamp), photographic optical filters blue (80B), yellow (Y2) and red (25A) providing coloured light (Figure 42), a water-jacketed cylindrical glass tube with a volume of *ca.* 30 cm^3 fitted with a rubber septum and a photon flux meter (LI-250 quantum

meter, Lincoln, LI-COR, USA). For the purpose of irradiation, the glass cylinder was covered with aluminum foil, except for the ends, eliminating all other sources of light.

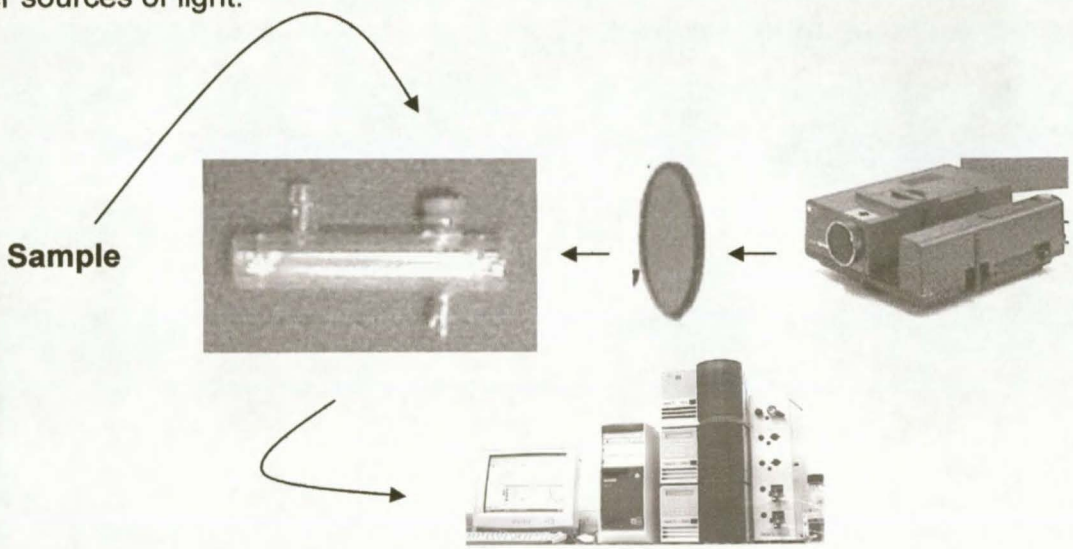

Figure 41. The controlled set-up used to study the *cis-trans* isomerisation of the ***cis***-[M(L-***S,O***)$_2$] complexes.

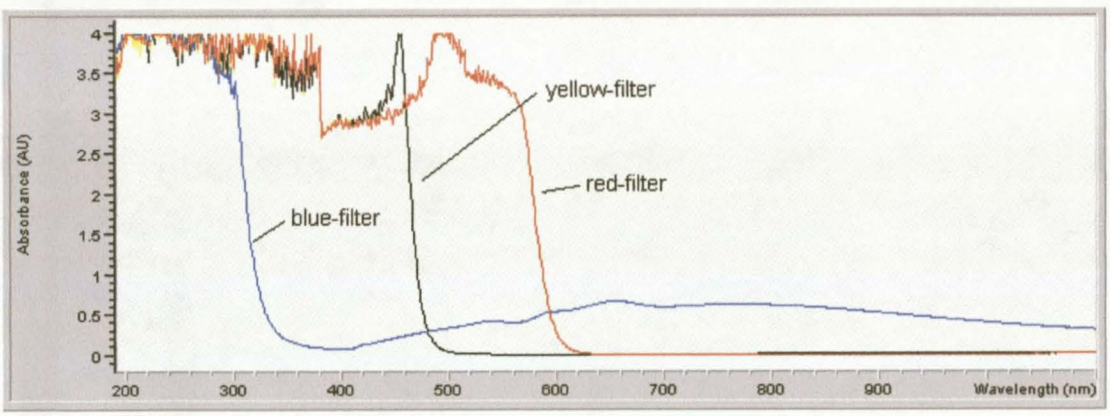

Figure 42. The UV/VIS spectra taken of the blue (80B), yellow (Y2) and red (25A) photographic filters used in the controlled set-up.

At this point it has to be reiterated that control experiments were performed at all times, at the same concentration, temperature and in the same solvent (acetonitrile unless otherwise stated). Subsequent injections of this sample at random times (kept in the dark) yielded chromatograms exactly like that depicted in Figure 43 for a fresh sample. Furthermore, the *cis-trans* isomer distribution will hereafter be discussed in terms of a defined K_e-value (K_e = [peak area]$_{trans}$/[peak area]$_{cis}$). This value can be defined as a conditional

steady-state and is not a true equilibrium value because the parameters controlled during irradiation change post-injection.

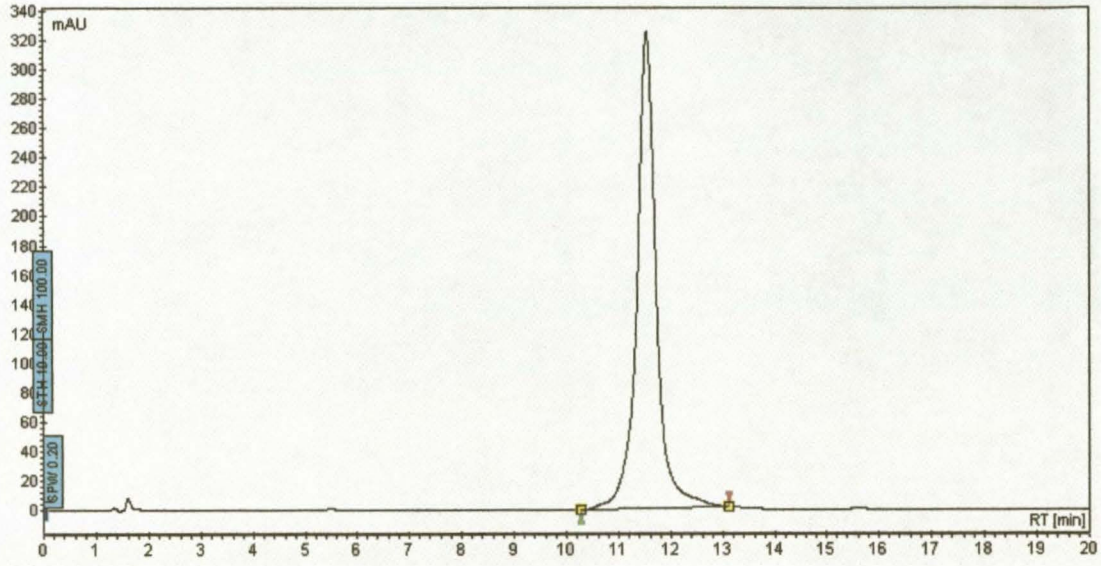

Figure 43. A chromatogram of a fresh solution of ***cis***-[Pt(L^3-***S,O***)$_2$] in acetonitrile (t_R = 11.5 min).

The sample, ***cis***-[Pt(L^3-***S,O***)$_2$], was dissolved at concentrations of 200µg.cm^{-3} (acetonitrile) in the water-jacketed glass cylinder. After injection of the fresh sample, the foil was removed from the ends of the glass cylinder and the light source was switched on. The results, in the form of K_e-values, can be summarised in a graph such as the one depicted in Figure 44.

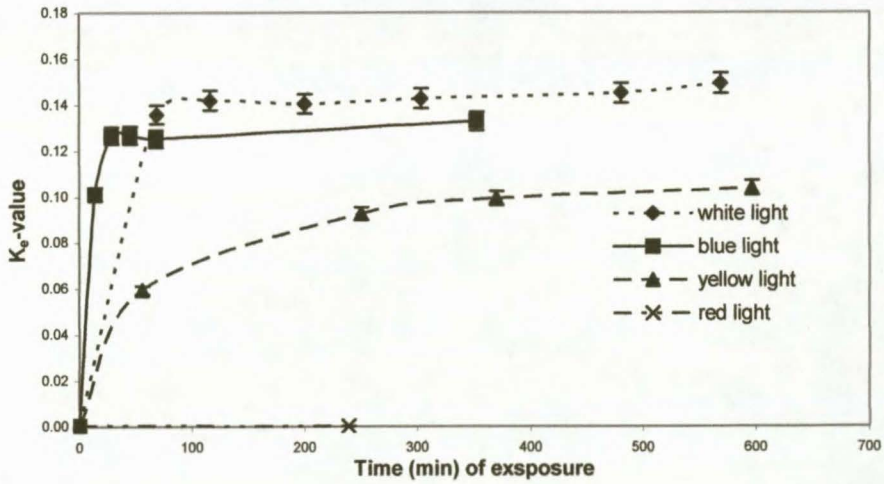

Figure 44. A plot of the K_e-values obtained for ***cis***-[Pt(L^3-***S,O***)$_2$] after irradiation with white, blue, yellow and red light respectively (MeCN, 20°C).

Figure 44 clearly shows that, when ***cis***-[Pt(L^3-***S,O***)$_2$] is irradiated, it reaches a *cis-trans* steady-state after a time of *ca.* 100 minutes for white, blue and yellow light. When this light was red (radiation cut-off at *ca.* 600nm from Figure 42), no isomerisation took place. When the irradiating light was white or blue (radiation cut-off at 300nm for blue light), K_e-values of *ca.* 0.14 were obtained in acetonitrile at 20°C. When the irradiating light was yellow (radiation cut-off at *ca.* 480nm) a K_e-value of *ca.* 0.09 was obtained.

3.3 The isomerisation of *cis*-[Pt(L^3-*S,O*)$_2$]: The effect of solvent

It is known that for monodentate complexes of this nature the polarity of the solvent of dissolution has an effect on the stability, and therefore equilibrium, of the two isomers.[7,13] The *trans* complex has a zero dipole moment by virtue of its planar symmetrical structure, while the *cis* complex is expected to have a non-zero dipole moment (δ^+). In solvents with a higher dielectric constant, the *cis* complexes are expected to be stabilized relative to the *trans* complexes.

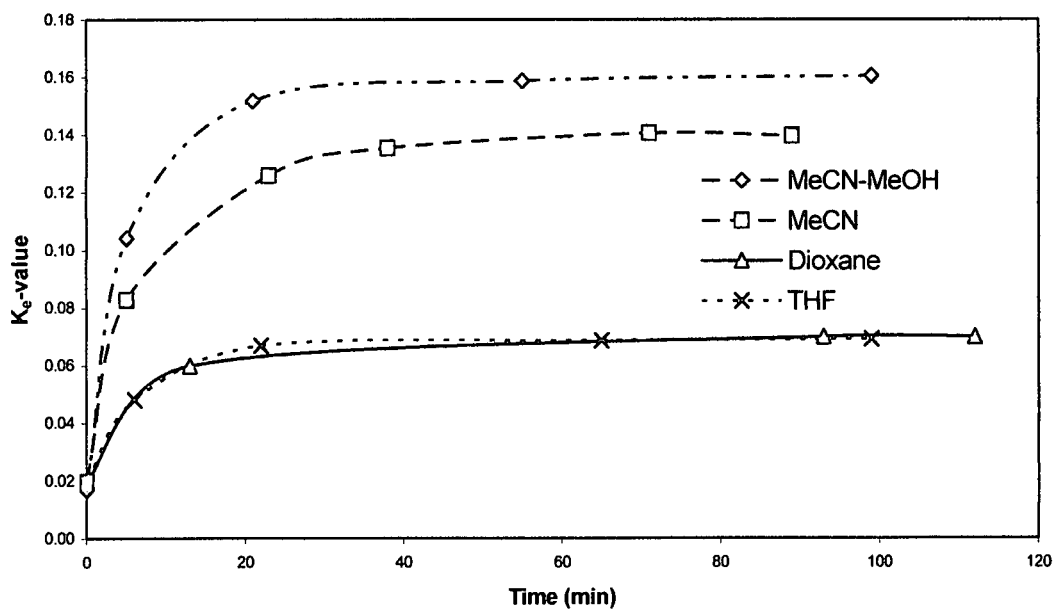

Figure 45. The K_e-values of 100 µg.cm^{-3} solutions of ***cis***-[Pt(L^3-***S,O***)$_2$] in solvents/solvent-mixtures of differing polarity.

Because ***cis***-[Pt(L^3-***S,O***)$_2$] was only slightly soluble in methanol at concentrations of 100 µg.cm^{-3}, a mixture of acetonitrile and methanol was used in the study of a possible solvent effect. Acetonitrile, THF and 1,4-dioxane were the other solvents used (in order of decreasing polarity). In contrast to what was observed for the (similar) monodentate complexes of platinum(II)[7], more polar solvents or solvent-mixtures appear to favour the *trans*-isomer in the case of the bidentate ***cis***-[Pt(L^3-***S,O***)$_2$]; as inferred from the respective K_e-values of the steady-state (Figure 45).

Table 5. Summary of solvents used, their dielectric constants and K_e-values obtained for ***cis***-[Pt(L^3-***S,O***)$_2$].

Solvent	MeCN	MeCN/MeOH	THF	Dioxane
Dielectric constant	36.6	36.6 and 32.9	7.6	2.2
K_e-value	0.14	0.16	0.07	0.07

This apparent increased stability of the *trans*-isomer in a more polar solvent suggests that other factors must be involved besides the polarity of the complex molecule (and the subsequent stabilization thereof) itself.

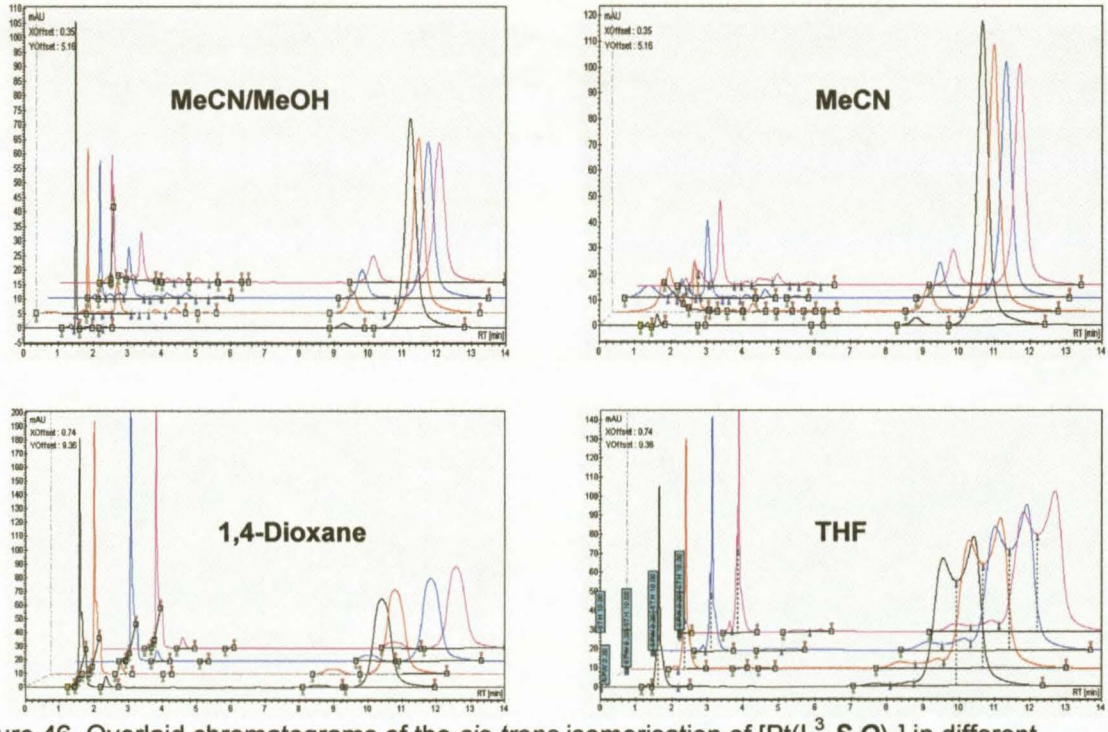

Figure 46. Overlaid chromatograms of the *cis-trans* isomerisation of [Pt(L^3-***S,O***)$_2$] in different solvents (white light, 20°C). Additional peaks could be photodecomposition products, see section 3.7.

With acetonitrile/methanol (50%, v/v) and pure acetonitrile solutions, adequate separation is obtained for the ***cis***- and ***trans***-isomers of [Pt(L^3-***S,O***)$_2$]. Although good symmetry and separation is still obtained, the chromatograms of [Pt(L^3-***S,O***)$_2$] dissolved in 1,4-dioxane show much broader peaks than those obtained in the more polar solvents. When dissolved in THF, the ***cis***- and ***trans***-peaks (which are both split) of [Pt(L^3-***S,O***)$_2$] are poorly separated and the resulting K_e-value therefore carries a greater margin of error.

3.4 Other platinum complexes studied in acetonitrile

The complexes, ***cis***-bis(*N,N*-diethyl-*N'*-camphanoylthioureato)platinum(II), ***cis***-[Pt(L^6-***S,O***)$_2$], and ***cis***-bis(*N,N*-diethyl-N'-pivaloylthioureato)platinum(II), ***cis***-[Pt(L^8-***S,O***)$_2$], were synthesized (donation from A. Westra in the case of ***cis***-[Pt(L^8-***S,O***)$_2$]) in order to investigate the effect of bulkiness and of having an acyl group on the carbonyl moiety instead of having an aroyl group on the carbonyl moiety.

Experiments were conducted at 20°C in acetonitrile at concentrations similar to that mentioned in section 3.2. White light was used for irradiation.

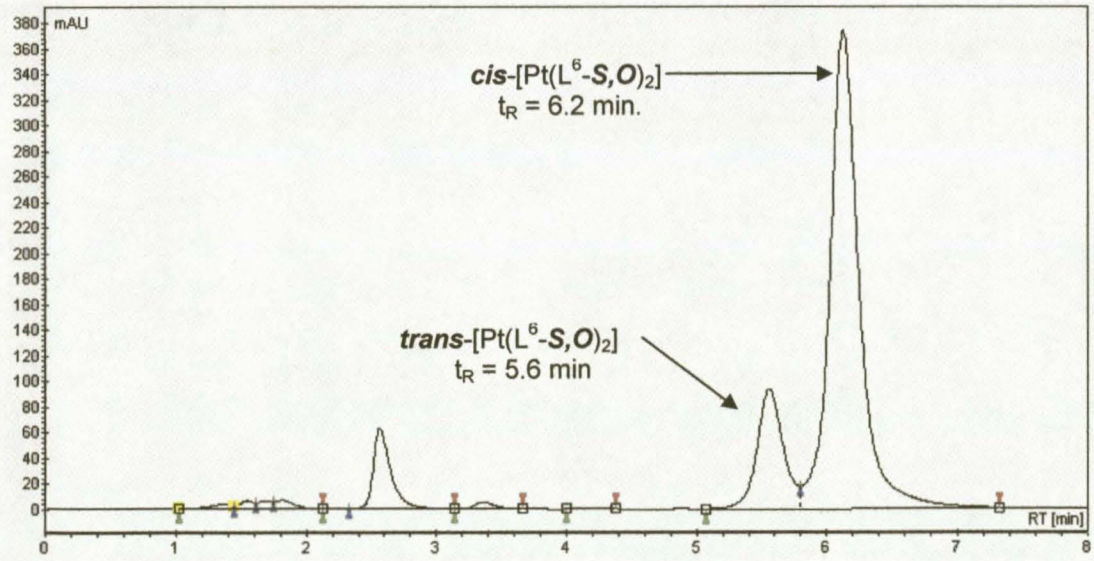

Figure 47. A chromatogram of an isomerised solution of ***cis***-[Pt(L^6-***S,O***)$_2$] in acetonitrile at 20°C (random time, $t \neq 0$). Additional peaks could be photodecomposition products, see section 3.7.

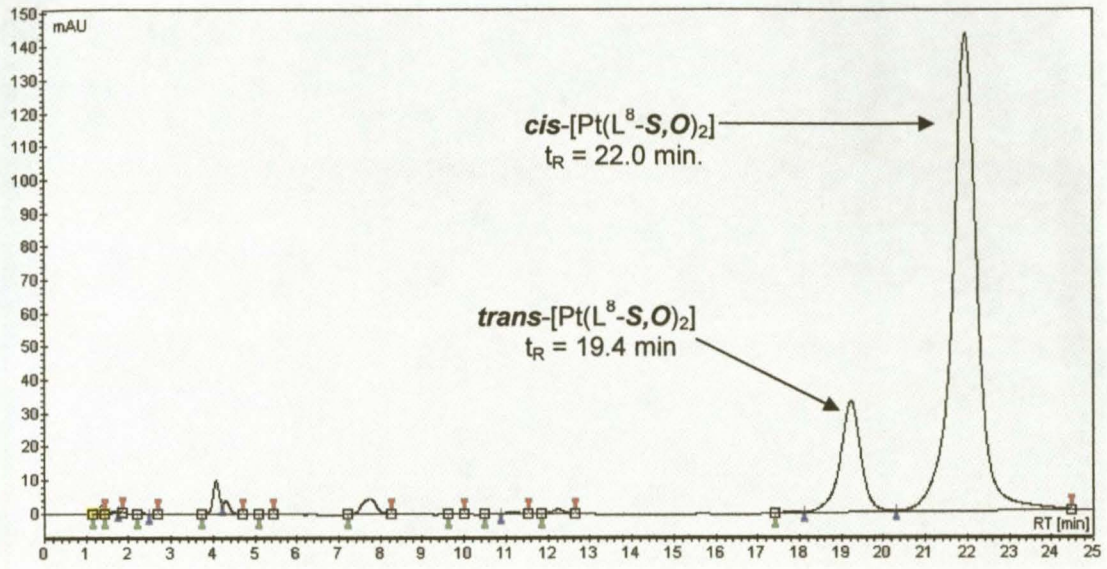

Figure 48. A chromatogram of an isomerised solution of ***cis***-[Pt(L^8-***S,O***)$_2$] in acetonitrile at 20°C (random time, t ≠ 0). Additional peaks could be photodecomposition products, see section 3.7.

Figure 49 on page 73 shows the K_e-values obtained for ***cis***-[Pt(L^6-***S,O***)$_2$] and ***cis***-[Pt(L^8-***S,O***)$_2$] with white light radiation in acetonitrile.

[Pt(L^6-***S,O***)$_2$] is the platinum complex with the highest K_e-value for which the isomerisation process was followed. The bulky camphanoyl moiety on the carbonyl end of the ligand might play a decisive role in this regard. However, [Pt(L^8-***S,O***)$_2$], which has a tertiary butyl group on the carbonyl side of the ligand, has a higher K_e-value than the larger more electron-donating trimethoxy, dimethoxy and monomethoxy variations of the complex. Therefore, it can be assumed that the electron donating abilities of the methoxy groups have a limited influence on the stabilization of the *trans*-isomer or an intermediate state during the reaction.

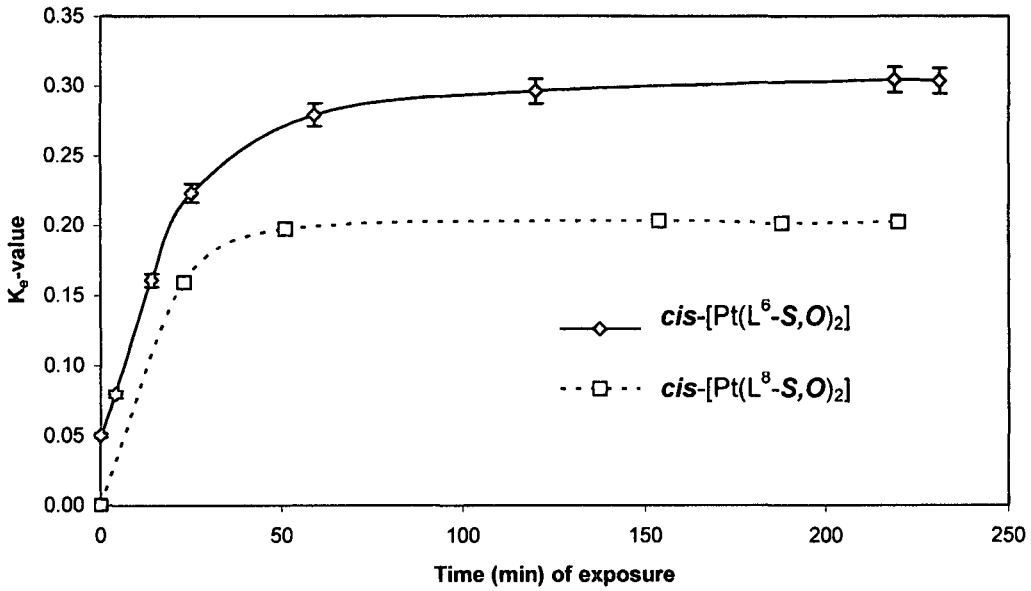

Figure 49. K_e-values of [Pt(L^6-***S,O***)$_2$] and [Pt(L^8-***S,O***)$_2$] dissolved in acetonitrile at 20°C, and irradiated with white light.

3.5 The isomerisation of *cis*-[Pd(L^3-*S,O*)$_2$] to *trans*-[Pd(L^3-*S,O*)$_2$]

After the observations of section 3.1 were made (photo-induced isomerisation of the platinum complexes), we were very interested in the behavior of the palladium analogues of these platinum complexes. Because palladium complexes are generally more facile than their platinum counterparts (although existing literature only deals with the isomerisation of monodentate palladium complexes), the palladium complexes posed an exciting prospect with regard to chromatographic time studies concerning the isomerisation process.

Solutions of 200 µg.cm^{-3} ***cis***-[Pd(L^3-***S,O***)$_2$] were prepared in volumetric flasks by dissolving crude complex in acetonitrile (HPLC grade). Two volumetric flasks were left on the windowsill of the laboratory; one exposed to the incoming light (sunlight and fluorescent) and the other covered in aluminum foil (control sample); the following was observed. Both solutions were injected

into the HPLC system at time zero. Thereafter, samples were injected at random, but recorded, times (Figure 50).

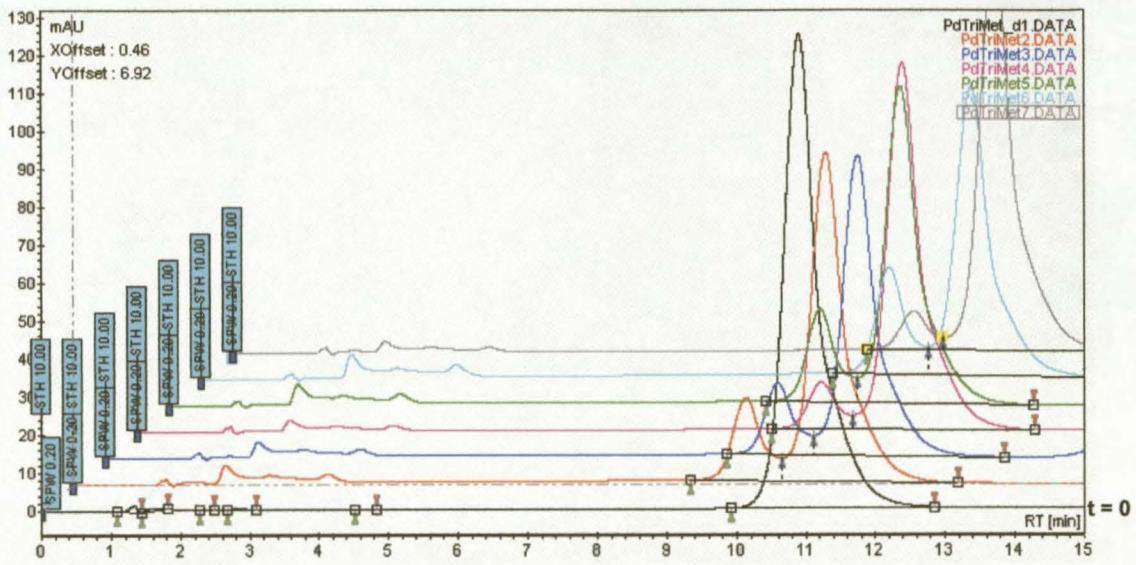

Figure 50. Overlaid chromatograms of [Pd(L^3-***S,O***)$_2$] exposed to sunlight and fluorescent light; injections made at random times (***cis***-[Pd(L^3-***S,O***)$_2$] and ***trans***-[Pd(L^3-***S,O***)$_2$], t_R's = 11 and 9 minutes respectively). Additional peaks could be photodecomposition products, see section 3.7.

From Figure 50 it is clear that there is only one main species present in the initial chromatogram (t = 0), ***cis***-[Pd(L^3-***S,O***)$_2$]. After injections were made at random times it became apparent that the *trans* species did not develop at a constant rate to a point of a *cis-trans* steady-state. In fact the isomer distribution varied with time. This isomerisation also clearly took place very rapidly, as it was observed then that higher K_e-values were obtained in the morning when the light was bright as opposed to in the evening (or in times of cloud cover) when the light was less intense. The control experiment always yielded the same chromatogram with only one peak corresponding to the *cis* isomer, i.e. no *cis-trans* isomerisation.

Solutions of ***cis***-[Pd(L^3-***S,O***)$_2$] in acetonitrile, at concentrations of 200 $\mu g.cm^{-3}$, were made up in acetonitrile and then subjected to irradiation using the system described in section 3.2. A sample was withdrawn and injected into the HPLC, after which the light source was switched on and the foil removed

from the ends of the cylinder. The results, in the form of K_e-values, are summarized in Figure 51.

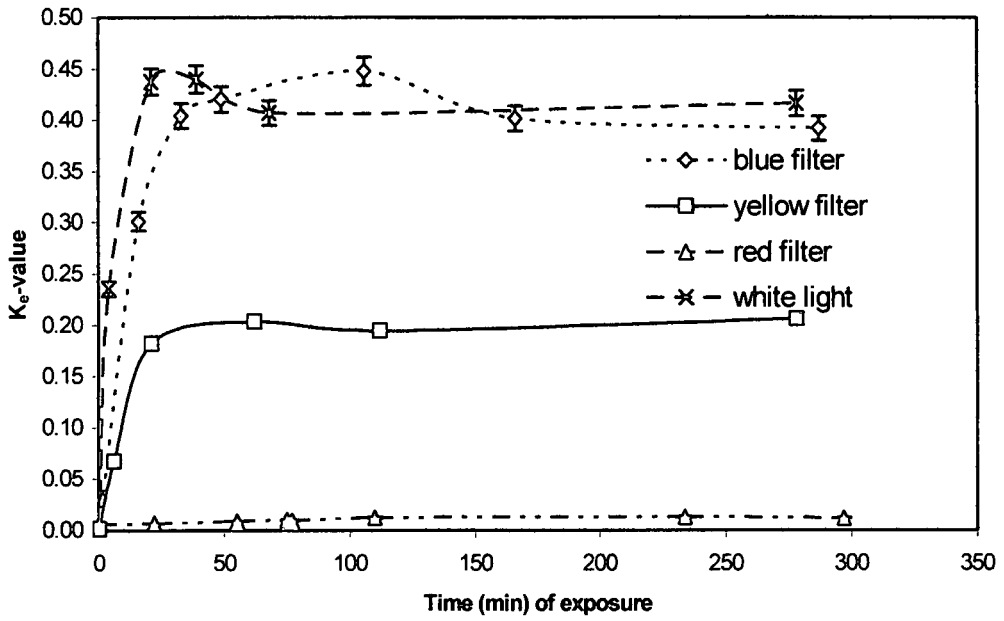

Figure 51. A plot of the K_e-values obtained for ***cis***-[Pd(L^3-***S,O***)$_2$] dissolved in MeCN after irradiation with white, blue, yellow and red light respectively (20°C).

Figure 51 clearly shows that when ***cis***-[Pd(L^3-***S,O***)$_2$] is irradiated it reaches a *cis-trans* steady-state at a time of *ca.* 50 minutes for white, blue and yellow light. When this light is red (radiation cut-off at ca. 600nm from Figure 42) no isomerisation takes place at all. The steady-state is reached markedly faster for the palladium analogue of the platinum complex (*ca.* 100 minutes). When the irradiating light was white or blue (radiation cut-off at 300nm for blue light), K_e-values of 0.40 were obtained in acetonitrile at 20°C.

As was the case with the ***cis***-[Pt(L^3-***S,O***)$_2$], the graph associated with yellow light poses an interesting question. A steady-state K_e-value of *ca.* 0.20 is obtained for ***cis***-[Pd(L^3-***S,O***)$_2$] in acetonitrile at 20°C irradiated with yellow light. Possibly this is because, when the yellow filter is used, fewer photons of the correct energy interacts with the system, therefore causing fewer *cis* complexes to isomerise to the *trans* complex. To test this theory, an experiment was set up were the light source was brought much closer to the glass cylinder, thereby reducing the loss of photons.

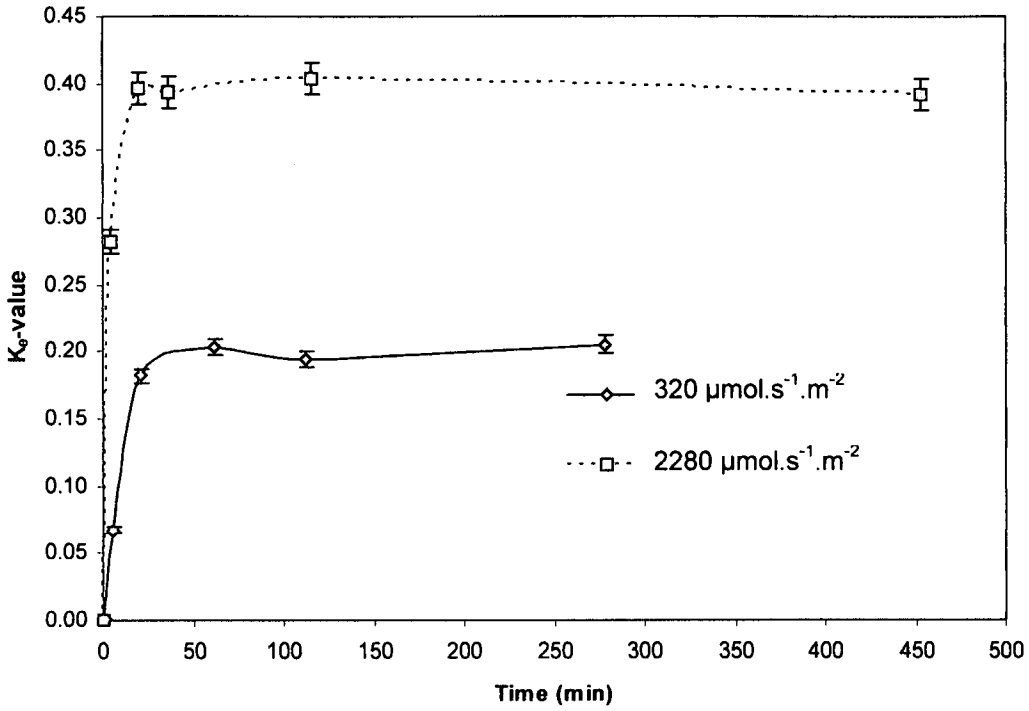

Figure 52. The comparative K_e-values obtained for ***cis***-[Pd(L^3-***S,O***)$_2$] in acetonitrile when lower and higher intensities of yellow light were employed.

Figure 52 clearly indicates that the flux of photons significantly influences the steady-state value K_e. When the intensity of the yellow light was increased from the initial 320 to 2280 µmol.s^{-1}.m^{-2}, the same K_e-value was obtained for yellow light (0.40) as was previously obtained for blue or white light irradiation.

The effect of temperature was subsequently investigated for a solution of ***cis***-[Pd(L^3-***S,O***)$_2$] in acetonitrile, also irradiated with yellow light. K_e-values obtained at "low" intensity and at 20°C (steady-state K_e-value = 0.20) were used as one set of data points and a second experiment was performed at 50°C with yellow light of equal intensity. The result obtained from this experiment clearly indicates that temperature has a definite effect on the *cis-trans* equilibrium. At 50°C an equilibrium K_e-value (acetonitrile) of 0.06 was obtained (Figure 53).

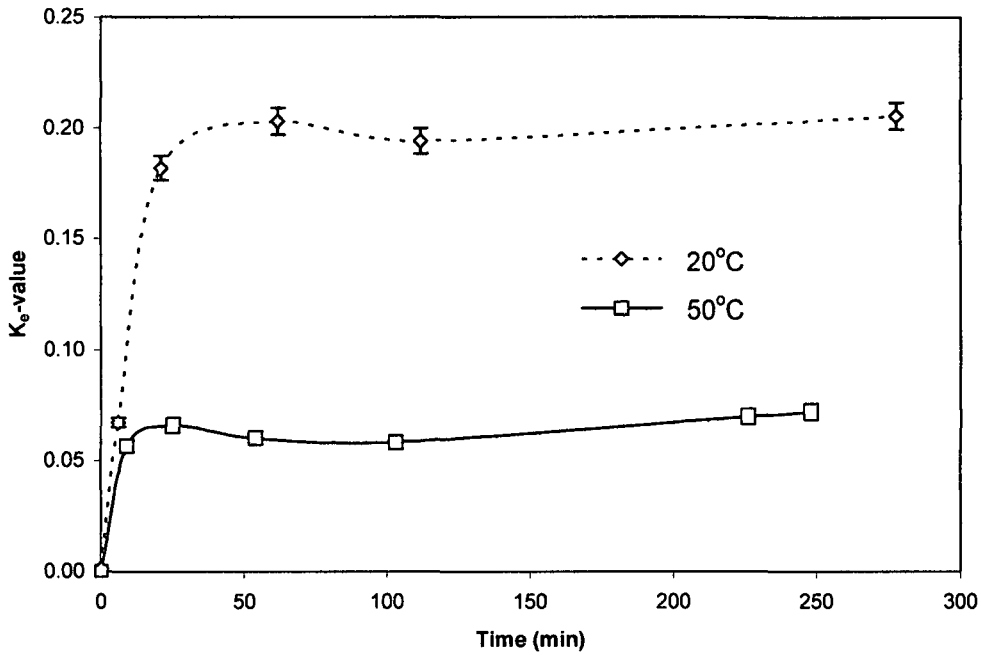

Figure 53. The comparative K_e-values obtained for ***cis***-[Pd(L^3-***S,O***)$_2$] in acetonitrile at 20°C and 50 °C.

For a six-coordinate, monodentate, ruthenium(II) complex a photo-induced isomerisation with thermal reversibility has been observed (see Figure 19, Chapter 1).[23] Because of the results depicted in Figure 53, the question arose whether a solution of [Pd(L-***S,O***)$_2$], at a *cis-trans* equilibrium, also possesses such a thermal backward reaction, thereby yielding pure ***cis***-[Pd(L-***S,O***)$_2$].

A solution of ***cis***-[Pd(L^3-***S,O***)$_2$] in acetonitrile was irradiated for a period of time until the solution reached it's *cis-trans* equilibrium (room temperature, K_e-value = 0.43). Three amber HPLC vials, also covered with aluminum foil, were filled with the above-mentioned isomerised solution. The three vials were kept at temperatures of 0°C, 20°C, and 40°C respectively. The chromatogram obtained at time = zero were used as the first data point for all three samples.

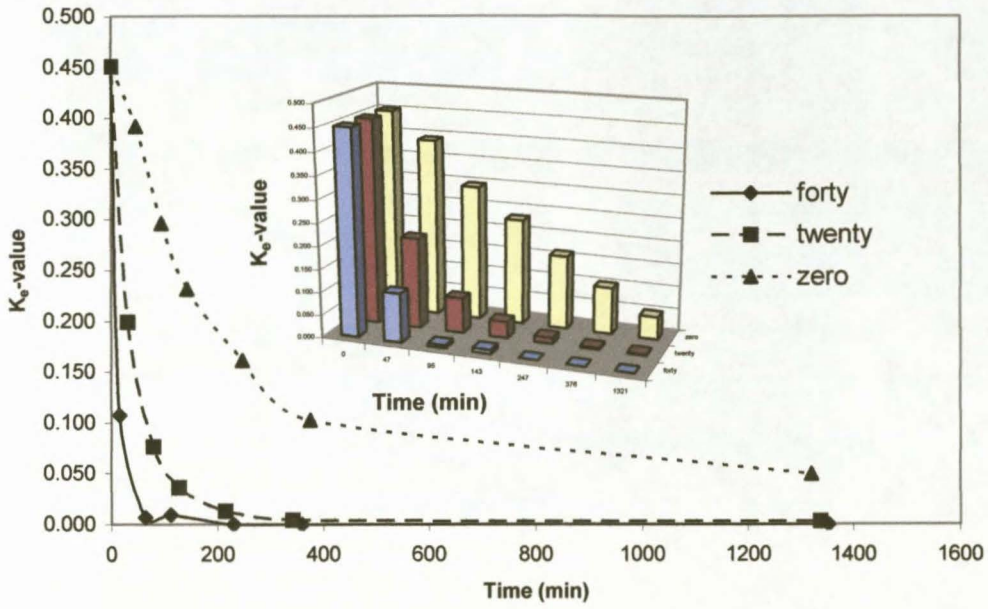

Figure 54. (including 3D inlay). Evidence of a thermally controlled *trans-cis* isomerisation of **Pd**(L^3-***S,O***)$_2$.

From Figure 54 it is clear that the *cis-trans* photo-induced isomerisation of Pd(L^3-***S,O***)$_2$ is thermally reversible. At a constant temperature of 40°C the system reaches a K_e-value of 0.007 after just 63 minutes, while at a constant temperature of 0°C the system still maintains a K_e-value of 0.30 after *ca.* 90 minutes (the second set of data points in the 0°C and 40°C series carries an inherent error originating from the time taken for the respective vials to reach the specified temperature). The isomerisation can therefore, at this stage, be represented as follows:

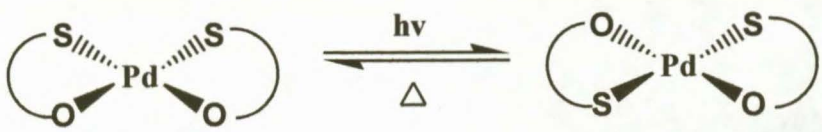

cis-[Pd(L-***S,O***)2] ***trans***-[Pd(L-***S,O***)2]

Figure 55. The photo-induced, thermally reversible, *cis-trans* isomerisation of [Pd(L-***S,O***)$_2$].

3.6 The *cis-trans* isomerisation of the methoxy-series of complexes for platinum and palladium

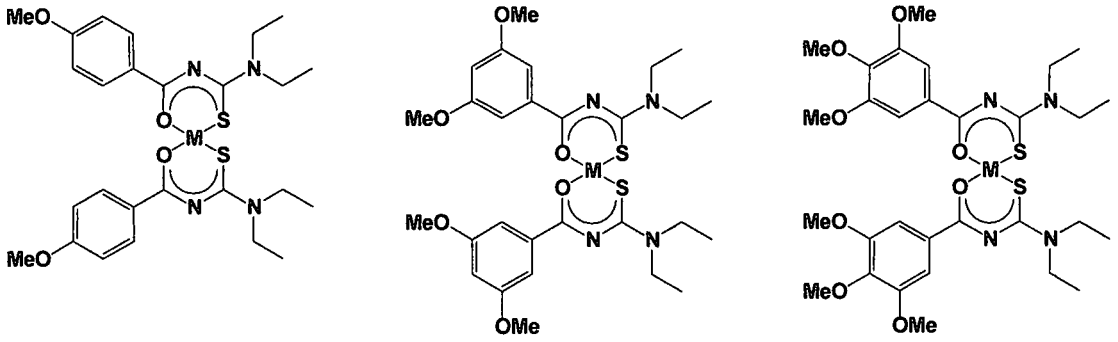

cis-[M(L^5-*S,O*)$_2$] *cis*-[M(L^4-*S,O*)$_2$] *cis*-[M(L^3-*S,O*)$_2$]

Figure 56. The series of ***cis***-[M(L-***S,O***)$_2$] complexes synthesized [M = Pt(II) and Pd(II)].

As was discussed in detail in chapter 2, a complete series of methoxy complexes (Figure 56) was synthesised for platinum(II) and palladium(II). Methoxy groups are known to be resonance-donating and, in the past, this has been argued to have an effect on the *cis-trans* distribution. The *cis* geometry is thought of as being more stable, since the two sulphur atoms (having a more significant *trans* influence) are not *trans* to one another, but rather *trans* to the oxygen donor atoms (smaller *trans* influence).

Solutions containing 200 µg.cm^{-3} pure ***cis***-[Pt(L^x-***S,O***)$_2$] (x = 3-5) complex were dissolved in acetonitrile inside the glass cylinder. An injection was made and a chromatogram obtained representing a fresh sample in all cases. For the investigation into the effect, one, two or three methoxy-groups might have on the isomerisation process, and possibly *cis-trans* equilibrium, white light was used as the light of irradiation.

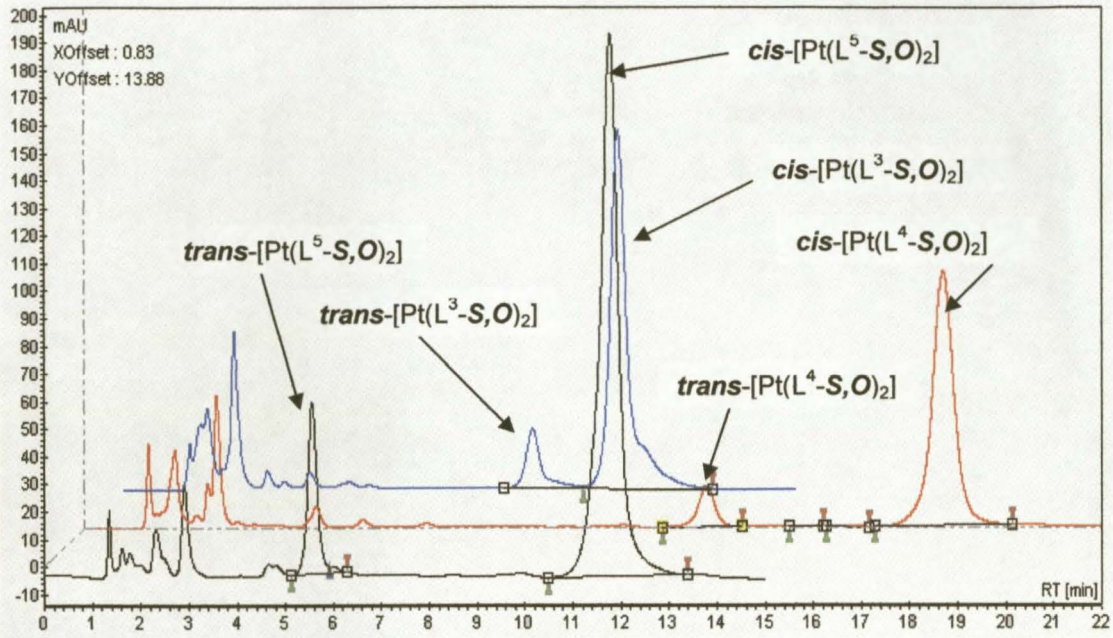

Figure 57. Chromatograms of isomerised acetonitrile solutions of [Pt($L^{3,4,5}$-***S,O***)$_2$] at 20°C (white light). Additional peaks could be photodecomposition products, see section 3.7.

Figure 57 is a representation of the chromatograms of isomerised solutions (random time, t ≠ 0) of ***cis***-[Pt(L^x-***S,O***)$_2$] (x = 3-5). As can be seen from the above overlaid representation, the separation and retention times (t_R's) of the *cis-* and *trans*-isomers differ greatly in going from the monomethoxy to the dimethoxy to the trimethoxy platinum(II) complexes (Table 6).

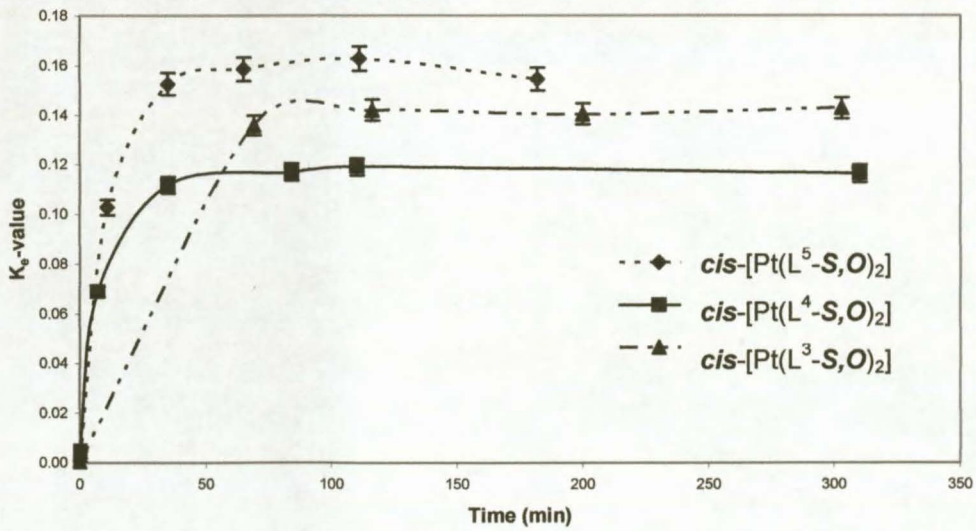

Figure 58. The K_e-values of [Pt(L^x-***S,O***)$_2$] (x = 3-5) in acetonitrile at 20°C.

Figure 58 indicates K_e-values of 0.12, 0.14 and 0.16 for ***cis***-[Pt(L^4-***S,O***)$_2$], ***cis***-[Pt(L^3-***S,O***)$_2$] and ***cis***-[Pt(L^5-***S,O***)$_2$] respectively. As discussed earlier in section 3.6 and also in section 2.2.3, it is speculated that the electron donating capabilities of the methoxy groups might increasingly stabilize a *trans* conformation. From Figure 58 the dimethoxy complex of platinum has a *cis-trans* equilibrium K_e-value of 0.12 in acetonitrile at 20°C. The trimethoxy complex of platinum shows increased *trans*-isomer stability over the dimethoxy complex with a *cis-trans* equilibrium K_e-value of 0.14 in acetonitrile at 20°C. However, this trend is not followed by the monomethoxy complex of platinum with ***cis***-[Pt(L^5-***S,O***)$_2$] exhibiting a K_e-value of 0.16 in acetonitrile at 20°C. Table 6 summarizes the *cis-trans* isomerisation results for ***cis***-[Pt(L^x-***S,O***)$_2$] (x = 3-5) in acetonitrile at 20°C (irradiation with white light).

Table 6. General information regarding Figure 57 and Figure 58.

Complex	[Pt(L^3-***S,O***)$_2$]		[Pt(L^4-***S,O***)$_2$]		[Pt(L^5-***S,O***)$_2$]	
Isomer	***cis***	***trans***	***cis***	***trans***	***cis***	***trans***
t_R/min	12.0	10.2	18.8	13.8	11.5	5.5
R_s	2.1		8.3		7.3	
K_e-value	0.14		0.12		0.16	

Solutions containing 200 µg.cm^{-3} pure ***cis***-[Pd(L^x-***S,O***)$_2$] (x = 3-5) complex were dissolved in acetonitrile inside the glass cylinder. An injection was made and a chromatogram obtained for a fresh sample in all cases. For the investigation into the effect that one, two or three methoxy-groups might have on the isomerisation process, and possibly *cis-trans* equilibrium, white light was used as the light of irradiation.

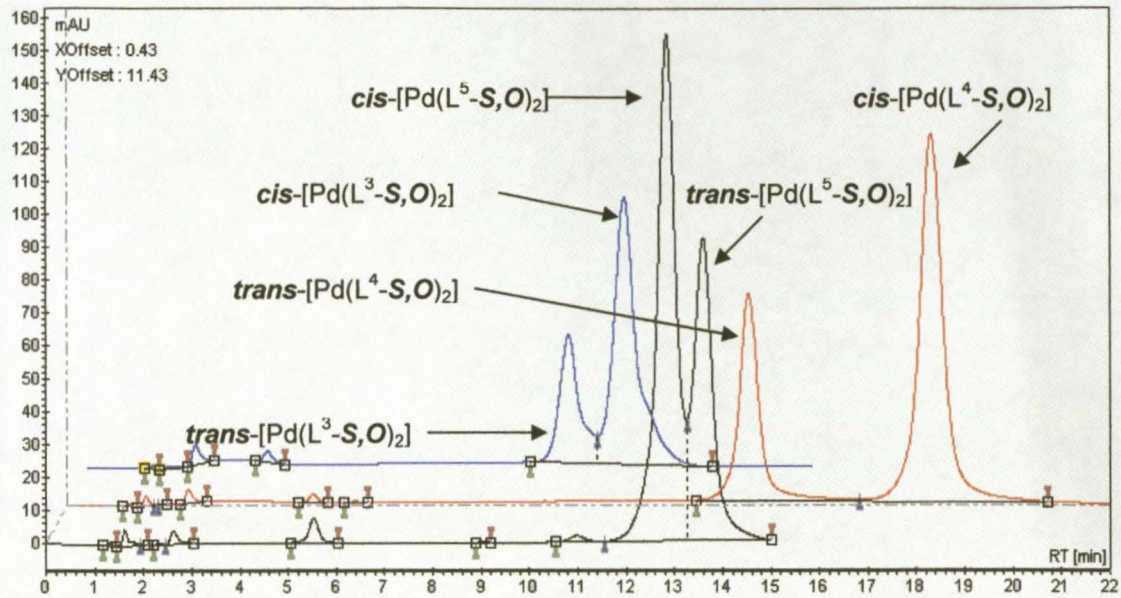

Figure 59. Chromatograms of isomerised acetonitrile solutions of [Pd(L^x-***S,O***)$_2$] (x = 3-5) at 20°C (white light). Additional peaks could be photodecomposition products, see section 3.7.

As was seen in the chromatograms of the isomerised solutions of the methoxy-platinum complexes (Figure 58 and Table 6), the t_R's and the separation of the *cis*- and *trans*-isomers differ greatly in going from monomethoxy to dimethoxy to trimethoxy substitution in the palladium complexes. The equilibrium K_e-values for ***cis***-[Pd(L^x-***S,O***)$_2$] (x = 3-5) in acetonitrile irradiated with white light at 20°C are plotted against time in Figure 60.

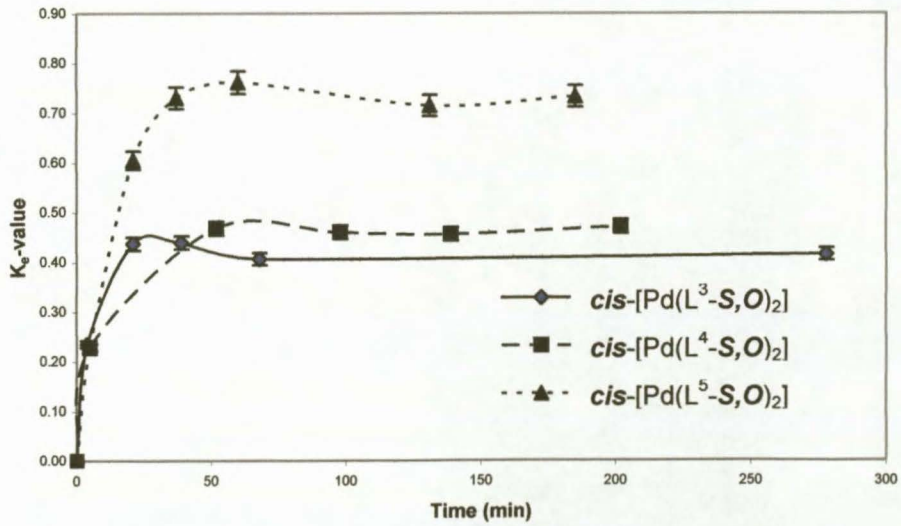

Figure 60. The K_e-values [Pd(L^x-***S,O***)$_2$] (x = 3-5) in acetonitrile at 20°C.

As for ***cis***-[Pt(L^5-***S,O***)$_2$] the K_e-value of ***cis***-[Pd(L^5-***S,O***)$_2$] was observed to be the highest relative to the other complexes. For the palladium complexes however, there seems to be a clearer trend. K_e-values of 0.40, 0.46 and 0.72 were obtained for ***cis***-[Pd(L^3-***S,O***)$_2$], ***cis***-[Pd(L^4-***S,O***)$_2$] and ***cis***-[Pd(L^5-***S,O***)$_2$] respectively. Although advanced software was used for the integration of the peaks, the poor separation obtained for ***cis***- and ***trans***-[Pd(L^5-***S,O***)$_2$] (and to a lesser extent ***cis***- and ***trans***-[Pd(L^3-***S,O***)$_2$]) adds a margin of error to the K_e-values of [Pd(L^5-***S,O***)$_2$] and [Pd(L^3-***S,O***)$_2$]. Despite this error margin, it can be said that [Pd(L^5-***S,O***)$_2$] has a higher K_e-value than [Pd(L^4-***S,O***)$_2$] which in turn has a higher K_e-value than [Pd(L^3-***S,O***)$_2$].

Table 7. General information regarding Figure 59 and Figure 60.

Complex	[Pd(L^3-***S,O***)$_2$]		[Pd(L^4-***S,O***)$_2$]		[Pd(L^5-***S,O***)$_2$]	
Isomer	***cis***	***trans***	***cis***	***trans***	***cis***	***trans***
t_R/min	12.0	10.8	18.4	14.5	12.8	13.6
R_s	1.0		3.4		0.64	
K_e-value	0.40		0.46		0.72	

3.7 Looking at a proposed mechanism

Although no specific attempts were made to investigate the mechanism involved in the *cis-trans* isomerisation process of these [M(L-***S,O***)$_2$] complexes, certain experiments lead to speculation concerning a possible mechanism.

It was discussed in section 3.1 that the isomerisation of ***cis***-[M(L-***S,O***)$_2$] to ***trans***-[M(L-***S,O***)$_2$] (M = Pt(II) and Pd(II)) is photo-induced and that no isomerisation could be identified in the absence of light. Moreover, no isomerisation process was observed on the heating of a 200 $\mu g.cm^{-3}$ solution of ***cis***-[Pt(L^3-***S,O***)$_2$] at 80°C for 100 hours, even when an excess of free ligand was added to the system.

Further comparison of the isomerisation and subsequent chromatograms of ***cis***-[Pt(L^3-***S,O***)$_2$] and ***cis***-[Pd(L^3-*S,O*)$_2$] after exposure to light is interesting. If the areas under the ***cis***- and ***trans***-[M(L-***S,O***)$_2$] peaks are taken as being equal to the total concentration of [M(L-***S,O***)$_2$] present in the solution, the following observations can made.

For both Pt(II) and Pd(II) the area under the *cis* and *trans* peaks is equal to *ca.* 99.80% before commencing with irradiation. After 300 minutes of irradiation the total percentage for [Pd(L^3-***S,O***)$_2$] (*cis* + *trans*) is calculated as: red light 99.5%, yellow light 97.6%, blue light 96.1% and white light 96.8%.

After a similar period of time the percentage for [Pt(L^3-***S,O***)$_2$] (*cis* + *trans*) is calculated as: red light 99.8%, yellow light 90.0%, blue light 60.0% and white light 51.28%.

For [Pd(L^3-***S,O***)$_2$] two peaks appear at 2.1 and 3.8 minutes (Figure 61, **1** and **2**) after irradiation. Although a number of additional peaks appear in the 2-4 minute retention time region for [Pt(L^3-***S,O***)$_2$], two similar peaks at 2.1 and 3.8 minutes are evident (Figure 62, **1** and **2**).

As previously stated the isomerisation reaction has been shown to be thermally reversible. When heat is applied, in the dark, to a previously irradiated solution of [Pt(L^3-***S,O***)$_2$], the peaks at 2.1 minutes (**1**), 3.8 minutes (**2**) and the peak attributed to the *trans* isomer (8 min) substantially diminish, while the peak attributed to the *cis* isomer (10 min) grows. The other peaks in the 2-4 minute region for [Pt(L^3-***S,O***)$_2$] do not indicate any such changes. These peaks could therefore be considered to be possible photodecomposition products related to the isomerisation process (Figure 63).

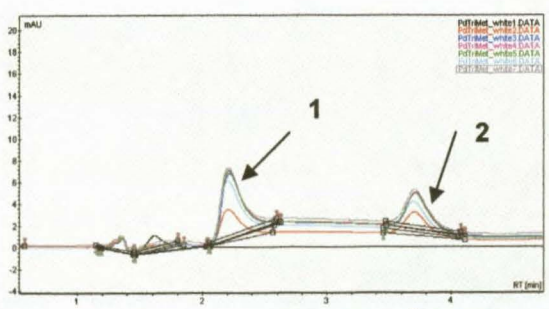

Figure 61. 2-4min. region for [Pd(L^3-***S,O***)$_2$]

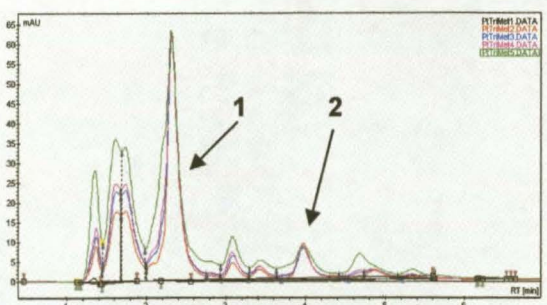

Figure 62. 2-4min. region for [Pt(L^3-***S,O***)$_2$]

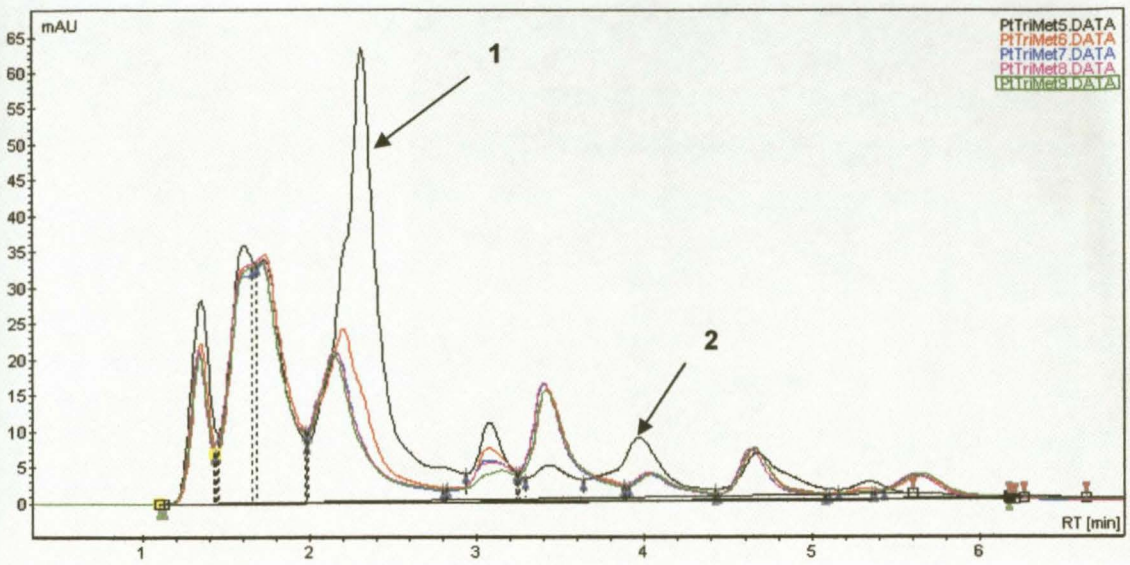

Figure 63. Chromatograms indicating that when a solution of [Pt(L^3-***S,O***)$_2$] is heated to 78°C, two similar peaks that were also evident in the chromatograms of [Pd(L^3-***S,O***)$_2$], diminish while the others remain unchanged.

The above evidence suggests that these peaks, in particular **1** and **2** in Figure 63, may be intermediate species with relatively long lifetimes as a consequence of irradiation with light. However, more evidence is needed to confirm this.

3.7.1 Evidence for ligand exchange in *cis*-[Pt(L-*S,O*)$_2$] complexes in acetonitrile.

In an unrelated experiment which was set up, pure ***cis***-[Pt(L^3-***S,O***)$_2$] was mixed with pure ***cis***-bis(*N,N*-diethyl-*N'*-naphtoylthioureato)platinum(II), ***cis***-[Pt(L^1-***S,O***)$_2$] (50:50, %(w/w)), both complexes at a concentration of 100 µg.cm^{-3} in acetonitrile. Two 50mL round bottom flasks, each containing 100 µg.cm^{-3} of both the aforementioned complexes in 25mL acetonitrile, were left on the bench-top for a period of two weeks. One of the flasks was covered in aluminum foil and the other was left exposed to the light (fluorescent and other).

Injections from both the light and dark experiments were made after a period of two weeks and the following chromatograms were obtained:

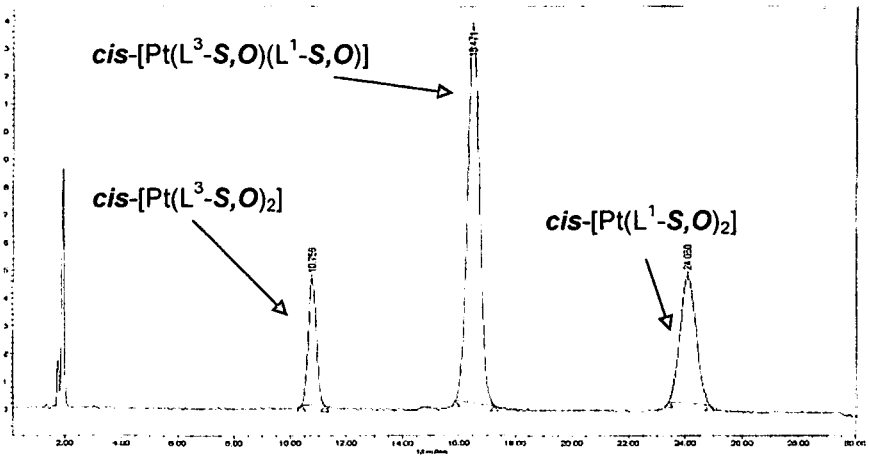

Figure 64. A chromatogram obtained for a two week old solution from the dark setup.

As can be seen from the chromatogram in Figure 64 an exchange reaction between ***cis***-[Pt(L^3-***S,O***)$_2$] and ***cis***-[Pt(L^1-***S,O***)$_2$] had taken place with the resulting mixed ***cis***-[Pt(L^3-***S,O***)(L^1-***S,O***)] complex having a t_r of 16.5 minutes (t_r ***cis***-[Pt(L^3-***S,O***)$_2$] = 11 minutes, t_r ***cis***-[Pt(L^1-***S,O***)$_2$] = 24 minutes). Again, no *trans*-isomers were evident from injections of the dark setup.

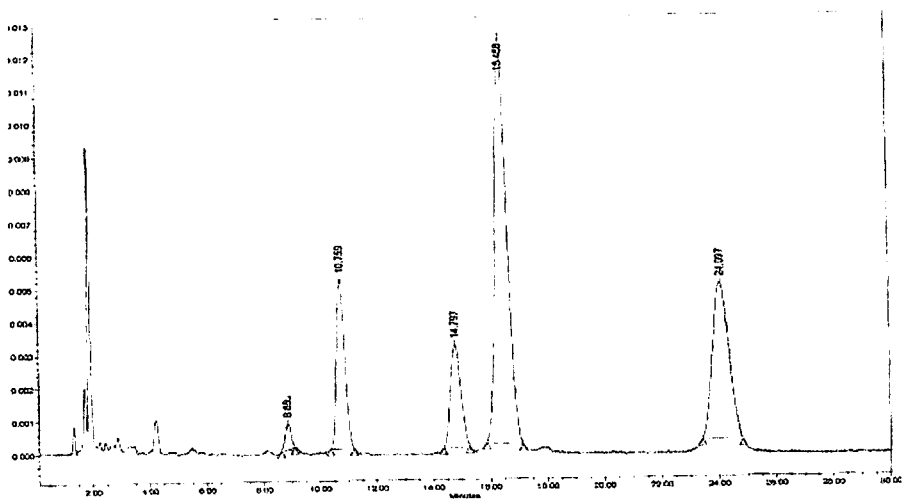

Figure 65. A chromatogram obtained of a two week old solution from the light setup.

From the chromatogram in Figure 65 it is clear that the same exchange reaction occurred in the light setup as in the dark setup. Moreover, in the light setup isomerisation of both ***cis***-[Pt(L^3-***S,O***)$_2$] and ***cis***-[Pt(L^3-***S,O***)(L^1-***S,O***)] to

their respective *trans*-isomers occurred within the period of two weeks. The separation of (possible) ***trans***- and ***cis***-[Pt(L^1-***S,O***)$_2$] isomers (as discussed in section 3.1) could not be achieved. Although initial injections were only made after two weeks, the exchange reaction between the chelated complexes seems to be rapid, as was evident from a relatively fresh injection of a mixed sample solution (Figure 66).

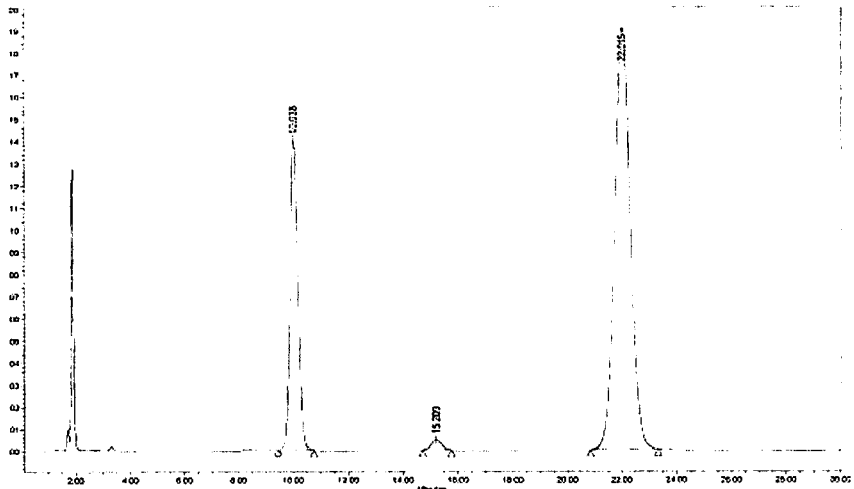

Figure 66. A relatively fresh injection of the mixed sample solution (MeCN), both complexes at a concentration of 100 µg.cm^{-3}.

An exchange reaction occurs when two chelated [Pt(L-***S,O***)$_2$] complexes are dissolved (100 µg.cm^{-3} of each) in acetonitrile. This process occurs in the absence of light and can be considered to be rapid. However, the same exchange reaction, and a *cis-trans* isomerisation of the *cis*-isomers occurs, in an experimental setup exposed to light. Although an exchange reaction is "allowed" in the dark, this possible bond breaking exchange reaction does not allow for a *cis-trans* isomerisation. This suggests that no bond breaking occurs in the isomerisation process and that the isomerisation is more probable to occur via a pseudorotation route, as previously speculated in literature (see Chapter 1).

Furthermore, it was found (as discussed in section 3.3) that a more polar solvent mixture seems to favour the *trans*-isomer of [Pt(L^3-***S,O***)$_2$]. Studies of the methoxy complexes were inconclusive as to the effect of electron-donating groups. A reverse, thermal, *trans-cis* isomerisation was identified

and followed for [Pd(L^3-***S,O***)$_2$] and it was also noted that no forward thermal isomerisation occurs (elevated temperatures initiate *trans-cis* isomerisation).

With the above in mind the following mechanism is proposed (Figure 67):

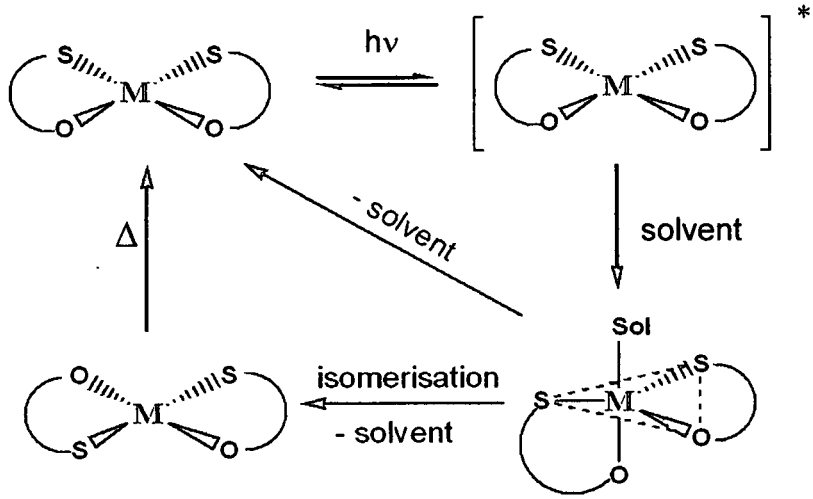

Figure 67. A proposed mechanism for the photo-induced, thermally reversible, *cis-trans* isomerisation of the [M(L-***S,O***)$_2$] complexes (M = Pt(II) and Pd(II)).

3.8 NMR evidence supporting the isomerisation process

A major drawback associated with studying these systems with the aid of RP-HPLC is the inherent delay, and therefore the on-column back-isomerisation of the ***trans***-[M(L-***S,O***)$_2$] isomer to the ***cis***-[M(L-***S,O***)$_2$] isomer. NMR could potentially solve this conundrum by allowing for real-time *cis-trans* ratio determination with the use of an optic-fibre probe as the source of irradiation.

Preliminary investigations were conducted by dissolving pure ***cis***-[M(L-***S,O***)$_2$] complexes (M = Pt(II) and Pd(II)), at concentrations of *ca.* 50 mg.cm^{-3}, in deuterated chloroform. While one solution of a specific complex was kept in a dark environment the other was exposed to white light irradiation using the same 150 W tungsten-halogen light source mentioned on page 66. The aluminum foil was removed just prior to the dark sample being inserted into the NMR instrument. The irradiated sample was analysed immediately after the period of irradiation.

The following table gives ^{195}Pt NMR shifts of the complexes that were investigated in the manner mentioned above:

Table 8. ^{195}Pt NMR shifts of irradiated solutions of ***cis***-[Pt(L-***S,O***)$_2$]. ^{195}Pt spectra were run at 30 °C and externally referenced to 500 mg.cm^{-3} H_2PtCl_6 in 30% (v/v) D_2O/1M HCl.

Complex	^{195}Pt NMR shifts (ppm)		
	cis-[Pt(L-***S,O***)$_2$]	***trans***-[Pt(L-***S,O***)$_2$]	-(shift$_{cis}$ - shift$_{trans}$)
[Pt(L^1-***S,O***)$_2$]	-2700.41	-1980.26	720.15
[Pt(L^3-***S,O***)$_2$]	-2723.49	-1982.51	740.98
[Pt(L^4-***S,O***)$_2$]	-2706.55	-1974.51	732.04
[Pt(L^5-***S,O***)$_2$]	-2733.79	-1990.95	742.84
[Pt(L^6-***S,O***)$_2$]	-2691.08	-1972.04	719.04
[Pt(L^7-***S,O***)$_2$]	-2720.14	-1980.83	739.31

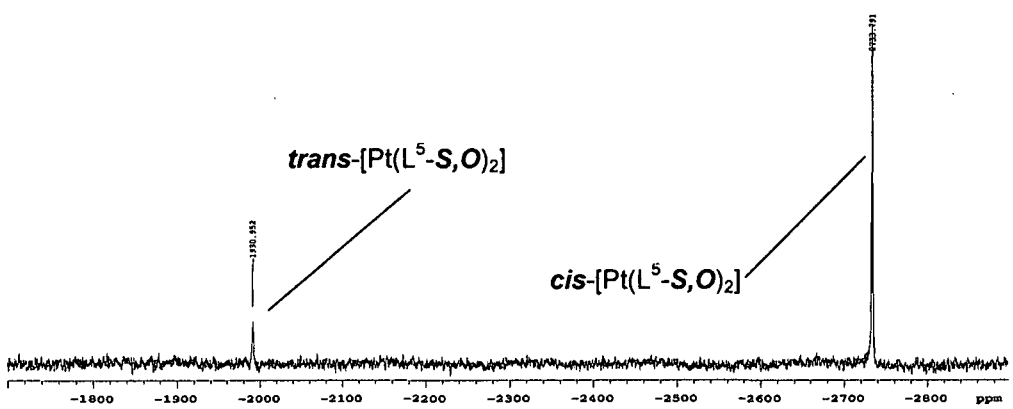

Figure 68. The ^{195}Pt NMR spectrum obtained for an irradiated solution of ***cis***-[Pt(L^5-***S,O***)$_2$]. The *cis*-isomer appears upfield at -2733.79ppm and the *trans*-isomer at -1990.95ppm.

3.9 Experimental details

Chromatographic analysis was performed on two systems. A Waters 2690 Alliance HPLC system equipped with an automatic sampling system, quaternary pumps and a Waters 996 photodiode array detector was initially used. Subsequent analyses were performed on a Varian Polaris system equipped with a 20µl Rheodyne sampling loop, Varian ProStar binary pumps and a Varian ProStar 325 variable-wavelength detector. A Zorbax XDB-C_{18} 150 x 4.6mm, 5µm, column was used at all times. The mobile phase was made up of 90:10 (%(v/v)) MeCN:0.1M acetate buffer (pH ≈ 6). An isocratic flow of 1ml.min^{-1} was used with photometric detection at 254nm. Only de-

ionized water and HPLC grade organic solvents, filtered through 0.22μm and 0.45μm respectively, were used to make up the mobile phase.

Chapter 4:

Concluding Remarks

4. Concluding remarks

4.1 Synthesis and characterisation of the *N,N*-dialkyl-*N'*-aroylthiourea ligands and their respective platinum(II) and palladium(II) complexes

Several ligands of the type *N,N*-dialkyl-*N'*-aroylthiourea were prepared with relative ease and in high yields. These ligands were characterised by means of ^{1}H and ^{13}C NMR as well as elemental analysis and melting point determination. All the ligands synthesised were of acceptable purity without the need for further purification steps.

Platinum(II) and base deprotonated HL^{x} complexed in a ***cis***-$[Pt(L^{x}\text{-}\boldsymbol{S,O})_2]$ (x = 1-7) orientation without exception. The crude product mixtures all contained some unreacted ligand after the standard reaction time of 60 minutes. The addition of metal to ligand, and ligand to metal afforded the same products. For the synthesis of ***cis***-$[Pt(L^{2}\text{-}\boldsymbol{S,O})_2]$, a reaction time of 48 hours was employed, which rendered the ^{1}H NMR spectrum free from any secondary species. Although a range of solvents was used during synthesis, no *trans* species could be isolated. ^{1}H, ^{13}C and ^{195}Pt NMR all confirmed the existence of only the *cis* isomer. Further analyses of the compounds included elemental analysis and melting point determination. The crystal structures of ***cis***-$[Pt(L^{3}\text{-}\boldsymbol{S,O})_2]$ and ***cis***-$[Pt(L^{4}\text{-}\boldsymbol{S,O})_2]$ were determined.

Palladium(II) and base deprotonated HL^{x} (x = 3-5) all resulted in a *cis* complex, as was the case with the platinum(II) analogues. The complexes were synthesised by the addition of the metal solution to the ligand solution, both in different ratios of acetonitrile and water. ^{1}H and ^{13}C NMR confirmed the existence of only the *cis* isomer. Further analyses of the compounds included elemental analysis and melting point determination. The crystal structures of ***cis***-$[Pd(L^{3}\text{-}\boldsymbol{S,O})_2]$ and ***cis***-$[Pd(L^{4}\text{-}\boldsymbol{S,O})_2]$ were determined.

4.2 The photo-induced, thermally reversible, *cis-trans* isomerisation process

Pure ***cis***-[M(L-***S,O***)$_2$] complexes [M = Pt(II) or Pd(II), L = *N,N*-dialkyl-*N'*-aroyl(acyl)thiourea] undergo a *cis-trans* isomerisation process that is photochemically induced and which is thermally reversible. This process can conveniently be followed by means of Reversed Phase High Performance Liquid Chromatography.

Solutions of ***cis***-[M(L^x-***S,O***)$_2$] [M = Pt(II) or Pd(II), x = 3-5] in acetonitrile (200 µg.cm^{-3}) were made up in a cylindrical, water-jacketed glass tube (l = 10cm, i.d. = 1,5cm) which was covered in foil. Irradiation of the sample commenced after a fresh sample was withdrawn and injected into a RP-HPLC system. The light source (150W tungsten halogen lamp) was generally kept at a constant distance of 15cm from the sample, giving rise to a light intensity of 320 µmol.s^{-1}.m^{-2}. Sequently samples were withdrawn at random times and injected.

K_e-values (K_e = [*trans*]/[*cis*]; [trans] and [cis] taken as area under the respective peaks) obtained for the Pt(II) and Pd(II) complexes with HL (MeCN, 20°C) indicate that, as expected, the [Pd(L-***S,O***)$_2$] complexes are more labile than their equivalent [Pt(L-***S,O***)$_2$] complexes. Optical filters with radiation cut-offs at 330nm, 480nm and 600nm were used to eleminate certain parts of the spectrum. For [Pt(L^3-***S,O***)$_2$] K_e-values of 0.14 were obtained when the complex was irradiated with white and blue light, 0.10 with yellow light and 0 when red light was the source of irradiation.

The results for experiments with ***cis***-[Pd(L^3-***S,O***)$_2$], using these filters, are illustrated in section 3.5 (Figure 51). No *cis-trans* isomerisation was observed when [Pd(L^3-***S,O***)$_2$] was irradiated with red light. When white or blue light was used for irradiation K_e-values of *ca.* 0.40 in MeCN were obtained. A steady-state K_e-value of 0.20 was obtained when a ***cis***-[Pd(L^3-***S,O***)$_2$] solution was irradiated with yellow light (acetonitrile, 20°C). When the light source was brought closer, minimising the loss of photons due to dispersion (intensity changed to 2280 µmol.s^{-1}.m^{-2}), the same K_e-values were obtained for yellow light (0.40) as for white and blue light. This would suggest that the photochemical excitation of the ***cis***-[Pd(L^3-***S,O***)$_2$] complex occurs in the

480nm to 600nm region of the spectrum and that it depends on the flux of photons. Similar results were obtained for the other ***cis***-[M(L-***S,O***)$_2$] (M = Pt(II), Pd(II)) complexes.

A sample of [Pd(L^3-***S,O***)$_2$] in acetonitrile was irradiated to its equilibruim *cis-trans* state at 20°C. Three separate vials were filled from the solution and kept in the dark at 0°C, 20°C and 40°C respectively. Injections were then made from these vials at random times. The *trans-cis* backward isomerisation was found to be temperature-dependant (Figure 50). After *ca.* 95 minutes the sample kept at 40°C had virtually fully back-isomerised to pure ***cis***-[Pd(L^3-***S,O***)$_2$] while the sample kept at 0°C still had a K_e-value of 0.1 after *ca.* 1200 minutes. To verify this ***cis***-[Pd(L^3-***S,O***)$_2$] was irradiated with yellow light at *ca.* 50°C. The complex isomerised to a equilibrium K_e-value of 0.07 as opposed to 0.20 at 20°C.

The question of how the addtion of electron donating groups to the benzoyl moiety affects the equilibrium *cis-trans* distribution was examined for both the Pt(II) and Pd(II) complexes with HL^3, HL^4 and HL^5. It would be reasonable to argue that the equilibruim K_e-value should increase in going from [M(L^5-***S,O***)$_2$] to [M(L^4-***S,O***)$_2$] to [M(L^3-***S,O***)$_2$], as the addition of these groups should render the oxygen atom softer, thereby making such a *trans* conformation more favourable. However, the opposite was observed for the Pd(II) complexes. White light irradiation of these complexes in MeCN gave rise to the following K_e-values: 0.40 for [Pd(L^3-***S,O***)$_2$], 0.47 for [Pd(L^4-***S,O***)$_2$] and 0.73 for [Pd(L^5-***S,O***)$_2$]. The isomerisation of the methoxy-series of Pt(II) gave rise to the following K_e-values: 0.14 for [Pt(L^3-***S,O***)$_2$], 0.12 for [Pt(L^4-***S,O***)$_2$] and 0.16 for [Pt(L^5-***S,O***)$_2$]. Clearly no simple conclusion can be made about the effect of the addition of electron-donating groups on the benzoyl moeity purely from a "softness of the oxygen" point of view.

A brief solvent study was carried out on the *cis-trans* isomerisation of ***cis***-[Pt(L^1-***S,O***)$_2$]. RP-HPLC was limiting in this instance as the solvent used to dissolve the sample had to be misicible with the mobile phase. ***trans***-[M(L-***S,O***)$_2$] complexes are thought of as being more non-polar than their equivalent ***cis***-[M(L-***S,O***)$_2$] complexes.[33] If the solvent effect is to be viewed purely from a

trans-cis equilibruim point of view more non-polar solvents should favour the *trans*-complexes and therefore lead to higher K_e-values. A K_e-value of 0.16 was obtained for the white light induced isomeristaion of ***cis***-[Pt(L^3-***S,O***)$_2$] dissolved in a (50:50, %(v/v)) mixture of MeCN:MeOH as opposed to 0.14 in pure MeCN. Both 1,4-dioxane and THF gave an equilibruim K_e-value of 0.07. Although the *trans*-complex is less polar, higher K_e-values are not obtained in more non-polar solvents as was previously observed for similar monodentate complexes. This would indicate that other solvent related factors play a significant role in the *trans-cis* equilibruim distribution.

Other complexes that were investigated included ***cis***-bis(*N,N*-diethyl-*N'*-camphanoylthioureato)platinum(II) and ***cis***-bis(*N,N*-diethyl-*N'*-pivaloyl-thioureato)platinum(II) with K_e-values of 0.30 and 0.20 respectively. The very bulky camphanoyl moiety as well as the acyl pivaloyl moiety both led to higher K_e-values than the methoxy-series of Pt(II) complexes did.

No separate forward thermal isomerisation mechanism has been observed as previously seen[19], even at temperatures of 80°C and, with the addition of an excess of free ligand, the solutions contained only ***cis***-[M(L-***S,O***)$_2$].

Because the reaction is thermally reversible, the HPLC data obtained can only be used to make comparisons between complexes with similar retention times, as the *trans*-species rapidly starts isomerising back to the *cis*-species, especially in the case of the palladium complexes, when light is absent. Prelimary ^{1}H NMR experiments have proven to be very promising and ^{195}Pt peaks for all the ***trans***-[Pt(L-***S,O***)$_2$] complexes have been observed after white light irradiation of the $CDCl_3$ solutions directly in the NMR tube. Because of the possibility of real-time data acquisition, monitoring the isomerisation reaction, induced by laser light *via* an optic fibre probe in the NMR instrument, would be ideal and is currently under investigation.

4.3 Future work

The photo-induced, thermally reversible, isomerisation reactions of these bis-chelated ***cis***-[M(L-***S,O***)$_2$] complexes (M = Pt(II), Pd(II)) have only been briefly studied in this dissertation. Although RP-HPLC offers an elagant window to the isomerisation reaction, and to *cis-trans* equilibruim distributions, the use of NMR would allow us to study the mechanism to a greater extent.

The *trans-cis* backward isomerisation of the palladium complexes in the NMR tube (pre-irradiated with white light to an equilibruim distribution) are currently being studied. This opens up the door for real-time data acquisition as well as a thorough solvent study. This has been well studied and documented for similiar monodentate complexes and data concerning *cis-trans* ratios of these bis-chelated complexes would be a valuable contribution to the literature. Moreover, Density Functional Theory (DFT) calculations are carried out and can assist in the elucidation of the mechanism. This will enhance our fundamental understanding of these molecules and their properties in solution.

Futhermore, the exchange reaction (non-photochemical) of these bis-chelated complexes, detailed in section 3.7, needs to be indepently studied.

References

References

1. http://www.matthey.com
2. http://www.vcarfueldata.com
3. Anglo American Platinum Corporation Limited, Annual Report, 2002, **1-2**
4. K.R. Koch, A. Irving, M. Matoetoe, *Inorg. Chim. Acta*, 1993, 206
5. a) K.R. Koch, J. du Toit, M.R. Caira, C. Sacht, *J. Chem. Soc. Dalton Trans.*, 1994, 785, b) F.H. Allen, The Cambridge Structural Database: a quarter of a million structures and rising, *Acta Crystallogr.*, 2002, **B58**, 380-388
6. K.R. Koch, A. Coetzee, Y. Wang, *J. Chem. Soc. Dalton Trans.*, 1999, 1013
7. K.R. Koch, Coord. *Chem. Rev.*, 2001, 473-488
8. K.R. Koch, T. Grimmbacher, C. Sacht, *Polyhedron*, 1998, 267-274
9. F. Basolo, R.G. Pearson, Mechanism of Inorganic Reactions, 2nd edn., Wiley, New York, 1967
10. A.N. Mautjana, J.D.S. Miller, A. Gie, S.A. Bourne, K.R. Koch, *Dalton Trans.*, 2003, 1952-1960
11. a) G.K. Anderson, R.J. Cross, *J. Chem. Soc. Quantum Rev.*, 1980, **9**, 185, b) J.S. Wood, *Progr. Inorg. Chem.*, 1972, **16**, 227
12. R.J. Cross, T.H. Green, R. Keat, *J. Chem. Soc. Dalton Trans.*, 1976, 382
13. D.A. Redfield, N.H. Nelson, *Inorg. Chem.*, 1973, **15**, 315
14. (a) A.J. Cheney, B.E. Mann, B.L. Shaw, R.M. Slade, *J. Chem. Soc. (A)*, 1971, 3833 (b) E.C. Algea, S.A. Dias, G. Ferguson, P.J. Roberts, *J. Chem. Soc. Dalton Trans.*, 1979, 948
15. (a) F.R. Hartley, J. Chem. Soc. Rev., 1973, **2**, 63 (b) T.G. Appleton, H.C. Clark, L.E. Manzer, *Coord. Chem.Rev.*, 1973, **10**, 335
16. P. Haacke, P.M. Pfeiffer, *Chem. Commun.*, 1969, 1330
17. W.J. Louw, *Inorg. Chem.*, 1977, **16**, 2147
18. W.J. Louw, D.J.A. de Waal, G.J. Kruger, *J. Chem. Soc. Dalton Trans.*, 1976, 2364

19. F. Scandola, O. Traverso, V. Balzani, G.L. Zucchini and V. Carassiti, *Inorg. Chim. Acta*, 1967, **1**, 76
20. S.H. Goh, C.Y. Mok, *J. Inorg. Nucl. Chem.*, 1977, **39**, 531
21. P. Haake, T.A. Hylton, *J. Am. Chem. Soc.*, 962, **84**, 3774
22. C.R. Bock, E.A. Koerner von Gustorf, *Advances in Photochemistry* (J.N. Pitts, G.S. Hammond, k. Gollnick, Eds.), Interscience, New York, **10**, 1974, 221
23. a) M. Wrighton, H.B. Gray, G.S. Hammond, *Mol. Photochem.*, 1973, **5**, 165, b) M. Wrighton, H.B. Gray, G.S. Hammond, *Mol. Photochem.*, 1973, **5**, 179, c) J.I. Zink, *Mol. Photochem.*, 1973, **5**, 151, d) J.I. Zink, *Inorg. Chem.*, 1973, 12, 1018, d) J.I. Zink, *J. Am. Chem. Soc.*, 1972, **94**, 8039
24. R.W. Callahan, G.M. Brown, T.J. Meyer, *J. Am. Chem. Soc.*, 1974, **96**, 7829
25. H.H. Willard, L. Merritt, J.A. Dean, S.A. Settle, *Instrumental Methods of Analysis*, 1988, 7th edition
26. D.A. Skoog, F.J. Holler, T.A. Nieman, *Principles of Instrumental Analysis*, 5th edition
27. I.B. Douglas, F.B. Dains, *J. Am. Chem. Soc.*, 1934, **56**, 719
28. S. Mtongana, V.Z. Brus'ko, K.R. Koch, unpublished results
29. G.M. Sheldrick, SHELXS 97, University of Göttingen, Germany
30. G.M. Sheldrick, SHELXL 97, University of Göttingen, Germany
31. L.J. Barbour, X-Seed, *J. Supramol. Chem.*, 2001, **1**, 189-191
32. A. Mautjana, MSc thesis, University of Cape Town, 2000
33. P. del Socorro Murdoch, J.D. Ranford, P.J. Sadler, S.J. Berners-Price, *Inorg. Chem.*, 1993, **32**, 2249-2255
34. a) J. Miller, Ph.D thesis, University of Cape Town, b) H.G. Berhe, M.Sc. thesis, University of Stellenbosch
35. R. Köhler, R. Richter, H. Tschö, M. Moll, L. Beyer and E. Hoyer, *Z. Chem.*,1988, **28**, 369
36. T. E. MacDermott, *Inorg. Chim. Acta*, 1968, **2:1**, 399-401
37. A. Mahipal Reddy, V. Raj Gopal and V. Jayathirtha Rao, *Radiat. Phys. Chem.*, 1997, **49**, 119-125
38. S. Mastin and P. Haake, *Chem. Commun.*, 1970, 202

39. J. Sieler, R. Richter, E. Hoyer, L. Beyer and R. Köhler, *Z. Anorg. Allg. Chem.*, 1991, **603**, 25-32

40. R. Rumin and P. Coutot, *J. Photochem.*, 1982, **20**, 107-122

41. L.L. Costanzo, S. Giuffrida and R. Romeo, *Inorg. Chim. Acta*, 1980, **38**, 31-35

42. J.H. Price, J.P. Birk, B.B. Wayland, *Inorg. Chem.*, 1978, **17**, 2245-2249

43. H. Nakai, S. Fukada and H. Nakatsuji, *J. Phys. Chem.*, 1997, **101**, 973-980

44. E.M. Jaryszak and P. Hoggard, *Inorg. Chim. Acta*, 1998, **282**, 217-221

45. M.F. Budyka, O.D. Laukhina and V.F. Razumov, *Chem. Phys. Lett.*, 1997, **279**, 327-332

46. L.I. Elding and A.B. Gröning, *Inorg. Chim. Acta*, 1978, **31**, 243-250

47. L.I. Elding and A.B. Gröning, *Inorg. Chim. Acta*, 1980, **38**, 59-66

48. C.Y. Mok, S.G. Tan and G.C. Chan, *Inorg. Chim. Acta*, 1990, **176**, 43-48

49. J. Real, E. Prat, A. Polo, A. Alvarez-Larena and J. Francesc Piniella, *Inorg. Chem. Commun.*, 2000, **3:5**, 221-223

50. D.V. Fomitchev, I.Novozhilova and P. Coppens, *Tetrahedron*, 2000, **56**, 6813-6820

51. O.V. Mikhailov, *Trans. Metal Chem.*, 1994, **19**, 387-389

52. P. O'Brien, *J. Chem. Educ.* 1982, **59**, 1052-1053

53. S.M. Moussa, R.R. Fenton, B.A. Hunter and B.J. Kennedy, *Austr. J. Chem.*, 2002, **55**, 3319

54. C.S. Trautermann, J. Sabalovic, A.F. Voegele and K.R. Liedl, *J. Phys. Chem.*, 2004, **88**, 2098

Appendices

Appendix A

Table 9. Crystal data and structure refinement for ***cis***-[Pt(L^3-***S,O***)$_2$].

Empirical Formula		$C_{30}H_{44}N_4O_8PtS_2$
Formula Weight/g.mol^{-1}		849.92
Crystal system		Monoclinic
Space Group		$P2_1/n$
Unit cell dimensions	*a*/Å	13.028(3)
	b/Å	8.2726(17)
	c/Å	31.150(6)
	β/°	90.46(3)
	V/Å^3	3357.2(12)
Z		4
Dc / g/cm^3		1.670
F(000)		1696
Temperature/K		173(2)
Absorption coefficient/mm^{-1}		4.356
Crystal size/mm^3		0.40 x 0.30 x 0.20
Theta range for data collection / °		1.31 – 27.88
Limiting Indices		-17≤h≤17 ; -10≤ k≤10 ; -40≤l≤40
Reflections collected / unique		98159 / 7977
Completeness to theta / %		99.9
Radiation		MoKα, graphite monochromated
Refinement method		Full-matrix-least-squares on F^2
Data / restraints / parameters		8003 / 398 / 6
Goodness-of-fit on F^2		1.058
Final *R* indices [I>2σ (I)]		5.68, 13.75%
R indices (all data)		R_1 = 0.0260, wR_2 = 0.0480
Largest diff. peak and hole		5.491, -2.581

Appendix B

Table 10.Crystal data and structure refinement for ***cis***-[Pt(L^4-***S,O***)$_2$].

Empirical Formula		$C_{28}H_{38}N_4O_6PtS_2$
Formula Weight/g.mol^{-1}		785.83
Crystal system		Monoclinic
Space Group		$P2_1/n$
Unit cell dimensions	*a*/Å	16.6195(10)
	b/Å	8.0537(5)
	c/Å	23.0932(13)
	β/°	104.1140(10)
	V/Å^3	2997.7(3)
Z		4
Dc / g/cm^3		1.741
F(000)		1568
Temperature/K		100(2)
Absorption coefficient/mm^{-1}		4.868
Crystal size/mm^3		0.1 x 0.1 x 0.1
Theta range for data collection / °		1.73 – 28.25
Limiting Indices		-22≤h≤15 ; -10≤ k≤10 ; -30≤l≤30
Reflections collected / unique		18028 / 6959
Completeness to theta / %		93.7
Radiation		MoKα, graphite monochromated
Refinement method		Full-matrix-least-squares on F^2
Data / restraints / parameters		6959 / 9 / 389
Goodness-of-fit on F^2		1.041
Final *R* indices [I>2σ (I)]		3.28, 8.03%
R indices (all data)		R_1 = 0.0328, wR_2 = 0.0803
Largest diff. peak and hole		2.312, -1.871

Appendix C

Table 11. Crystal data and structure refinement for ***cis***-[Pd(L^3-***S,O***)$_2$].

Empirical Formula		$C_{30}H_{42}N_4O_8PdS_2$
Formula Weight/g.mol^{-1}		757.20
Crystal system		Monoclinic
Space Group		$P2_1/n$
Unit cell dimensions	*a*/Å	12.7960(10)
	b/Å	8.3492 (6)
	c/Å	30.886(2)
	β/°	90.282(2)
	V/Å^3	3299.7(4)
Z		4
Dc / g/cm^3		1.524
F(000)		1568
Temperature/K		125(2)
Absorption coefficient/mm^{-1}		0.744
Crystal size/mm^3		0.1 x 0.1 x 0.1
Theta range for data collection / °		1.72 – 28.29
Limiting Indices		-12≤h≤16 ; -10≤ k≤11 ; -41≤l≤40
Reflections collected / unique		20115 / 7657
Completeness to theta / %		93.5
Radiation		MoKα, graphite monochromated
Refinement method		Full-matrix-least-squares on F^2
Data / restraints / parameters		5946 / 0 / 416
Goodness-of-fit on F^2		1.038
Final *R* indices [I>2σ (I)]		5.24, 11.40%
R indices (all data)		R_1 = 0.0524, wR_2 = 0.1140
Largest diff. peak and hole		1.336, -1.191

Appendix D

Table 12. Crystal data and structure refinement for ***cis***-[Pd(L^4-***S,O***)$_2$].

Empirical Formula		$C_{28}H_{38}N_4O_6PdS_2$
Formula Weight/g.mol^{-1}		697.14
Crystal system		Monoclinic
Space Group		$P2_1/n$
Unit cell dimensions	*a*/Å	16.6169(8)
	b/Å	8.0810(4)
	c/Å	23.0400(11)
	β/°	104.0310(10)
	V/Å^3	3001.5(3)
Z		4
Dc / g/cm^3		1.543
F(000)		1440
Temperature/K		100(2)
Absorption coefficient/mm^{-1}		0.805
Crystal size/mm^3		0.1 x 0.1 x 0.1
Theta range for data collection / °		1.73 - 26.00
Limiting Indices		-20≤h≤20 ; -9≤ k≤9 ; -28≤l≤28
Reflections collected / unique		30314 / 5890
Completeness to theta / %		99.9
Radiation		MoKα, graphite monochromated
Refinement method		Full-matrix-least-squares on F^2
Data / restraints / parameters		5454 / 74 / 446
Goodness-of-fit on F^2		1.077
Final *R* indices [I>2σ (I)]		3.91, 8.35%
R indices (all data)		R_1 = 0.0391, wR_2 = 0.0835
Largest diff. peak and hole		0.833, -0.538